UC Merced
UC Merced Electronic Theses and Dissertations

Title
Enabling Ex Vivo Heart Studies on Stem Cell Differentiation, Integration, and Repair

Permalink
https://escholarship.org/uc/item/3bj2j94x

Author
Tefera, Anley

Publication Date
2019

Copyright Information
This work is made available under the terms of a Creative Commons Attribution-NonCommercial License, availalbe at https://creativecommons.org/licenses/by-nc/4.0/

Peer reviewed|Thesis/dissertation

eScholarship.org Powered by the California Digital Library
University of California

UNIVERSITY OF CALIFORNIA, MERCED

ENABLING *EX VIVO* HEART STUDIES ON STEM CELL DIFFERENTIATION, INTEGRATION, AND REPAIR

A dissertation submitted in partial satisfaction of the requirements
for the degree of Doctor of Philosophy

In

Materials and Biomaterials Science and Engineering

by:

Anley E. Tefera, MS

Research Committee

Professor Christopher Viney, Founding Faculty, UC Merced, School of Engineering – Chair
Professor Valerie Leppert, Founding Faculty, UC Merced, School of Engineering
Professor Changqing Li, UC Merced, School of Engineering
Professor Kara McCloskey, Founding Faculty, UC Merced, School of Engineering – Primary Advisor

2019

Enabling *Ex Vivo* Heart Studies On Stem Cell Differentiation, Integration, And Repair

Copyright
Anley E. Tefera, 2019
All rights reserved

The Dissertation of Anley E. Tefera is approved, and it is acceptable in quality and form for publication on microfilm and electronically

Professor Kara McCloskey, Primary Advisor

Professor Valerie Leppert

Professor Changqing Li

Professor Christopher Viney, Committee Chair

University of California, Merced

2019

DEDICATIONS

To the best educator: You have inspired, installed confidence, cultivated, and motivated many students over the years. I have learned a lot about life from you and enjoyed every second you were kind enough to share with me. It took sometime for your humor to click for me but once it did, I realized you could have been a stand up comedian. I hope to become the man you are and positively impact as many young lives as you have. I have never met anyone who has made an impression on me as you have. Dr. Christopher Viney, you are the real MVP!!!!

&

To my transformer: You completely changed me since the day you came into my life. You forced me to grow up quickly and showed me a lot about myself. I was able to see the world from your perspective and there is a whole lot of world I otherwise would have never seen. You find the beauty in everyone and everything, which makes you unique. You introduced me to a lot of new things and I am a better person for it. I am proud of the amazing young lady you have become shattering all the limiting expectations the world placed upon you. You are a history in the making lovely girl. I love you!!!! Keep thriving Promise Alay'ja Rodriguez!!!!

I do not intend to make a living; I intend to make a difference!!!!

TABLE OF CONTENTS

LIST OF FIGURES vii
LIST OF TABLES ix
LIST OF ABBREVIATIONS x
LIST OF SYMBOLS xiii
ACKNOWLEDGMENTS viv
CURRICULUM VITA xvi
ABSTRACT xix

CHAPTER 1. INTRODUCTION 1

1.1 BACKGROUND 1
1.1.1 Cardiovascular Diseases (CVDs) 3
1.1.2 Treatment History 5
1.1.3 Stem Cell Based Cardiac Therapy 6
1.1.4 Tissue Slice As a Model 11
1.1.5 Mechanical Stimulation 12
1.2 GOALS AND OVERVIEW OF THE DISSERTATION 13

CHAPTER 2. REPROGRAMMING ORAL MUCOSA EPHITHELIAL (OME) CELLS FROM BUCCAL SWAB FOR GENERATING PATIENT-SPECIFIC STEM CELLS 16

2.1 INTRODUCTION 17
2.1.1 Current Reprogramming Methods and Challenges 17
2.1.2 Somatic Cell Sources for Reprogramming 18
2.1.3 Oral Mucosa Epithelial Cells 19
2.1.4 Extraction and Culturing Substrates 20
2.2 MATERIALS AND METHODS 21
2.2.1 Obtaining and Culturing Oral Mucosa Epithelial (OME) Cells 21
2.2.2 Oral Mucosa Epithelial (OME) Cell Culture Substrates 22
2.2.3 Substrate Preparation 22
2.2.4 Oral Mucosa Epithelial (OME) Cell Viability 23
2.2.5 Immunohistochemistry Staining 23
2.2.6 Cellular Reprogramming 24
2.2.7 Alkaline Phosphatase Live Stain 25
2.2.8 Statistical Analysis 25
2.3 RESULTS 25
2.3.1 Buccal Swab Cells are Viable, Express Epithelial Cell Markers, And Test Negative for Pluripotency 25
2.3.2 Collagen IV is Suitable Substrate for Oral Mucosa Epithelial Cell Culture 27
2.3.3 Reprogrammed Oral Mucosa Epithelial Cells have Stem Cell like Morphology, And Show Pluripotency with Alkaline Phosphatase Live Staining 29
2.4 DISCUSSIONS AND CONCLUSIONS 31

CHAPTER 3. STRETCHING DEVICE FOR HEART TISSUE MODEL PRESERVATION 33

3.1 INTRODUCTION 33
3.1.1 Advantages and Limitations of Current Tissue/Cell Stretchers 35
3.1.2 DTSD 4.0s Design Specification 36
3.2 MATERIALS AND METHODS 37
3.2.1 Tissue Stretching Device 37
3.2.2 Design and Fabrication 38
3.2.3 Slice Preparation 40
3.2.4 Tissue Loading and Device Characterization 40
3.2.5 Device General Setup 41
3.2.6 Statistical Analysis 42

3.3 RESULTS 42
3.3.1 Device Calibration 42
3.3.2 Device Strain profile 43
3.4 DISCUSSIONS AND CONCLUSIONS 46

CHAPTER 4. CHARACTERIZATION OF MECHANICALLY STIMULATED CARDIAC TISSUE SLICES 48

4.1 INTRODUCTION 48
4.1.1 Cardiovascular Research Platforms 48
4.1.2 Cardiac Organotypic Tissue Slices as a Model 50
4.1.3 Role of Mechanical Stimulation in Cardiac Remodeling 52
4.2 MATERIALS AND METHODS 53
4.2.1 Heart Collection 53
4.2.2 Slice Preparation 54
4.2.3 Tissue Culture 55
4.2.4 Hematoxylin & Eosin (H&E) Staining 56
4.2.5 Fixation and Histological/Immunohistochemical Staining 56
4.2.6 Stimulation Protocol 56
4.2.7 Statistical Analysis 56
4.3 RESULTS 57
4.3.1 Cardiac Slice Preparations 57
4.3.2 Static Cultured slices lose their tissue integrity over time 58
4.3.3 Mechanical stimulation improves structure and function 59
4.4 DISCUSSIONS AND CONCLUSIONS 60

CHAPTER 5. DERIVATION OF CM FROM PSC: OPTIMIZING CULTURE SUBSTRATE 63

5.1 INTRODUCTION 63
5.1.1 Cardiac Cell Therapy 63
5.1.2 Cell Sources 63
5.1.3 Cardiac Differentiation 65
5.2 MATERIALS AND METHODS 66
5.2.1 Stem Cell Culture 66
5.2.2 Differentiation 66
5.2.3 Fixing and Staining 68
5.3 RESULTS AND DISCUSSIONS 68
5.3.1 Cardiac Induction: EB method 68
5.3.2 Cardiac Induction: Monolayer method 70
5.3.3 ITGB 4 and ITGB 5 localization 71
5.4 CONCLUSIONS 72

CHAPTER 6. CONCLUSIONS 73

REFERENCES 76

LIST OF FIGURES

Figure 1	Percentage change in age adjusted death rate from CVD, Non-CVD, and Stroke in the United States since 1950.	1
Figure 2	2015 data on leading causes of death in the United States. Heart disease continues to kill more Americans than any other cause.	2
Figure 3	Myocardial infarction (MI), or a heart attach is caused by occlusion of a coronary artery by atherosclerosis	4
Figure 4	History of Myocardial Infarction (MI) Treatment Over the Last 100 Years	6
Figure 5	Adult Stem Cell sources for cell based regenerative medicine	8
Figure 6	Comparison of Transfecting Vectors Used for Reprogramming	18
Figure 7	Classification of Epithelial cells	20
Figure 8	Schematic representation of the process utilized to obtain epithelial cells from oral mucosa	21
Figure 9	Schematic for reprogramming Buccal cells	24
Figure 10	Oral Mucosa Epithelial Cell Extraction: Comparison of two subsequent swabs/washes	26
Figure 11	Oral Mucosa Epithelial Cell Extraction: Cell viability Via Trypan Blue exclusion	26
Figure 12	Oral Mucosa Epithelial Cell Characterization. Stained for Cheek cell and Stem cell markers	27
Figure 13	Substrate for Buccal Cell Culture	28
Figure 14	Characterization of iPS cells	29
Figure 15	Characterization of iPS cells. NHLF iPS cells maintain colony shape, and stain positive for the pluripotent markers	30
Figure 16	Reprogrammed Buccal cells on inactivated MEF feeder layer	30
Figure 17	Reprogrammed & Stained Buccal cells on iMEF feeder layer	31
Figure 18	Cellular Mechanotransduction: Cells display biological responses to mechanical cues such as sheer stress, interstitial flow, substrate strain, or compression	33
Figure 19	Frank-Starling curve relating the left ventricular End Diastolic Pressure (EDV) to the Stroke Volume (SV)	34
Figure 20	Prior generation devices	36

Figure 21	DTSD 4s design and fabrication	39
Figure 22	Tissue loading and displacement measurement	40
Figure 23	General Device setup: DTSD4s is depicted on the right with the five chambers labeled 1 through 5 (positioner)	41
Figure 24	Relationship between Input and Output distances for all five chambers	43
Figure 25	Device characterization: Simulation of force applied on a 3D model of tissue slice preparations	44
Figure 26	Young's Modulus (E) of biological tissues and Organs	45
Figure 27	*In vitro* experimental model systems for cardiovascular research	49
Figure 28	Electrophysiological parameters and mechanical properties of acute vs. cultured slices	51
Figure 29	Porcine heart block preparation for slicing	55
Figure 30	Myocardial Tissue slice preparation	57
Figure 31	Optimization of tissue slicing speed by altering cutting orientation	58
Figure 32	H&E staining reveals chronically unloaded tissue slices lose structural integrity	59
Figure 33	Cardiac tissue slices stained for structural and functional proteins	60
Figure 34	Injected cells can potentially improve cardiac function	64
Figure 35	CM induction from human ESC (hESC)	65
Figure 36	Time line and description of small molecule modulated induction	67
Figure 37	Induction of CM from hESC-HES2, iPSC, H9, and H7 via EB method	69
Figure 38	After 21 days of induction, CM were stained for cardiac specific markers	70
Figure 39	Induction of CM from ESC H9 via small molecule monolayer method	71
Figure 40	Human ESC-CMs (H9) stained from Cardiac Troponin I, ITGB4, and ITGB5	71
Figure 41	Summary of our work towards realizing Cardiac Cell Therapy	73

LIST OF TABLES

Table 1	Summary of cell sources as a potential for myocardial repair after infarction	9
Table 2	Oral Mucosa Epithelial Culture Conditions and Viability	22
Table 3	Design specification, constraints that guided the design and considerations taken for the DTSD 4s	37
Table 4	Preparation of 1 liter of cardioplegia solution	54
Table 5	Preparation of 1 liter of slicing solution (Tyrode's solution + 30 mM BDM)	55

LIST OF ABBREVIATIONS

Abbrev.	Word or Term
2D	2-Dimentional
3D	3-Dimentional
µm	Micrometer
AAS	Antibiotic Antimycotic Solution
AP	Alkaline phosphatase
BDM	2,3-Butanedione monoxime
bFGF	Basic fibroblast growth factor
BMMNC	Bone marrow mononuclear cells
BSA	Bovine serum albumin
c-myc	Cellular Myelocytomatosis
CA	California
CAD	Computer Aided Design
CAD	Coronary Artery Disease
CCU	Coronary Care Unit
CHD	Cardiac Heart Disease
CK 10	CytoKeratin 10
CK 13	CytoKeratin 13
CM	Cardiomyocytes
CMPC	Cardiomyocyte Progenitor Cell
COL 1	Type I Collagen
COL IV	Type IV Collagen
CPC	Cardiac Progenitor Cells
cTnT	Cardiac Troponin T
CVD	Cardiovascular Disease
DAPI	4′,6-diamidino-2-phenylindole
DBME	Dilute Beta-mercaptoethanol
DC	Direct Current
dH2O	Distilled Water
DIC	Digital Image Correlation
DMEM	Dulbecco's Modified Eagle Medium
DMEM/F-12	Gibco Dulbecco's Modified Eagle Medium: Nutrient Mixture F-12
DNA	Deoxyribonucleic acid
DTSD	Dynamic Tissue Stretching Device
EC	Endothelial cell
ECG	Electrocardiogram
ECM	Extracellular Matrix

EDV	End Diastolic Volume
EHT	Engineered Heart Tissues
EKG	Electrocardiogram
Endo	Endocardium
EOM	Epithelial Oral Mucosa
EPC	Endothelial Progenitor Cell
Epi	Epicardium
ESC	Embryonic Stem Cell
ESTRN	Strain
F	Force
FEA	Finite Element Analysis
FITC	Fluorescein isothiocyanate
FN	Fibronectin
g	Gram
G-CODE	Geometric – Code
Gel	Gelatin
HEPES	4-(2-hydroxyethyl)-1-piperazineethanesulfonic acid
hESC	Human Embryonic Stem Cell
hiPS	Human induced Pluripotent Stem
HiPSC	Human induced Pluripotent Stem Cell
iMEF	Inactivated Mouse Embryonic Fibroblast
iPSC	Induced Pluripotent Stem Cell
iPSC-CM	iPSC derived Cardiomyocyte
ITGB1	Integrin beta-1
klf-4	Kruppel-like factor 4
KOS	Klf4–Oct3/4–Sox2
kPa	Kilo Pascal
KSR	Knockout Serum Replacement
LASER	Light Amplification by Stimulated Emission of Radiation
LN	Laminin
M	Molar (concentration, Mole/Liter)
M4	Metric 4 (4 millimeter)
MB	Molecular Beacons
MEF	Mouse Embryonic Fibroblast
Mgel	Matrigel
MHC	Myosin heavy chain
MI	Myocardial infarction

Mid	Mid-myocardium
mL	Milliliter
mm	Millimeter
mM	Millimolar
MOI	Multiplicity of infection
MPS	Myocardial Perfusion Scintigraphy
MRI	Magnetic Resonance Imaging
MSC	Mesenchymal stem cells
N	Newton
NC	Numerical Control
NEAA	Non-Essential Amino Acids
NHLF	Normal Human Lung Fibroblast
NHLF-iPS	NHLF – Induced Pluripotent Stem
NS	Not Significant
OCT 3/4	Octamer-binding transcription factor 3/4
OME	Oral Mucosa Epithelial
PBS	Phosphate-buffered saline
PFA	Paraformaldehyde
PI	Physik Instrumente
PIV	Particle Image Velocimetry
PMMA	Poly(methyl methacrylate)
PSC	Pluripotent Stem Cell
RNA	Ribonucleic acid
SAAS	Software As A Server
SE	Standard Error
SeV	Sendai Virus
SkM	Skeletal muscle
Sox-2	Sex determining region Y-box 2
SSEA 4	Stage-specific embryonic antigen-4
STL	Standard Triangle Language
TfR	Transferrin receptor
URES	Resultant Displacement
USB	Universal Serial Bus
UVO	Ultraviolet-Ozone
VCAM	Vascular cell adhesion protein
VDC	Volts Direct Current
VEGF	Vascular endothelial growth factor

LIST OF SYMBOLS

Symbol	Definition
E	Elastic modulus
Δ	"The change in"
σ	Stress
ε	Strain
ν	Poisson's ratio
L_0	Initial length
$\sqrt{}$	Square root

ACKNOWLEDGMENTS

"Always give without remembering and always receive without forgetting." **Brian Tracy**

I would like to start by acknowledging my funding sources. The National Science Foundation (NSF) STC EBICS And UC Merced Graduate division Faculty mentor program.

I received tremendous support and insight from my committee members, and for that I am thankful. They helped guide my work by asking the right questions and providing advice when needed. My committee chair, Dr. Viney in particular, spent significant amount of time helping me think through some of the project challenges and teaching me his approach to problem solving.

The McCloskey lab has been good to me over the years, showering me with love and by treating me like the big brother in the lab. I was able to discus some of my work with a lot of them over the years and they have supported my work in various capacities. I would like to thank all members of the McCloskey lab past and present. In particular, I would like to thank the undergraduates who were directly involved in my project over the years and have significant contributions (Ian Buczko, Michael Brooks, Selasie De-Souza, Mohammed Amwas, Meer Mohamad, and Maha Zaman).

I would also like to extend my heartfelt gratitude to Dr. Saha and lab for graciously allowing me to use their vibratome, UC Merced machine shop (Ed Silva), School of Engineering instructional and prototyping lab (Dr. Neeraj Sharma, Salvador Diaz, Dr. Luke Reed), Merced Screw Products, and everyone directly involved in the process of developing my device.

The support I received from graduate division staff is considerable. They have treated me with respect and were extremely helpful navigating some of the administrative streets. Some have became good friends of mine (Tsu Ya, Jesus Cisneros, and Iqbal Atwal).

A lot of individuals on campus were on my corner over the years with encouragement, advice, friendship, and love. Tomiko Hale et al. from school of engineering, Dr. Teamrat Ghezzehei & Dr. Asmeret Berhe, Mr. Guillermo Rivas, Angela Winek et al. from UC Merced staff, and many others.

My life in Merced would not have been the same without Merced Pickup Soccer group, Minds in Motion Track Club, Northern California Oromo Community, and Tokkuummaa FC. They have greatly enhanced my wellbeing physically and mentally and they are big part of my sanity.

All my family and friends (too many to name all of you and you know who you are), thank you for your continued support, unconditional love and unwavering confidence in me. My foundation and my rock have been Emanuel Tefera, Fikerte Duguma, Adisalem Duguma (and family), Eba Amanuel (and family), Tsegab Amanuel, and Hawi Emanuel (plus Moti Daba).

I have no words to express the gratitude I have for my advisor Dr. Kara E. McCloskey. Thank you for the amazing opportunity and experience. I have learned a lot from you and I will use all of it in my future endeavors. The work I started under your guidance in a passion I want to continue to peruse for the rest of my life.

Last but not least, I would like to express my love for my lovely, feisty, sweet wife Mon'Leisha

Lynn Tefera, who was by my side before it all started, my little precious ones (Promise Rodriguez, Namari & Nalaali Tefera), and my acquired brother William Douandju. Thanks for tolerating me, supporting me and showing me a new kind of love.

CURRICULUM VITA

EDUCATION

Ph.D., Materials and Biomaterials Science and Engineering; University of California, Merced Dec, 2019
Advisor: Kara E. McCloskey

- Address challenges in cardiovascular tissue engineering, mainly regenerative medicine to enable *ex vivo* heart studies on stem cell differentiation, integration, and repair. Find suitable and novel cell sources for patient specific repair and developing model system that incorporates mechanical stimulation to enable long-term chronic studies.

M.S., Biological Engineering and Small-scale Technologies (BEST); University of California, Merced
May 2012

- Research: Finding functional information on the primary release site of Ca^{2+} from the SR of Cardiomyoctyes Techniques: Confocal microscope, electrical, and optical measurements of Action Potentials and Ca-Transients

B.S., Bioengineering with Honors; University of California, Merced
May 2009

- Undergraduate Research: Microfluidic aptamer array for multiplexed quantitative protein analysis. Center of Integrated Nanomechanical Systems (COINS) – University of California Berkley

AWARDS/FELLOWSHIPS

- Outstanding Graduate Student Award, 2018
- Outstanding Teaching Assistant Award, 2018
- Sara Collins Fernandis Award: Commitment to the Future, 2018
- EBICS Award, 2015-2016
- BEST Bobcat Award, 2015-2016
- Bobcat Travel Award; School of Engineering, UC Merced, 2015-2016
- Distinguished Leader Finalist, 2015
- UCM Faculty Mentor Research Fellow, 2013-2014
- NSF-funded STC Diversity Fellow, 2011 - 2013
- California Senate Pillar of Community Hope Leadership Award, 2013
- Certificate of Special Congressional Recognition, 2013
- California Stat Assembly Certificate of Recognition, 2013
- Pillar of the Community Lighthouse Keepers Award, 2013
- Commitment to the future: Recognition of engagement with students, 2013
- Dean's List, 2007-2009
- Chancellor's Honor List, 2007 – 2009
- National Society of Black Engineers (NSBE) Region 6 Academic Tech Bowl Championship team Captain, 2008

ADDITIONAL SKILLS DEVELOPMENT

NSF-Emergent Behaviors of Integrated Cellular Systems (EBICS) STC-Trainee, Spring 2013–present
EBICS Student Leadership Council (SLC) Spring 2013- Fall 2017
Certificate in General Pedagogy (CRTE) Mastering the classroom with 1st generation college students Spring 2015
Certificate of Completion, Undergraduate Learning Outcomes Assessment: Pedagogy and program Planning Fall 2014
NSF-Certificate of Completion Science: Becoming the Messenger, August 2014
McNair Scholars Program Graduate student advisor U.S. Department of Education funded program designed to encourage and prepare talented and eligible undergraduate students from low-income, first

generation, and/or historically underrepresented backgrounds to peruse doctoral studies through involvement in faculty mentored independent research, GRE training, graduate preparation seminars, leadership development, January – August 2012

Third annual McNair and SSS Best Practices and Professional Development Seminar, Long Beach California staff participant February 24-25, 2012

III Latin-American Postgraduate Program of Biophysics Workshop and biophysical Labs Federal University of Rio de Janeiro, August 30 – September 9, 2010

CITI Program training

Animal Skills Training

Center of Integrated Nanomechanical Systems (COINS) Intern, UC Berkeley Dr. Luke P. Lee Summer 2008

TEACHING EXPERIENCE

Teaching Assistant, UC Merced, Spring 2019. COGS 105: Research methods for cognitive scientists

Teaching Assistant, UC Merced, Spring 2016 – Fall 2018. ENGR 45: Introduction to Materials Science and Engineering

Teaching Assistant, UC Merced, Fall 2015. ENGR 65: Circuit Theory

Teaching Assistant, UC Merced, Fall 2014 - Spring 2015. ENGR 45: Introduction to Materials Science and Engineering

Teaching Assistant, UC Merced, Fall 2011. ENGR 155: Engineering Economic Analysis

Teaching Assistant, UC Merced, Fall 2011. ENGR 166: Digital and Analog Electronics

Tutor, UC Merced, Spring 2009. ENGR 45: Introduction to Materials Science and Engineering

SELECTED ORAL PRESENTATIONS

Tefera AE, Assessment of Student Learning and Developing Learning Pedagogy in a Penalty Free Environment*,* The third annual assessment and research symposium sharing practices, successes, and lessons learned, UC Merced, March 2016

Tefera AE, Assessment of Student Learning and Developing Learning Pedagogy in a Penalty Free Environment*,* the 2nd symposium on assessment of learning, UC Santa Cruz, November 2015

SELECTED INVITED LECTURES

Guest Lecturer: Cardiovascular Tissue Engineering; Dos Palos High school

Guest Lecturer: Introduction to Materials Science and Engineering (ENGR 45); UC Merced

Imperfections in solids, diffusion, mechanical properties of metals, dislocations and strengthening mechanisms, failure, phase diagram, polymer structure, characteristics, application and processing of polymers 2014-2018

Guest Lecturer: Tissue Engineering and Design (BIOE 114/BEST214); UC Merced

Time constant

Guest Lecturer: Physiology for Engineers (BIOE 100); UC Merced

Cardiac cellular and molecular physiology

POSTER PRESENTATIONS

Tefera AE, McCloskey KE. *Stretching Cardiac Tissue: Towards ex-vivo studies on stem cell differentiation, integration, and repair*, EBICS annual retreat, University of Illinois Urbana Champaign. June 24, 2014

Tefera AE, Lee LP. Microfluidic Aptamer array for multiplexed quantitative protein analysis, NSBE National convention, Las Vegas Nevada. March 2009

Tefera AE, Lee LP. Microfluidic Aptamer array for multiplexed quantitative protein analysis, California Alliance for Minority Participation in Science (CAMP) undergraduate research symposium, UC, Irvine. February 2009

SERVICE, OUTREACH AND MENTORING EXPERIENCE

- **Graduate Student Mentor: Mentoring Undergraduate students in research skills,** 2009 – Present

- **African Student Union UC Merced Chapter Faculty Advisor,** Advice, coach, mentor student leaders to achieve their potential and highly involved in conflict resolution Spring 2013 – Spring 2019
- **Competitive Edge Summer Bridge Program: Adjusting to graduate school panel,** July 2016
- **National Society of Black Engineers (NSBE) graduate student mentor,** mentor, motivate, and inspire 2009 – 2014
- **Graduate Student Association (GSA) Delegate to BEST group,** bridge the gap between leadership and graduate group 2013 – 2014
- **Graduate Student Association (GSA) Delegate to BEST group,**
- **African Student union UC Merced Chapter Founding member,** 2011
- **Graduate Student recruitment rep and chaperon NSBE 36th annual National convention,** Toronto ON march 31-April 4 2010
- **Graduate Student recruitment rep and chaperon NSBE Fall Regional conference for Region VI,** Long Beach CA. Nov 20 – 22, 2009
- **National Society of Black Engineers (NSBE) Chapter inter club council chair,** 2008 – 2009
- **Engineering Service Learning Sub Team Leader,** 2008 – 2009
- **Vanguard Engineering Student Organization Rep.,** 2007 – 2009
- **National Society of Black Engineers (NSBE) Chapter Vice President,** 2007 – 2008

ABSTRACT

Enabling *Ex Vivo* Heart Studies On Stem Cell Differentiation, Integration, And Repair

By

Anley E. Tefera

In

Materials and Biomaterials Science and Engineering

UNIVERSITY OF CALIFORNIA, MERCED

Research Committee

Professor Christopher Viney – Chair
Professor Valerie Leppert
Professor Changqing Li
Professor Kara McCloskey – Primary Advisor

2019

Cardiovascular diseases remain the leading causes of death, affecting one in three adults worldwide. The most common form of cardiovascular disease is the coronary heart disease (CHD)[1], which can lead to a myocardial infarction (MI), or heart attack. The heart does not contain a significant pool of endogenous stem cells for intrinsic regeneration and is, therefore, incapable of repairing itself. Stem cell therapy can potentially improve heart function after MI; however, it is difficult to conduct controlled studies on cell and tissue integration of *in vivo* MI models. Therefore, there is a need for an *ex vivo* model that can help assess the survival, differentiation, and integration of injected cells. Here, I first generate induced pluripotent stem cells (iPSC) from a non-invasive cell source by first establishing a stable cell culture system for these cells. I then developed a tissue-stretching device that is able to secure fragile heart tissue slices and provide uniaxial cyclic mechanical stimulation to cardiac tissue slices that will preserve their native physiology for up to 3 months. Tissue slices supported with device for 10 days show over 50% improvement in cxn43 expression and display higher alignment compared with slices that are unloaded. Lastly, I differentiated PSCs into cardiomyocyte cells and have verified that laminin and fibronectin matrix direct high number of cardiac cells containing distinct ITGB4 and ITGB5 cell populations. The *ex vivo* tissue model developed will enable longer-term studies of cell and tissue grafting onto the heart.

Chapter 1. Introduction

1.1 Background

Over the last one hundred years, life expectancy and quality of life in the western world has seen significant improvement as a result of advancement in prevention and treatment of two human diseases. The first revolutionary success story is elimination and reduction of infections diseases via public health measures and drug developments. The second, decline in cardiovascular disease consequences, was driven by innovations in procedures and operation for acute diseases and the discovery and implementation of drugs for long-term use. Since the 1970s, age adjusted death rate from cardiovascular disease (CVD) has seen a significant decline [2][Figure 1].

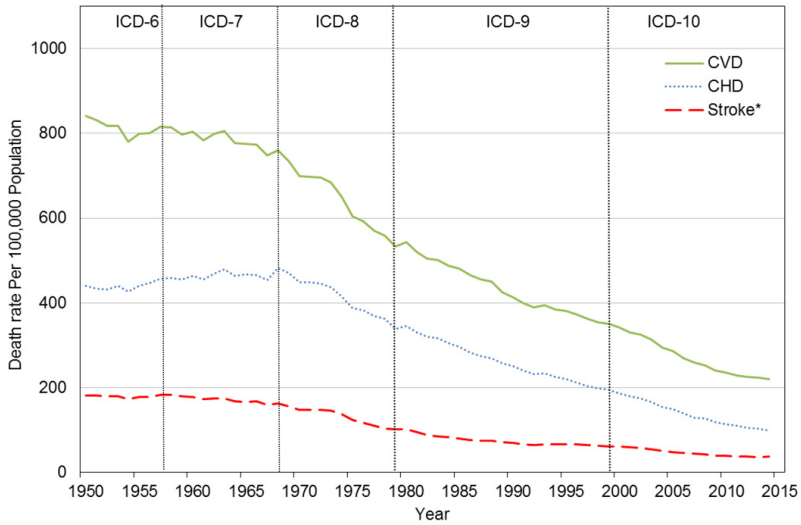

Figure 1: Percentage change in age adjusted death rate from CVD, Non-CVD, and Stroke in the United States since 1950. The decline of coronary heart disease started approximately in 1970 and by 2015 it has declined by over 75 percent.

Unfortunately, cardiovascular diseases still remain the leading causes of death, affecting one in three adults worldwide. It accounts for over 800,000 deaths annually in the US claiming about 2300 American lives each day (1 death every 40 seconds) and well over 300 billion dollars of economic burden to our nation every year, which is expected to more than double in the next two decades projected to cost over one trillion dollars in 2035. According to 2015 data from center for disease control & prevention, cardiovascular diseases claim comparable number of lives as all forms of cancer and chronic lower respiratory diseases combined each year [Figure 2]. At any given moment, over 90 million American adults are living with some form of cardiovascular disease. It accounts for approximately 18 million deaths every year worldwide with the number that is expected to increase by 33% in a little over a

decade[3].

The most common form of cardiovascular disease is the coronary heart disease (CHD)[1], which is defined by thrombosis (build up clots around raptured plaque) on inner walls of coronary arteries, impeding flow of blood to downstream areas of cardiac muscle walls. These obstructions lead to perfusion imbalance and hinder oxygen and nutrient delivery to the heart muscle leading to myocardial hypoxia and accumulation of waste metabolites [4, 5]. If the blockage is severe enough, or if the thrombosis breaks off the artery and moves through circulation, it can lead to a Myocardial Infarction (MI). An MI, commonly referred to as a heart attack, starves the heart tissue of oxygen for a period of time, and subsequent damage and remodeling can often lead to progression towards heart failure. Heart failure is the final clinical manifestation of a variety of cardiovascular diseases where the heart fails to pump enough blood to meet demands of the body. Furthermore, those who survive an ischemic heart event are left with permanent scar tissue.

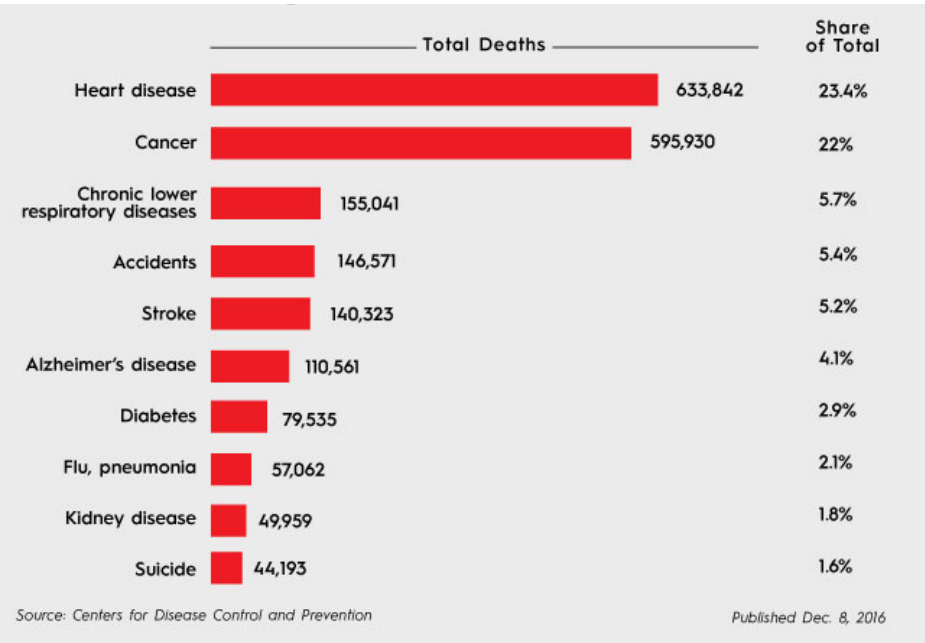

Figure 2: 2015 data on leading causes of death in the United States. Heart disease continues to kill more Americans than any other cause.

The heart is traditionally considered as an organ incapable of repairing itself since it is unable to effectively regenerate after notable injury, as it does not contain a significant pool of endogenous stem, or reserve cells[6, 7]. Treatments of heart attack over the last century have been palliative, focused on managing, reducing, or preventing further damages to the heart and fail to address the underlying problem: loss of functional cardiomyocytes and lack of replacement and/or repair therapies. The current gold

standard therapy that is curative that addresses the underlying problem of CM death is heart transplant, but it is limited by donor supply, organ mismatch, and immunosuppression. At any given time, there are ten times more patients who would benefit from cardiac transplantation than available donor hearts. In addition, this gold standard treatment's long-term prognosis is disappointing at best with marginal improvement of quality of life and pedestrian promise for long term survival. Given these facts, much attention has recently been directed at regenerative medicine using cell transplantation approaches as an alternative strategy to address the underlying problem of CM loss and restore cardiac functions in failing hearts. Despite an abundance of research manpower and funding towards this approach, a cost effective and robust solution for replacing or repairing post infarct scar tissue is far from patient use.

1.1.1 Cardiovascular Diseases (CVDs)

The cardiovascular system, an organ system composed of two pumps in series (the heart with right and left chambers), ascending & descending tubes (blood vessels), and fluid (blood) is responsible to circulate blood throughout the body to supply essential nutrients and oxygen to cells and tissues and remove metabolic waste from the body. It facilitates the body's ability to fight diseases, maintain homeostasis, and provide nourishment. Unfortunately, this remarkable system is prone to assaults and breakdowns from variety of factors that are genetic and non-genetic mishaps referred collectively as cardiovascular diseases (CVD)[8]. CVD, a condition that has been affecting human lives for thousands of years, results from abnormal function of the heart and the blood vessels[9]. Over the past several decades, U.S age adjusted mortality from CVD has greatly declined with increased understanding and development of technology to prevent, diagnose, and treat CVD[8]. However, to date, CVD remains to be the leading cause of disability and death worldwide claiming approximately 20 million lives a year (one in three deaths). In addition, the economic burden is estimated to be over three hundred billion dollars in direct and indirect costs each year in the United States alone [1, 10]. To combat heart disease, the first line of defense is to incorporate healthy lifestyle choices in our daily lives. However, often the disease only manifests after an artery has already clogged to cause perfusion imbalance in down stream tissue causing ischemia.

MI is the major manifestation of CVDs: Coronary heart disease (CHD) also called coronary artery disease (CAD) is the major contributor to cardiovascular morbidity and mortality accounting for 60% - 80% of all deaths. Other types of CVD include hypertension, stroke, congestive heart failure, peripheral artery disease, aortic aneurysm, and other cardiovascular disorders (tumor of the heart, cardiomyopathy). CHD is a reduction of blood flow to an area of cardiac muscle wall due to atherosclerosis (thrombosis that forms around ruptured plaque) on inner walls (lumen) of coronary arteries, impeding the flow of blood to downstream areas of cardiac muscle walls [Figure 3A].

These obstructions will not only cause a perfusion imbalance, but will also hinder oxygen and nutrient delivery to the affected areas leading to myocardial

hypoxia and accumulation of waste metabolites[5]. Partial occlusion of arteries will lead to ischemic angina, and if ischemic assault is severe enough (a complete cut off of blood supply), it will cause contractile dysfunction as in a stunned myocardium and ultimately irreversible narcosis of functional cardiac cells causing (MI). Failure of endogenous repair mechanism will evoke a secondary mechanism resulting in scar formation. The subsequent compensation efforts and remodeling of the affected area will lead to heart wall thinning [Figure 3B & C] and will eventually lead to heart failure.

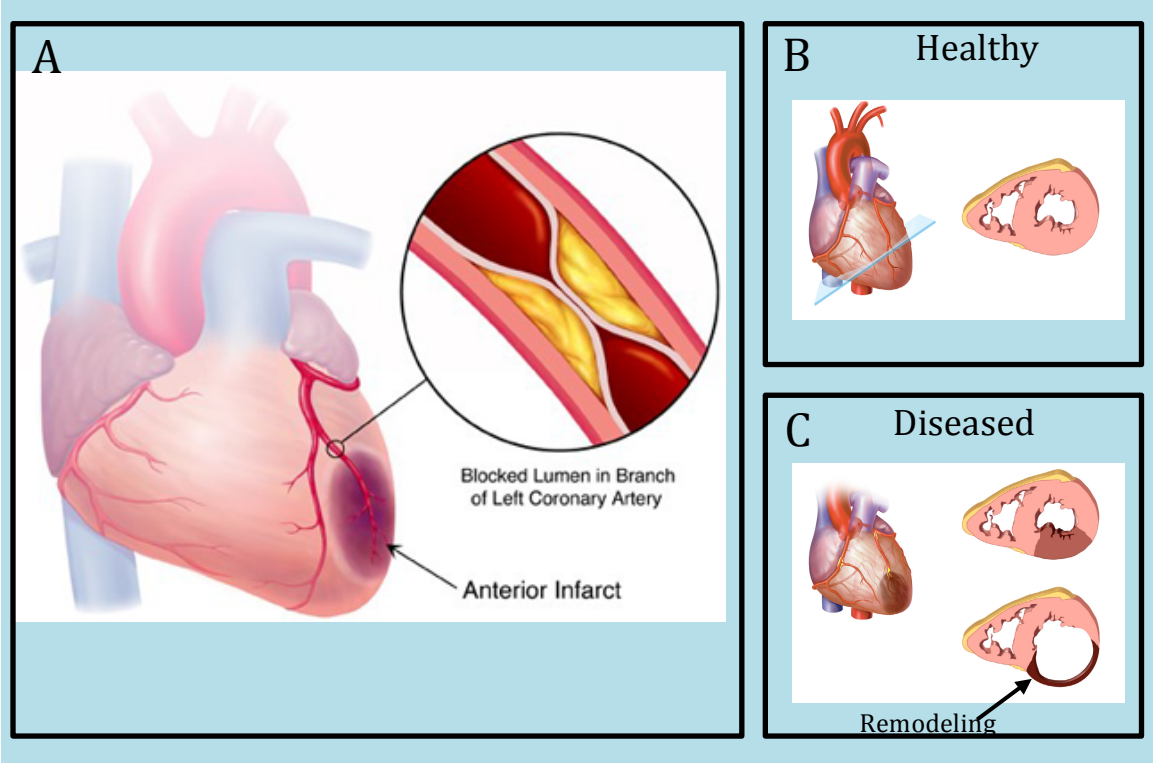

Figure 3: Myocardial infarction (MI), or a heart attack is caused by occlusion of a coronary artery by atherosclerosis. A) The imbalance of perfusion (ischemic conditions) will cause myocardial cells downstream from the occlusion to undergo necrosis. Limited capacity of adult heart regeneration will lead to scar formation and remodeling of the heart. B) Cross section of a healthy heart. C) Cross section of a diseased remodeled heart with thinning ventricular wall.

Myocardial infarction (MI) can often lead to progression towards heart failure. Because the heart does not contain a significant pool of endogenous stem, or reserve cells, it is unable to effectively regenerate after injury[11]. The subsequent changes in the workload of the heart may, if the infarct is large enough, deteriorate further leading to congestive heart failure. By 2030, CVD are projected (by world health organization[12]) to remain the single leading cause of death. There are various methods to diagnose MI: however, a combination of diagnostics efforts surely yields a more definitive determination. One method is an indirect but qualitative functional diagnosis using time-course electrocardiography to noninvasively identify

pathological conditions such as infarct expansion and infarct size. In addition, novel imaging techniques such as coronary angiography, myocardial perfusion scintigraphy (MPS), and magnetic resonance imaging (MRI) can also be utilized to examine myocyte viability, cardiac wall thickness, cardiac perfusion, and other morphological defects/changes of the heart. The increase in the level of biomarkers such as cardiac troponin T (cTnT), a protein of the contractile apparatus unique to cardiomyocytes, is indicative of myocardial narcosis and can be used as a diagnostic tool.

1.1.2 Treatment History

There are numerous pathophysiologies that can lead to damaged ventricular wall and hinder the heart's performance. Pharmaceutical agents along with healthy eating and regular exercise play a major role in prevention of the genesis of atheroma and thrombosis. There has also been a great deal of research into cardiac physiology, pathology, and development of experimental and/or therapeutic devices to treat MI. In addition, the development of accurate diagnostic imaging tools has contributed to improved assessments of heart function. The treatment of MI has greatly evolved over the last century as summarized in Figure 4. In much of the last century (1912-1962) physicians recognized the importance of absolute bed rest and used it as a foundation for their treatment of MI. This strategy improved the conditions of some patients with ischemic hearts by decreasing the workload; hence decreasing demand for oxygen and nutrients.

However, the high death rate among patients with damaged cardiac walls coupled with the fact that MI leads to other complications such as arrhythmias along with the development of electrocardiogram (ECG, EKG) prompted the transition to the next treatment phase. During this time, MI could only be definitively diagnosed on the autopsy table.

The following years (1961-74) saw the development of coronary care unit (CCU) to provide special care for heart patients. Combination of trained personnel and availability of medical gadgets reduced death rates from subsequent complications like arrhythmias but death due to heart failure caused by myocardial narcosis remained the same. Should a serious arrhythmia occur, staffs trained in closed chest resuscitation and/or external defibrillation were able to respond immediately. Unfortunately, coronary artery obstructions and occlusions will always result in perfusion imbalance and growth of infarcted area. Animal studies demonstrated that altering the oxygen demand of an infarcted heart or reperfusion of the ischemic area can potentially have a positive effect. Therefore, efforts were focused on reperfusion of damaged area by agents that open up the occluded artery or by surgeries that bypass the blockage. To offset reperfusion injury caused by sudden change in the environment, the damaged area is often preconditioned before treatment[13]. As a last resort, organ transplant is a feasible and currently a gold standard option, but limited supply of donors, organ mismatch, and complications

associated with immunosuppressant drug regiments beg for better solutions. With all the above-mentioned treatments, the underlying problem still remains: the lack of contractile heart muscle. The future aims to address this predicament by utilizing special cells that are able to renew themselves and can be directed to give rise to other types of cells including cardiomyocytes.

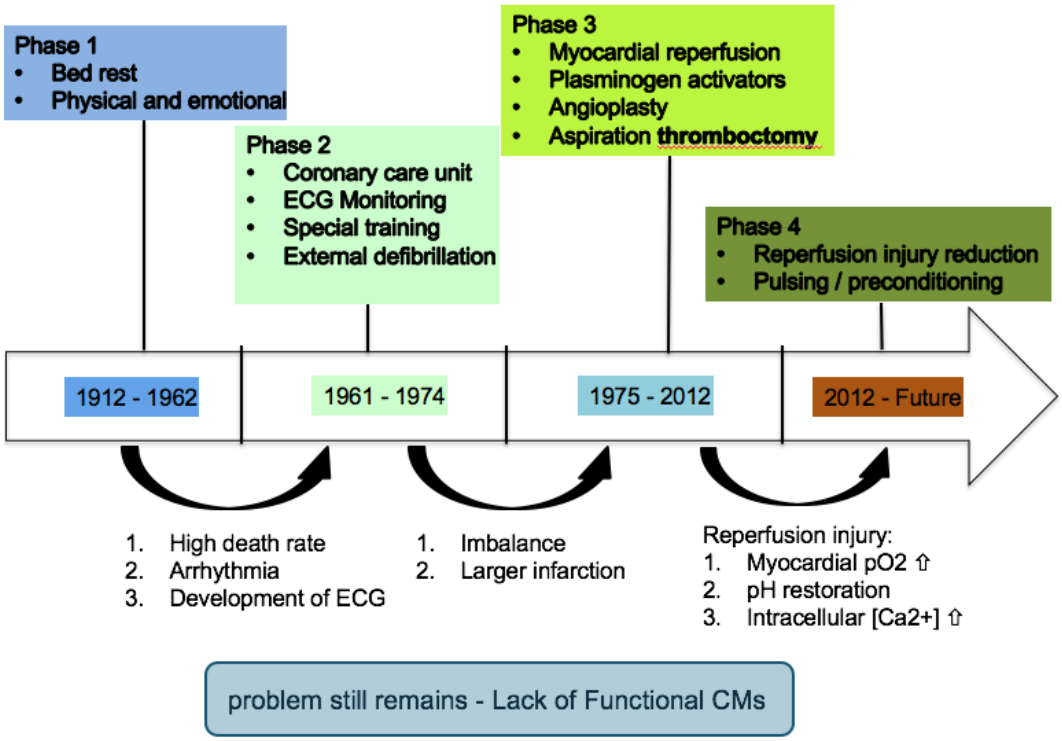

Figure 4: History of myocardial infarction (MI) treatment over the last 100 years. In phase 1, complete rest alleviated patient pain by reducing the workload (oxygen demand) of heart walls. However, it did not help reduce the development of arrhythmias and death rate. That brought about phase 2, where trained and well-equipped professionals were monitoring and treating patients. Since the perfusion to infarcted area remains impeded, the damage gets bigger calling for interventions of Phase 3. With flow restoration sudden change of environment preconditioning was required, phase 4. The future aims to address the underlying problem: replacing or repairing the damaged area with cells with regeneration potential.

1.1.3 Stem Cell Based Cardiac Therapy

In stem cell transplantation, stem cells are introduced into damaged areas of a tissue to treat disease or mitigate injuries. Cell therapy can potentially improve heart function after MI, but there remains the question of proper cell source accompanied with sufficient derivation and/or purification methodologies for cardiac cells [14]. Pluripotent stem cells (PSCs) including: multipotent adult stem cells, embryonic stem cells (ESCs) and induced-pluripotent stem (iPS) cells have emerged as a

promising therapeutic options for repairing cardiac damage. However, successful cell therapy of the myocardium is yet to be realized due to lack of efficient delivery methods to enable the integration and post implantation survival of *in vitro*-derived CM. Moreover, various methods for generating CMs from PSCs have been reported (reviewed in[15]), but these methods still produce heterogeneous mixtures of CMs and non-CMs cells (other cell types and undifferentiated cells). Therefore, it is vital to seek various non-genetic CM purification methodologies that can be used to enrich purified CMs. Non-genetic methods are desired not only for the ease of process but also to avoid undesirable results, solving the major problem in clinical use of PSC derived CMs. Methodologies that require genetic modifications are accompanied by several risk factors and complications that include, but are not limited to, incompatibility with clinical use, potentially silenced extrinsic genes, need for species specific constructs, possibility of tumor formation & genetic instability, and cumbersome integration process. It is extremely clear and important that non-genetic methods for purification are necessary for clinical applications of PSC derived CMs to repair MI. Non-genetic purifications have been shown to yield higher percentages of CM using CM-specific molecular beacons (MBs)[16], CM-specific surface markers such as VCAM-1[17], and other metabolic/ morphology differences between CM and non-CM[18-21]. Even before the stages of derivation and injection for integration, we are faced with a challenge of choosing suitable and non-controversial cell source for regeneration therapy.

Cell Source: There are two mechanisms of utilizing stem cells in cardiac repair: a myogenic strategy and a vascular strategy. A myogenic strategy injects either stem cells, which may differentiate into CM *in vivo*, or stem cell-derived CM directly in the heart[22-29]. An angiogenic or vascular strategy injects stem cells that can differentiate into cardiovascular cell types to promote angiogenic processes and increase neovascularization[30-32]. Various sources of adult stem cells have been studied in preclinical models and early-stage clinical trials (summarized in Table 1 and Figure 6), including human bone marrow-derived mononuclear cells (BMMNC), human skeletal muscle myoblasts (SkM), human mesenchymal stem cells (MSC), endothelial progenitor cells (EPC) and cardiac progenitor cells (CPC) [28-31, 33-35].

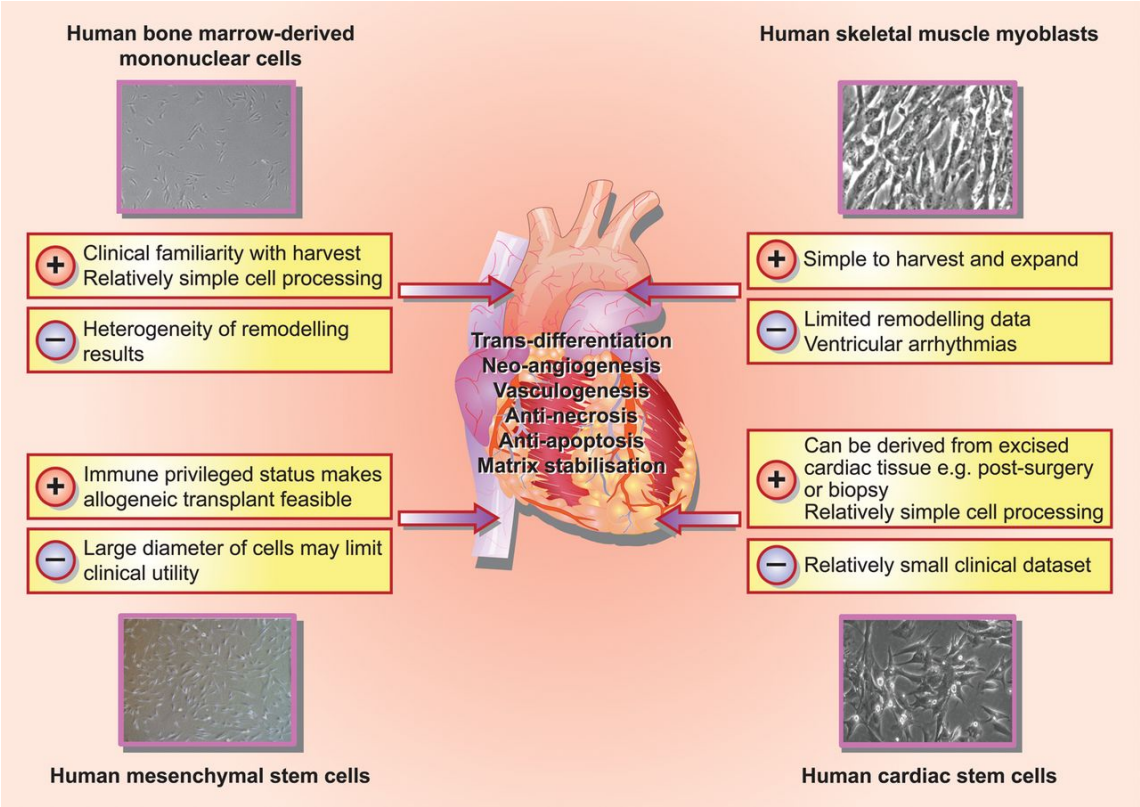

Figure 5: Adult stem cell sources for cell based regenerative medicine. Potential for repairing damaged tissue is not only limited to differentiating to cardiac cells but also other mechanisms such as angiogenesis and anti-necrosis. Their downside hinders them from being the cell source for clinical purposes.

Potential and early results of successful engraftment in injured hearts, has made cell transplantation using these adult donor cells attractive and realistic for treating cardiac diseases. These adult stem cells could be autologous, and therefore currently the only cells used in clinical studies. Unfortunately, most of these cells exhibit only limited proliferation potential, and/or plasticity to differentiate into cardiac cells, and are not significantly repairing the heart muscle. Though human bone marrow-derived stem cells are the most frequently used cell product in cardiac stem cell transplantation because of relatively simple cell processing and clinical familiarity with harvest, their heterogeneous population renders heterogeneity of remodeling results.

Table 1: Summary of cell sources as a potential for myocardial repair after infarction.

Cell sources for Cardiac Repair			
Cell Source	**Origin**	**Clinical potential**	**Limit of clinical potential**
Embryonic Stem Cells (ESC)	Inner cell mass of pre implantation blastocyst	Able to generate CMs [36, 37]	Ethical issues and teratoma formation [38]
Induced Pluripotent Stem Cells (iPSC)	Reprogrammed somatic cells[39]	Patient specific autologous grafts, generate CMs [40]	Low efficiency, reprogramming time and tumorigenic
Cardiac Stem Cells	Special niches in the myocardium [41]	Expand *ex vivo*, reduced tumor formation	Highly invasive procurement
Mesenchymal stem cells	Bone marrow, adipose tissue	Easy and safe to acquire and expand in culture	Large heterogeneity and not able to generate CMs
Endothelial progenitor cells	Bone marrow, peripheral blood	Important in neovasculogen esis	Heterogeneity and small population
Skeletal myoblasts	Between sarcolemma and basement membrane of muscle	Resistance to ischemia, no teratoma formation	Potential for arrhythmias and not Cardiogenic
Hematopoietic Stem Cells	Bone marrow, peripheral blood	Easy and safe to isolate	No true CM differentiat ion

Similarly, skeletal muscle satellite cells, progenitor cells resident within the skeletal muscle, were originally utilized extensively in cell based cardiac repair therapies because of their relative ease in harvesting and expansion *in vitro*. They were the pioneer cell type used in clinical trials as a result of their relatively superior success in preclinical studies, higher survival after implantation, and permit autologous transplantation in addition to the above mentioned ease of harvesting and expanding *in vitro*. However, there are limited remodeling data on outcome of such transplantations with apparent ventricular arrhythmia where the donor cells with skeletal background clearly show a different electrical property from host cardiac cells. Indicating that skeletal myoblasts do not readily transdifferentiate into CMs and remain committed to their parent skeletal lineage. Furthermore, MSCs can be expanded in culture and have the ability to differentiate into cells of mesenchymal origin *in vitro*. Under suitable conditions, even though it is at an extremely low rate, they are shown to differentiate into CMs *in vitro* or *in vivo* if injected into diseased animal infarct model. Interestingly,

therapy with EPCs has shown improved cardiac function but it is more likely that the cells are contributing in promoting angiogenesis rather than differentiating towards Cardiac lineage. Perhaps the more plausible adult stem cell for cardiac cell therapy is the resident CPCs. Several investigators have identified these resident cells with capacity to differentiate into CMs. The usage of these CPCs to repair cardiac infarctions though logical, no one is yet to identify a single population with a known niche with consistent phenotype to be used for clinical treatments.

In contrast, human ESC, multipotent cells isolated from blastocyst-stage preimplantation embryos, can be expanded *in vitro* while maintaining the potential to differentiate into all three embryonic germ layers; ectoderm, endoderm and mesoderm. Therefore, their extensive capacity for differentiation has garnered tremendous interest for their use in regenerative medicine and revolutionized the field by allowing the establishment of therapeutic solutions for several life-threatening disorders. Since their derivation in the late 1900s, they offered significant contribution by presenting models that could be closer to *in vivo* than any other available platforms. ESCs have been instrumental in advancement of disease treatments, drug discoveries, and mechanistic studies of pathologies. However, the procedure by which they are obtained and manipulated for use has engaged scientists and skeptics in an intense ethical and social debate because it mainly involves destroying embryos. Furthermore, even though teratoma formation is considered an important indicator of ESC pluripotency, the ability of these cells to form cancerous phenotypes introduces a potential concern for their use in cell-based therapy. These risks are further augmented by the fact that ESC is not patient specific. They were found to elicit immune response and may serve as major graft rejection antigens to the immune system of allogeneic hosts since they do not originate from individuals in need of interventions.

In the mid 2000s, the Yamanaka group showed that stem cells with properties similar to ES cells could be generated by ectopic expression of four genes in mouse fibroblasts and called them induced pluripotent stem cells (iPSC). Human induced pluripotent stem (hiPS) cells were first generated from dermal fibroblast by overexpression of oct 3/4, sox-2, klf4, c-myc, called yamanaka factors, in 2006. Even though fibroblasts are easy to maintain and expand in culture, their relatively low reprogramming efficiency and requirement of uncomfortable biopsies has prompted researchers to search for alternative sources [42]. Since then others have showed that these ESC like pluripotent cells could similarly be reprogrammed from other somatic cells. The other important challenge is the choice of a superior reprogramming method, as some methods leave unwanted “footprint” in the reprogrammed pluripotent cells. In the early days, integration of the reprogramming factors into the genome by retroviral or lentiviral transductions were also utilized [43]. The use of these integrating viruses may carry an oncogenic potential to the patient, resulting in iPS cells that are not safe to use as cell therapies. To avoid these, alternative reprogramming methods have been developed in recent years that use plasmids [44, 45], temperature sensitive Sendai viruses [46], small molecules [47, 48], and modified RNA [49]. CytoTune-iPS reprograming system that uses replication incompetent Sendai virus (SeV) to safely deliver and express the

yamanaka genetic factors required for reprogramming a somatic cell back into a pluripotent stem cell is utilized for this study. Like ESC, human iPSC can be expanded *in vitro* while maintaining the potential to differentiate into all three embryonic germ layers including the ability to differentiate into functional CMs, and thus iPS cells are a viable option as an autologous cell source for cardiac repair [50]. Fortunately, the usage of iPSC for cell based therapy circumvents the intense ethical debate triggered by ESC. However, the main advantage of iPSC over ESC is the possibility to generate patient-specific pluripotent stem cells, thus avoiding the risk of immune rejection. This procedure is time-consuming and may preclude its wide use for treating acute myocardial infarction [32]. Since then, over 37 clinical trials have explored the potential for injected pluripotent and derived cells to aid in preventing heart failure [51]. Although these treatments have shown mild improvement, the low retention rate of introduced cells suggests this is due mainly to an increase in vascularization to the infarcted area, as well as paracrine signaling, for host cardiac cell survival, and not a regeneration of the heart muscle tissue.

1.1.4 Tissue Slice As a Model

Adult hearts have inadequate pool of endogenous stem cells; therefore, mature cardiac cells exhibit only limited proliferative capabilities after injury. Derivation of CM from stem cells is a critical aspect in future strategies of heart repair; however, direct injection of cells alone is not sufficient [5]. Additional challenges in cardiovascular tissue engineering include packaging these cells in a manner that enables effective delivery of densely-packed cells, survival of the cells as well as host integration, and then facilitating vascularization of the implant to meet the high oxygen and nutrient demands of newly constructed tissue. To understand the repair mechanism and/or assess contribution of each factor mentioned above to functional improvements observed during cell therapy, an *ex vivo* model that mimics physiological cardiac niche simultaneously rendering the experimentalist a precisely controlled electromechanical environment is almost a requirement. With lack of adequate *in vitro* tissue explants it is difficult to examine potential therapeutic solutions for MI. Cell-based transplantation models have been useful in understanding and defining many aspects of cardiac function [52, 53]. However, under physiological conditions, cardiac cells are coupled to each other electrically, mechanically and metabolically. Therefore, use of a multi-cellular tissue is a more relevant model that will provide a similar physiological environment as a whole intact heart.

Organotypic tissue slices have been utilized and proven useful as a model in many organ systems such as the brain [54], kidney [55], and liver [56]. In recent years, cardiac tissue slice preparations has also showed promising potential as it has the desired balance between simplicity and accurate representation of physiological niche. Like coronary perfused heart preparations, slices contain all physiologically relevant cell types and architecture that isolated primary cells do not have, but are simple enough for better control than perfused heart preparations. Cardiac tissue slices preserve the native tissue

environment, permitting cells to have physiological contacts with the extracellular matrix and intercellular communications. In recent years, it has been validated through multi-electrode measurements that slice from mouse, guinea pigs, rabbit, and others exhibit similar electrophysiology to the intact heart. Similarly, pharmacology studies revealed similar effects in slices versus coronary perfused preparations. However, organotypic studies employing *in vitro* culture of human cardiac tissue slices have observed a significant and rapid decline in force generation over 1 month of culture [57]. To address this predicament it is necessary to incorporate a dynamic *ex vivo* parameter to stimulate slices and keep the preparations active. The active model could maintain physiology of slice and could potential serve as a model to examine graft-tissue integration and maturation of human iPSC-CMs.

1.1.5 Mechanical Stimulation

Mechanical forces are significant in all cell types, especially in dynamic organ such as the heart. Under physiological condition, the myocardium undergoes stress with every heartbeat. When the heart muscle is stretched (increased end diastolic volume (EDV)), its force of contraction increases according to the Frank-Sterling law. Human ESC and iPSC-derived CM express fetal-like spontaneous contraction, ion channel expression [58], electrical propagation [59], and physical characteristics. In order to further CM maturation, researchers are beginning to engineer stem cell microenvironments that incorporate mechanical signals along with cell-cell contacts and soluble growth factors that have been previously optimized [60, 61]. Over the past five years, it has become increasingly apparent that mechanical signaling is a critical component of this cardiovascular microenvironment. Mechanical loading has a dramatic effect on the ECM production of CM [62], increases intracellular protein content [63], as well as their cytoskeletal organization, alignment, and proliferation [64]. Therefore, a number of groups have begun using micromanipulation devices for stretching cardiac cells (reviewed in [65]). Specifically, when cyclic strain was applied to stem cell-derived CM, the fetal-like CM exhibited elevated cardiac markers. When implanted into a mouse, stretched cells also had less scar tissue formation, lower apoptotic activity, higher VEGF expression, and increased angiogenic activity [66].

External load plays a critical role in determining muscle mass and its phenotype in CM. They have the ability to sense mechanical stretch and convert it into intracellular growth signals, which lead to hypertrophy. Mechanical stretch of CM *in vitro* increases calcium sensitivity of the heart's contractile machinery and causes activation of multiple second messenger systems that are very similar to growth factor-induced cell signaling systems. Another significant component of heart tissue is the micro and nano extracellular architecture. Mature adult cardiomyocytes (CM) exhibit an elongated rod-like shape, and contain well-developed contractile apparatus with intercalated discs as electromechanical cell end-to-end couplings. Existence of an organized contractile apparatus in cardiac cells can be identified by the striated pattern observed after staining for contractile proteins. Gap junctions, located in intercalated discs at the ends of cardiac

cells, are responsible for rapid propagation of electrical signals between cells. However, in standard tissue culture set-ups, CMs will often undergo dedifferentiation and lose many of these key physiological features, including their elongated shape and defined contractile apparatus. It is thought that the dedifferentiation is due to the lack of appropriate micro-environmental cues in prolonged cultures. It has been shown that alignment of cardiac cells, not only helps limit cell dedifferentiation by increasing the continuity of cell-to-cell connections, but also has a profound effect on impulse initiation and propagation velocities [67]. Moreover, cell culture systems that additionally provide signals to induce anatomical anisotropy of cardiac cells leads to larger cellular coupling resistance in the transverse (along short cell axis) compared with the longitudinal (along long cell axis) direction, resulting in a smaller velocity, but larger maximum slope of action potential upstroke [67]. Mimicking the heart's unique topographical signals induces alignment of both CM[68] and endothelial cells (EC) [69], facilitating more uniform electrical propagation and subsequent mechanical contraction of the heart cells [68].

1.2 Goals and Overview of The Dissertation

Cardiovascular diseases are leading causes of death and hospitalization, affecting one in three adults worldwide. It claims more lives than all forms of cancer and chronic lower respiratory diseases combined each year. At any given moment, over 90 million Americans are living with some form of cardiovascular disease. Ultimately, the underline cause of heat failure is irreversible narcosis of functional cardiac cells causing myocardial infarction. The heart does not contain a significant pool of endogenous stem cells and is unable to effectively regenerate after injury. The subsequent changes in the workload of the heart may deteriorate further leading to heart failure. Stem cell transplantation is a therapeutic strategy that has potential in replacing damaged or lost myocardial tissue and restoring cardiac function. Because of this potential, immense resources and intensive efforts have been invested in developing stem cell based strategies for cardiac repair. Various types of stem cells are currently being investigated for their potential in preclinical studies and some early stage clinical trials. Compared to adult stem cells with limited plasticity and in some cases low availability, embryonic stem cells (ESC) have proven to be a promising alternative population for cardiac repair. They theoretically possess extensive capacity to differentiate into all three embryonic germ layers as well as self-renew and most importantly they can be isolated and expanded *in vitro* using well established protocols. In addition, donor ESC derived CMs are viable cells that can functionally integrate with recipient organ attracting interest for their use in regenerative medicine.

Like ESC, human iPSC can differentiate into functional CMs, and thus iPS cells are a viable option as an autologous cell source for cardiac repair. The main advantage of iPSC over ESC is the possibility to generate patient-specific pluripotent stem cells for application to personalized therapy, thus avoiding risk of immune rejection. Furthermore, iPSCs circumvent many of the ethical concerns

associated with use of embryonic material, garnering them an ideal candidate for cell-based regenerative medicine. However, method of acquisition of starting somatic cell for reprogramming is one of the major drawbacks for utilizing iPSCs. For example, dermal fibroblast is readily available and relatively easy to isolate and expand in culture. However, its extraction requires painful process of invasive skin biopsy. Interestingly, more studies have been emerging presenting better alternative starting material for reprogramming. Although cells isolated from blood samples, urine, mesenchymal stromal cells from wisdom teeth, and others show promising characteristics for reprograming strategy, a simple, non invasive, and pain free extraction of starting somatic cell will make iPSC a more attractive option especially for the young and elderly population.

In addition, it is expensive and challenging to conduct controlled studies of graft cells or tissue integration in current *in vivo* MI models even if potential for cell and tissue therapy to improve heart function after MI is evident. It is difficult to identify precise repair mechanism in the absence of *in vitro* models that allow long-term assessment of transplanted cells. Clearly, there is a need for *ex vivo* model that can facilitate assessment of survival, differentiation, and integration of injected donor cells. Organotypic tissue slice cultures have been widely utilized as a platform to study diverse mechanisms in various organs such as liver [70], brain (Reviewed [71]), and kidney [72]. In the past decade, living cardiac tissue slices are becoming increasingly popular as a platform to study the heart and supplement findings from isolated cell, co-cultures, and perfused whole/wedge heart preparations [57, 73-76]. These slice preparations preserve the native tissue environment with intact cell to cell and cell to matrix electrical and mechanical communications and have been shown [in slices from various animals] to exhibit similar electrophysiology to the intact heart. They have several advantages as they only present moderate complexity and allow the experimentalist reasonable control while possessing all cell types found in the native tissue. Although these living cardiac tissue slice preparations have previously shown robust survivability in culture, significant mechanical and electrophysiological remodeling has been observed in long-term cultures [57].

Our cardiovascular tissue engineering laboratory is utilizing cells with promising results as a potential to literally mend broken hearts and contribute to advancement of regenerative medicine. We are working on 1) developing cutting age non-invasive methods of obtaining cells for reprograming to patient specific stem cells for therapy and 2) understand mechanism of how these cell are involved in the repair process. Currently, it is not well understood if the cells are directly involved in repair or are indirectly participating by providing protective environment and signals that aid repair. To undertake such a mechanistic study requires an excellent *ex vivo* (outside body) model that gives the experimentalist control to an extent but keeps complexity of the native heart. Current studies utilize reduced models that are very poor representation of the actual heart, or whole heart models that give us wonderful insights albeit with results that need to be validated because of lack of direct control. Even though model cultured human

heart slices posses native heart physiology, they will lose their properties in a very short time in such an environment. Therefore, the goal of this work in this thesis is to identify a simple none-invasive pain-free method of acquiring somatic cell as a starting cell source for reprogramming and to develop a suitable *ex vivo* platform that can facilitate assessment of survival and integration of injected iPSC derived donor CMs. The following chapter, chapter 2, describes derivation of transgene-free hiPSC from cells obtained via routine human cheek swab. Cheek swab is not only non-invasive and painless but it can also be performed anywhere and without any special skills. The chapter delineates novel functional cellular reprogramming of cells obtained by simple pain free method suitable even for young and elderly population for potential patient specific disease therapies. Chapter 3 shows design, development, and characterization of a tissue stretching device that mechanically stimulates tissue slices: a platform to allow long-*term ex vivo* cardiac repair mechanism studies to serve as an *ex vivo* model of dynamic heart tissue. Chapter 4 presents optimization of cardiac slice preparations followed by structural and functional assessment of cardiac tissue slices mechanically stimulated by developed device for up to ten days. In chapter 5, current protocol by Lian et al. [77] was utilized to direct cardiomyocyte differentiation from human pluripotent stem cells on specific combination and ratio of substrates optimized by our laboratory. The last chapter concludes this dissertation by delineating the big picture and my contribution to it.

Chapter 2. Reprogramming Oral Mucosa Epithelial (OME) Cells from Buccal Swab for Generating Patient-Specific Stem Cells

ABSTRACT

Induced pluripotent stem cells (iPSCs) derived from somatic cells of patients have an immense potential to be used as a platform to study therapeutic regenerative medicine and as patient specific disease model. Current methods to establish human iPSC lines face several challenges including identification, availabilities, and collection of starting somatic cell sources for reprogramming. *In this study, we describe derivation of transgene-free hiPSCs [using CytoTune-iPS reprograming system that uses replication incompetent Sendai virus (SeV) to safely deliver and express the Yamanaka genetic factors required for reprogramming cells] obtained via routine human cheek swab back into a pluripotent stem cell.* Procuring cells via cheek swab is not only non invasive and painless but it can also be performed anywhere and without any special expertise. We show that cheek swab samples are sufficient for performing functional cellular reprogramming. Our novel method has potential to make patient specific disease therapies simple and pain free [especially for the young and elderly]. In addition, it will facilitate development of large-scale hiPSC banking.

2.1 Introduction

Embryonic stem cells (ESC), cells derived from inner cell mass of five-day mammalian blastula, with their ability to grow indefinitely while maintaining pluripotency, have been instrumental in advancement of disease treatments, drug discoveries, and mechanistic studies of pathologies [78]. However, generation of ESC comes with several ethical controversies since it involves destruction of embryos [79, 80]. In addition, these cells are not patient/disease specific, as they do not originate from individuals in need of interventions. In 2006, the Yamanaka group demonstrated that stem cells possessing properties of ESC could be generated from terminally differentiated somatic cells by force expression of four sufficient and necessary genes [39]. These stem like cells (iPSC), similar to ESC, have the ability to maintain pluripotency and unlimited potential to differentiate into functional cell lineages. Moreover, their usage circumvents ethical controversies and addresses patient/disease specificity since starting cells can potentially originate from patients. Obtained pluripotent cells exhibit donor/patient's specific genetic information, revealing a possibility to characterize disease related phenotypic changes in patient derived stem cells and their differentiated cell products (reviewed in [81]). Unfortunately, generation (reprogramming of somatic cells into stem cells) has its own challenges that must be tackled before we see them as a cell therapy source in clinical setting.

2.1.1 Current Reprogramming Methods and Challenges

Induced pluripotent stem (hiPS) cells were first generated from dermal fibroblast by overexpression of oct ¾, sox-2, klf4, and c-myc, Yamanaka factors, in 2006 [39]. One significant challenge to overcome is finding a superior reprogramming method, as some methods leave unwanted "footprint" in the reprogrammed pluripotent cells. In the early days, integration of reprogramming factors into the genome by retroviral or lentiviral transductions were utilized [43]. Use of these integrating viruses may carry an oncogenic potential to patients, resulting in iPS cells that are not safe to use for cell based therapies. To avoid these, alternative reprogramming methods have been developed in recent years that use plasmids [44, 45], temperature sensitive Sendai viruses [46], small molecules [47, 48], and modified RNA [49]. In this study, we used CytoTune-iPS reprogramming system that uses replication incompetent sendai virus (SeV) to safely deliver and express yamanaka genetic factors required for reprogramming somatic cells back into a pluripotent stem cell. It utilizes modified, non-transmissible form of sendai virus that does not integrate into host genome or alter genetic makeup of host cell to deliver necessary reprogramming genetic factors [82][Figure 6].

While fibroblasts are easy to maintain and expand in culture, their relatively low reprogramming efficiency and requirement of uncomfortable biopsies has prompted researchers to explore alternative somatic cell sources [42]. It has been shown that reprogramming efficiency varies depending on the molecular properties of the starting

material. The challenge is to find a starting cell source with a superior reprogramming efficiency combined with ease of obtaining it.

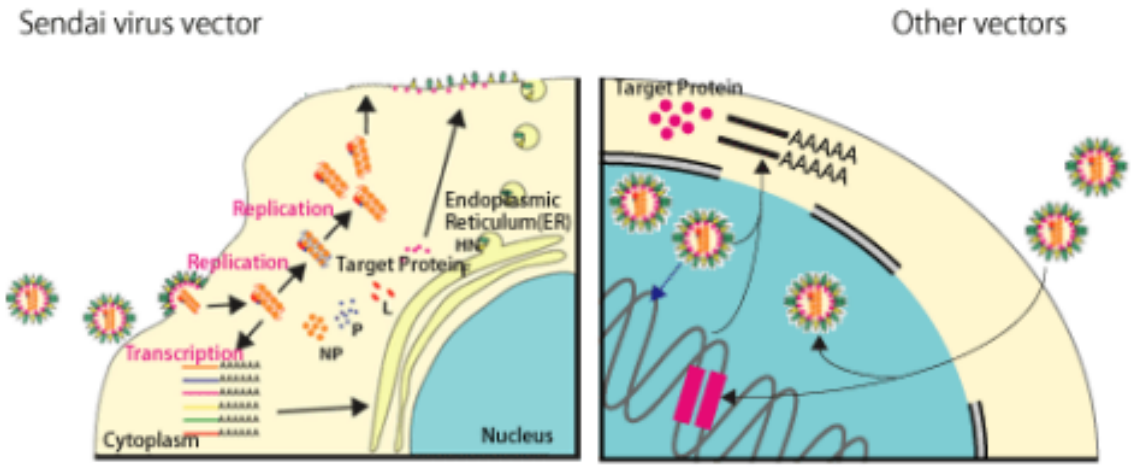

Figure 6: Comparison of transfecting vectors used for reprogramming. Sendai virus vector is superior because it does not integrate into the host genome and does not leave footprint [82].

2.1.2 Somatic Cell Sources for Reprogramming

The choice of starting somatic cell material should take into consideration the method of extraction, as some require special training and painful process. There has been exploration with various cell types, with some relatively easy to obtain compared to invasive and extremely painful biopsies. Cells from sources such as blood [83], keratinocytes from hair root [84], and exfoliated epithelial cells found in urine [85] are obtained non-invasively or with minimally invasive methods. Cells from hair root and urine in particular have shown promising reprogramming efficiency and they are relatively easy to handle and require minimal expertise. Alternative simple way of obtaining primary starting material is by performing buccal swabs. The oral mucosa contains a non-karatinized stratified squamous epithelium at the surface, which is routinely extracted for the purpose of collecting DNA samples for various studies [86-89]. Usually, buccal swabs are used to perform a one time molecular study or for the purpose of obtaining DNA for quick analysis. To our knowledge, up to date, no work has been done directly describing the use of buccal swab as a starting material for functional cellular reprogramming. The possibility to utilize mature somatic cell sources of patients suffering from various genetically defined diseases has rendered iPSC the advantage over the use of ESC for clinical research. Typically, epithelial cells from oral mucosa are collected by painful and invasive biopsy extraction process [90-92]. Here, we utilize a non-invasive and pain free scraping of oral mucosa as an alterative method to collect epithelial cells from oral cavity. Obtaining epithelial cells via non-invasive scraping

avoids discomfort and pain associated with tissue biopsy and venipuncture; thus, is suitable for children and elderly. After establishing buccal swab culture, they may be reprogrammed into iPSC using sendai virus. Furthermore, ease of obtaining the cells alleviates challenges of recruiting a large number of potential donors and avoids requirement for any special training. In this study, we report successful reprogramming of epithelial cells obtained by simple cheek swab method, albeit there is a need for further confirmation. The hiPSC line are theoretically transgene free and do not contain any genomic alteration. To the best of our knowledge, this is the first time such a non invasive and pain free buccal swab method is utilized to obtain starting cell source for reprogramming and our finding will greatly enhance development of patient specific therapeutic interventions.

2.1.3 Oral Mucosa Epithelial Cells

The epithelium is one of the four primary tissues in the human body. It is comprised of closely aggregated and tightly connected cells that cover most of our body surfaces exposed to external environments. These surfaces include skin, gastrointestinal tract, genital tract, urinary tract, oral mucosa, and other surfaces with potential exposure to external milieus. The epithelium not only provides physical protection from outside assault but also aids in various important selective transport phenomena such as diffusion, absorption, and secretion in the body. Oral mucosa epithelial cells are responsible for important functions in addition to providing mechanical barrier for physical protection of the oral mucosa against external intruders. They secrete important molecules for various functions and also aid in thermal regulation [93-95]. Epithelial cells from oral mucosa have great potential in serving as a tool for cellular and molecular research. They are usually collected via painful invasive biopsy methods [96, 97], however, scraping as in buccal swab can potentially yield viable cells for various studies. Oral mucosa epithelial cells are non-keratinized stratified squamous cells with cells in top surface viable unlike their keratinized counterparts [98] [Figure 7].

Non-keratinized stratified squamous epithelium has multiple layers of squamous cells resting on a basal membrane, where none of the cells are dead. However, sloughing (falling of the outermost superficial layer) can be seen indicating turnover. Buccal swabs are pain free non-invasive way to obtain cheek cells and are traditionally utilized to gather molecular or DNA samples from the cells for various analyses ranging from disease diagnostics to forensic identifications. Unlike skin epithelial cells, even their superficial layer is viable making them an attractive source of starting cell material for reprogramming. In addition, oral mucosa epithelial cells are superior candidates for such a study because they are less exposed to mutation agents [99].

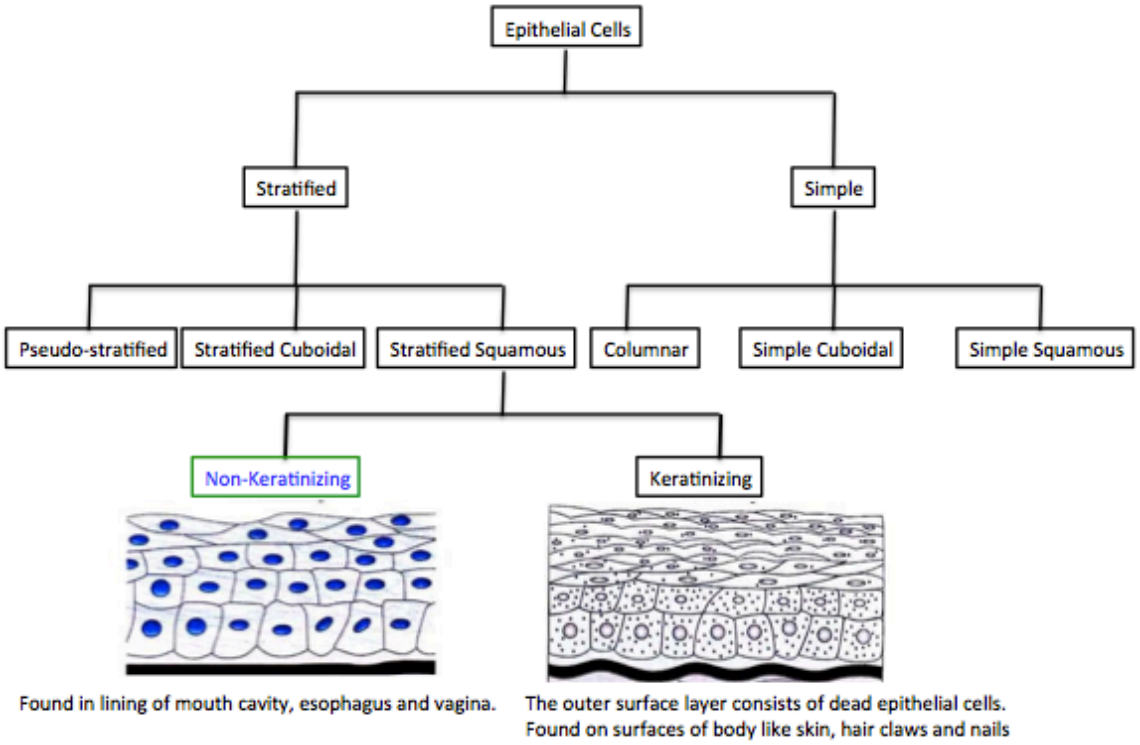

Figure 7: Classification of epithelial cells: Oral mucosa epithelial cells are non-keratinized stratified squamous cells found in lining of mouth cavity. There are several layers on top of each other will all layers viable.

2.1.4 Extraction and Culturing Substrates

Oral Mucosa Epithelial cell culture methods have been well established for many years. However, most of the developed methods utilize a painful invasive process to acquire starting cells [100, 101]. Establishing a culture method traditionally calls for optimizing media and/or choosing an appropriate substrate or mixture of substrates for culture surface. In this study, we optimized and describe a superior method to culture epithelial cells from buccal swab oral mucosa. Furthermore, we identified a substrate that is suitable and may represent physiological basal membrane. The basal lamina is composed of mixtures of substrates with collagen IV being the primary type of collagen found [102, 103]. Its main function is to anchor epithelium to layer underneath via cell-matrix adhesions aided by substrate adhesion molecules [104, 105]. The goal is to successfully establish a simplified monolayer primary oral epithelial cell culture method that avoids using fibroblast feeder layer as seeding substrate, priming it for use as a superior starting material for reprograming. Our method delivers a good alternative to culture oral mucosa epithelial cells, which will open new doors for various studies including cell therapy for regenerative medicine.

2.2 Materials and Methods

2.2.1 Obtaining and Culturing OME Cells

The University of California, Merced Institutional Review Board, holding Department of Health and Human Services Federal wide Assurance #00005105 has reviewed and approved Protocol ID #UCM15-0020 for ethical collection of human cells. A group of collage-aged volunteers of all genders were enrolled to participate and donors were asked to sign our "consent to participate in a research study" form for Biomedical studies with cell collection. Donors were then asked to brush their teeth as they would normally brush for hygiene. While they brush, a wash buffer was prepared in sterile 15mL conical tube containing 95% phosphate buffered saline (PBS) solution at room temperature with 5% antibiotic-antimycotic to prevent bacterial and fungal contamination. After twenty minutes of wait time, donors (4 male and 4 female) were asked to gently scrape cheek cells from palate and gum using sterile soft pack nylon bristle buccal brush (MasterAmp™ Cat. No. MB100SP) and collect cells in wash buffer [Figure 8].

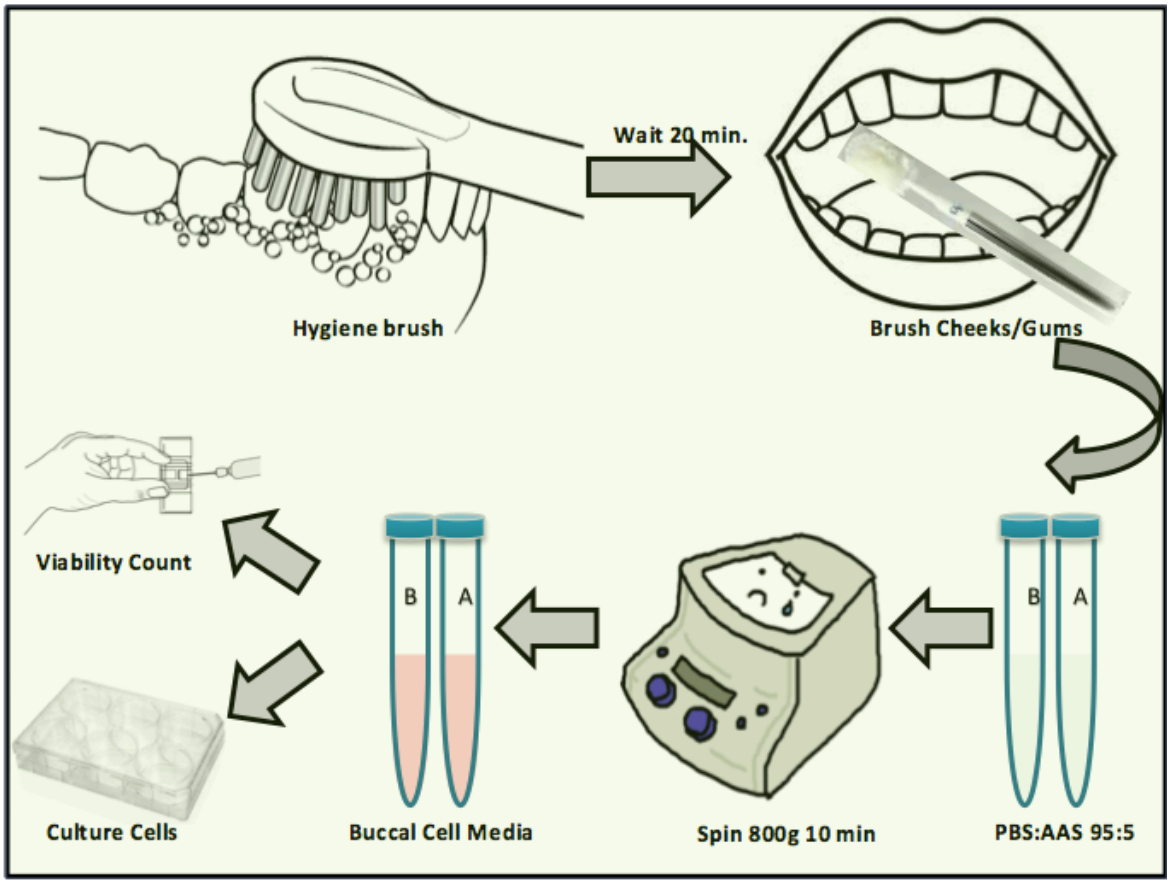

Figure 8: Schematic representation of the process utilized to obtain epithelial cells from oral mucosa.

Centrifuge cell-buffer solution for 10 min at 800*g* and aspirate supernatant to resuspend pellet in 3 mL of cheek cell media (84% High Glucose DMEM, 15% FBS, and 1% AAS). Resuspended cells were counted using (equal parts) 50 µL of cell suspension and 50 µL of trypan blue, plated at high density (p $\geq$17,000 cells/cm^2) on a 24 well plate, and placed in incubator (37°C, 95% relative humidity and 5% CO_2 level). Twenty-four hours after seeding, media were carefully aspirated from wells and gently fed with cheek cell media. Continue to feed cells daily until wells are ~30-60% confluent.

2.2.2 OME Cell Culture Substrates

In order to establish cheek cell epithelial cell culture, several different culture substrates were investigated as shown in table 2 below. (1) Culturing buccal swab on Laminin extracellular matrix; (2) Culturing buccal swab on Fibronectin extracellular matrix; (3) Culturing buccal swab on top of inactivated mouse embryonic fibroblast (iMEF) feeder layer; (4) Culturing buccal swab on Collagen I extracellular matrix; (5) Culturing buccal swab on Collagen IV extracellular matrix; (6) Culturing buccal swab on mixture of Collagen I and Fibronectin extracellular matrix; (7) Culturing buccal swab on Matrigel extracellular matrix; (8) Culturing buccal swab on Gelatin extracellular matrix. For all conditions, cells were cultured using cheek cell media described above and maintained in a standard incubator.

Table 2: Oral Mucosa Epithelial Culture Conditions and Viability

Cell	Substrate	Viability in culture (Days)
Oral Mucosa Epithelial	Laminin	6
Oral Mucosa Epithelial	Fibronectin	6
Oral Mucosa Epithelial	iMEF	12
Oral Mucosa Epithelial	Collagen I	6
Oral Mucosa Epithelial	Collagen IV	>60
Oral Mucosa Epithelial	Collagen I and Fibronectin	6
Oral Mucosa Epithelial	Matrigel	6
Oral Mucosa Epithelial	Gelatin	7

2.2.3 Substrate Preparation

Method 1: Stock Collagen IV was thawed on ice for several hours and plates and tips to be used were placed in a freezer overnight. In a tissue culture biosafety cabinet, collagen

IV stock solution was diluted with PBS or DI water to concentration of 25µg/mL. Ice for placing culture plates on top was prepared and quickly transferred the cold Collagen IV solution to wells of the plate such that bottom of plate was completely covered (for 24 well, used 150-200µL of solution per well). Wells [with Collagen IV solution] were dried down at room temperature overnight. Wells were rinsed with cold sterile cell culture medium prior to seeding cells.

Method 2: Stock Collagen IV was thawed on ice over several hours and then diluted with cold PBS to 25µg/mL. The solution was transferred to the wells [a cold plate (24-well)], such that bottom of plate was completely covered. Plates were sealed with parafilm and refrigerated at 4^0C for 2-3 days. After cells have been suspended in media, substrate was aspirated from plate, wells washed with cold media, and immediately seeded cells onto the plate such that bottom of the plate was covered in high-density cell solution (500µL on the 24 well plate). Incubated for an hour, then gently added 1000µL of cell media (to ensure binding of cheek cells to substrate on plate and reduce risk of Collagen IV denaturing), and incubated.

2.2.4 OME Cell Viability

For trypan blue exclusion test, equal parts of freshly obtained buccal cell suspension (50µl) and 0.4% trypan blue dye (ThermoFisher Scientific Cat. No. 1525006) (50 µl) were placed in a cryo-vial to obtain 1 to 2 dilution and gently mixed by pipetting up and down with a micropipette. The mixture was incubated at room temperature for no more than 2 minutes. Longer incubation will cause cell death and lead to inaccurate viability results. 14 µl of the mixture was loaded on to a standard Hemacytometer counter and observed under a light microscope. Number of viable cells [clear cells] and non-viable cells [blue cells] were counted and recorded. Percentages of viable cells were calculated by dividing number of viable cells by total number of cells and multiply by 100.

2.2.5 Immunohistochemistry Staining

Media was removed from cells and washed with Phosphate-Buffered Saline (PBS) then fixed in 4% paraformaldehyde (PFA) for 15 minutes. Cells were then permeablized with 0.1% Triton X-100 for 30 minutes and blocked in bovine serum albumin (BSA) for another 30 minutes. Cells were incubated with primary antibodies overnight at 4°C, washed, and incubated with secondary antibodies for a minimum of 2 hours [if primary is fluorophore-conjugated this step is not necessary]. Cells were stained by 4',6-Diamidino-2-Phenylindole (DAPI) for 5 minutes before imaging. oct ¾ and SSEA-4 antibodies were obtained from eBioscience. Ck 10, Ck 13, ITGB 1, Tf were obtained from Abcam. For live staining to check pluripotency, alkaline phosphatase live stain (ThermoFisher Scientific Cat. No. A14353) was used according to the manufacturer's protocol.

2.2.6 Cellular Reprogramming

The schematic shown in [Figure 9] below describes the functional cellular reprogramming of oral mucosa epithelial cells. Once cheek cells reach confluency of 30-60%, cheek cells were transduced using CytoTune^{TM}-iPS 2.0 Sendai Reprogramming Kit (Cat. No. A16517: KOS MOI=5, hc-Myc MOI=5, hKlf4 MOI=3).

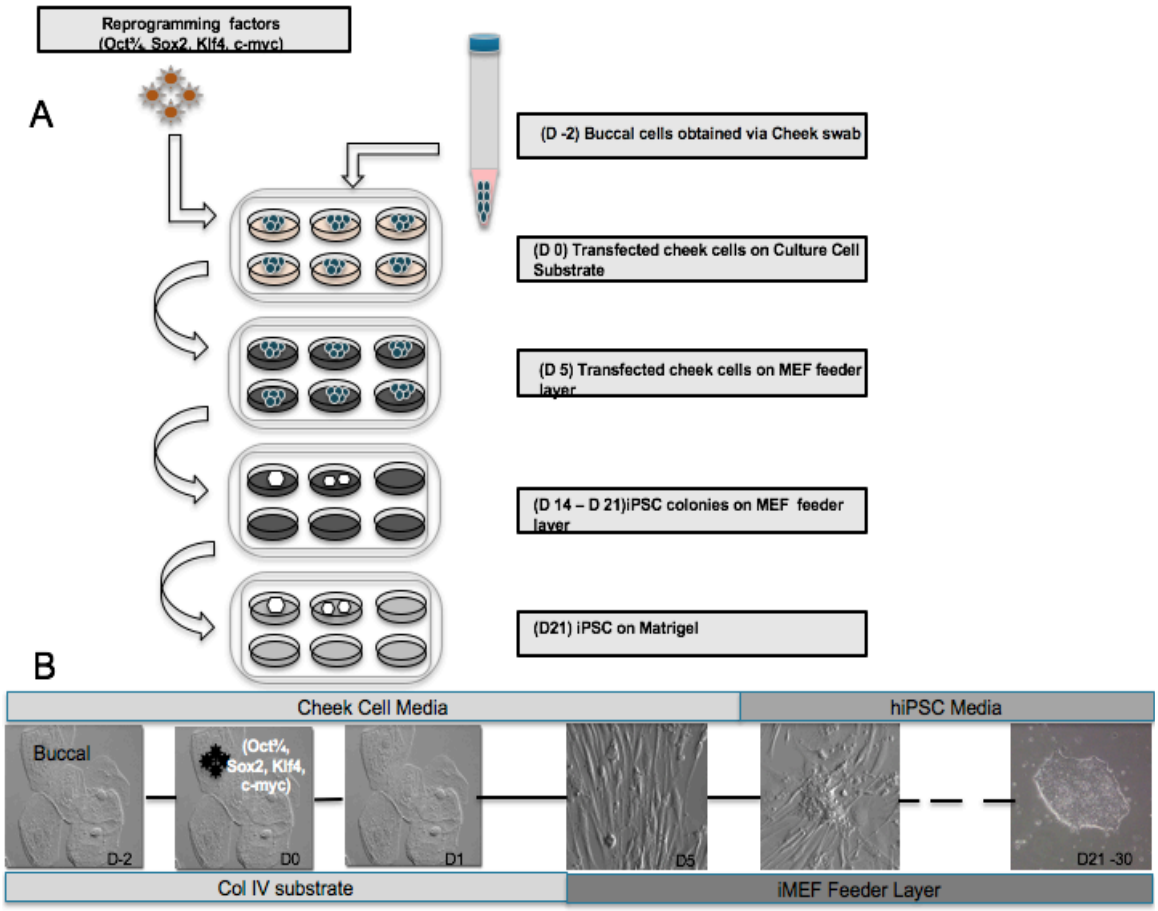

Figure 9: Schematic for reprogramming buccal cells. A) Cells were obtained via cheek swab into a conical tube and plated at high density on sterile tissue culture plates coated with a substrate. After two days, when cells were about 40% confluent, cells were transfected using CytoTune-iPS 2.0 sendai reprogramming kit and transferred onto MEF feeder layer after five days in culture. When colonies are large enough, they were picked and plated onto Matrigel. B) Time course, media, and substrate used to culture buccal cells and reprogram them into pluripotent state

To terminate transduction, media was replaced with fresh cheek cell media after 24 hours post transduction. On Day 2 post-transduction cells were fed with equal rations of iPSC media (DMEM F12 Advanced 77mL, KSR 20mL, NEAA 1mL, AAS 1mL, L-Glutamate 1mL, bFGF 20 µl, DBME 100 µl) and Cheek Cell media. Starting at day 3, cells were fed with 100% iPSC media daily. On Day 8 post-transduction, cells were lifted using 1 mL trypsin (incubating at 37^{0}C for 5 min then neutralizing after with media) and

centrifuged for 10 minute at 1000 rpm. Aspirate out media and resuspend pellet in iPSC media, then transfer cells to MEF feeder layer. Feed with iPSC medium daily until stem cell like colonies emerge (~day 11 - 21). Check colonies for pluripotency using alkaline phosphate live stain and once confirmed pick colonies manually and expand in culture on Matrigel. Schematic of method is shown in figure 9 below.

2.2.7 Alkaline Phosphatase Live Stain

To live stain cells, growth medium was removed from culture and washed with pre-warmed DMEM/F-12 twice for 2-3 minutes. 1X AP live staining working solution was prepared by diluting 500X stock solution in DMEM/F-12 solution and applied directly to cell culture. Culture was incubated for 30 minutes and then AP live stain was removed by gently washing twice with DMEM/F-12 for 5 minutes per wash to remove excess AP live stain and reduce background signal. Fresh DMEM/F-12 was added after final wash prior to visualization of fluorescent-labeled colonies under fluorescent microscope using FITC filter. Images were captured within 30 – 90 minutes of staining.

2.2.8 Statistical Analysis

All experiments were performed at least 3 times and analyzed by GraphPad Software Prism. Comparisons were done with student t test and differences were considered significant at the $p \leq 0.05$ *level.*

2.3 Results

2.3.1 Buccal Swab Cells are Viable, Express Epithelial Cell Markers, and Test Negative for Pluripotency.

Unlike the usual painful and invasive process of collecting cheek cells, we collected Buccal cells by non-invasive pain free scraping of oral mucosa, ordinarily considered superficial dead cells or used as a source for single molecular or cellular analysis. Initially we noticed a slight difference between a first scrape and a subsequent second scrape where the second one seemed to have fewer cells but more viable cells. Before proceeding with cell culture protocols, plates were checked for cell viability using trypan blue staining for both 1st and 2nd scrape, Brush A & Brush B [Figure 10A & B].

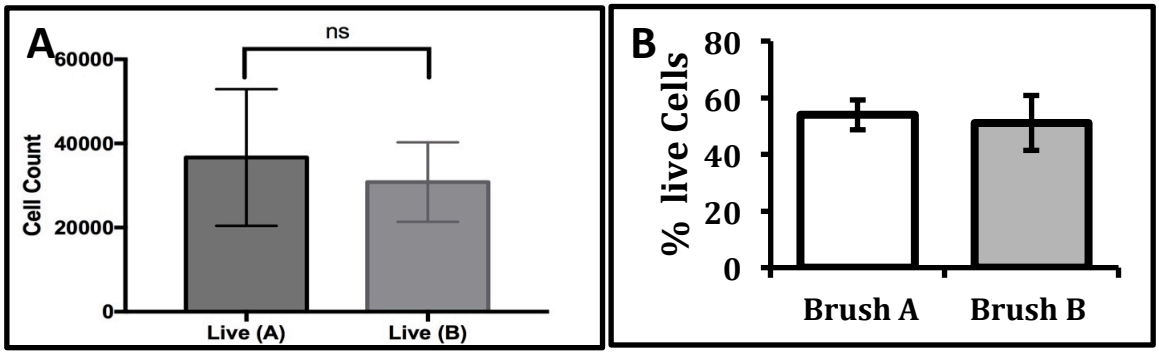

Figure 10: Oral mucosa epithelial cell extraction: Comparison of two subsequent swabs/Brushes A) Brush A and B have no significant difference in the amount of live cells obtained. B) The percentage of live cells obtained from both brushes has also no significant difference.

Even though slight differences were noticed in cell number and appearance between the two consecutive scrapes (brushes), our results show there is no significant difference ($P > 0.05$; t-test) as both brushes have between 30000 – 40000 live cells [Figure 10A]. The percentage of live cells out of total collected cells has also no significant difference between both brushes, brush A and brush B. Both yielded 55± 5% and 53 ± 6% respectively.

Samples collected consistently contained viability of 54 ± 4% with values ranging from 50% to 58% as shown by trypan blue exclusion test conducted [Figure 11A & B].

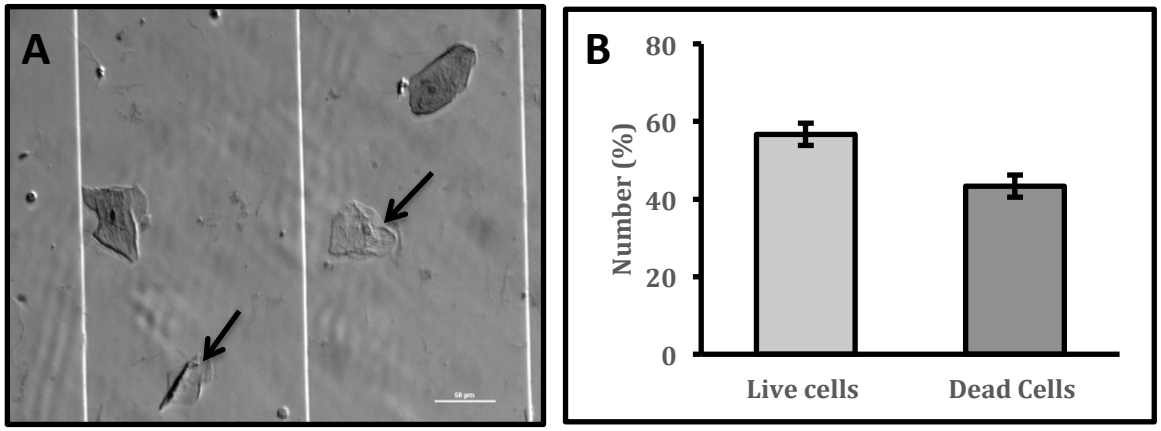

Figure 11: Oral mucosa epithelial cell extraction: Cell viability via trypan blue exclusion. A) Trypan blue dead/live assay, arrows show cells that are alive (light in color did not take up die) darker cells took up trypan blue and are not viable. B) Quantification of live and dead cells obtained by cheek swab method. Approximately 60% of cells of freshly obtained cheek cells are live cells.

Since we sought after culturing cheek cells to utilize as a starting somatic cell source for functional cellular reprogramming, it was necessary to establish identity of cells obtained via mouthwash and plated on a substrate by conducting molecular characterization. Immunofluorescence assay was used to detect presence of oral mucosa epithelial cell specific markers. Cytokeratin-10 (CK -10) and Cytokeratin-13 (CK-13), intermediate filament proteins responsible for structural integrity of epithelial cells, were detected in almost all cells plated on collagen IV substrate [Figure 12 A & B]. Epithelial

surface markers transferrin receptors (TfR), transmembrane carrier protein and transmembrane integrin β_1 (ITGB 1), collagen receptor were also detected in all cells and a few cells respectively (Figure 12 C & D). Absence of stem cells from collected cells was also confirmed by checking for human stem cell markers oct ¾ and SSEA 4 expression (Figure 12 E & F)

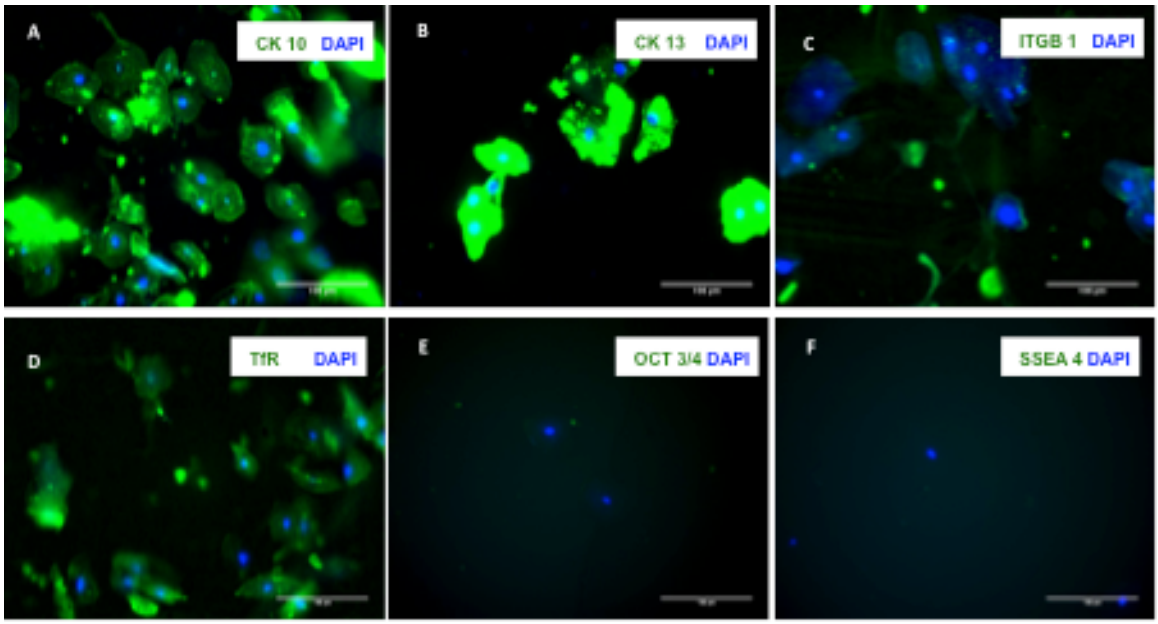

Figure 12: Oral Mucosa epithelial cell characterization. Stained for cheek cell and stem cell markers. A) Cytoplasmic intermediate filament marker Cytokeratin-10 (CK-10) was found in almost all cells in green. B) Cytokeratin-13 (CK-13) was also found in all cells in green. C) Cell surface marker integrin beta-1 (ITGB-1) was found in a lot of cells in green. D) Stained for transferrin receptor (Tf) in green. E &F) Stained for pluripotency markers oct 3 / 4 and SSEA 4 respectively showing the absence of pluripotent cells in the starting cell population. Blue is DAPI marking the nucleus.

2.3.2 Collagen IV is Suitable Substrate for Oral Mucosa Epithelial Cell Culture.

Oral mucosa epithelial cells cultured on the substrate Fibronectin immediately sat on sterile culture plate and several remained attached to culture plate after one day in the incubator. Starting day one, there was significant loss of cells during careful feed (media change) as floating cells were discarded with old media. Usually, cells that did not sit after one day in culture remain floating even if we avoid disposing them when feeding and keep them in culture (data not shown). The cells seemed to exhibit minor proliferation for two days, showing some promise on day 5 [Figure 13 A & J] when suddenly all cells died after six days in culture.

Similar behavior was observed with cells cultured on other substrates as well. Oral mucosa epithelial cells cultured on Collagen I, Laminin, Matrigel, and a combination of Fibronectin and Collagen I all lasted for six days in culture (see Table 2 in methods section of this chapter). In addition, we observed no significant difference between cells on the mentioned substrates on day five. On average there are slightly more cells on culture dishes coated with Laminin and matrigel than Fibronectin and Collagen I.

Oral mucosa epithelial cells seeded on the combination of Fibronectin and Collagen I on average showed slightly higher numbers than on Laminin and Matrigel [Figure 13].

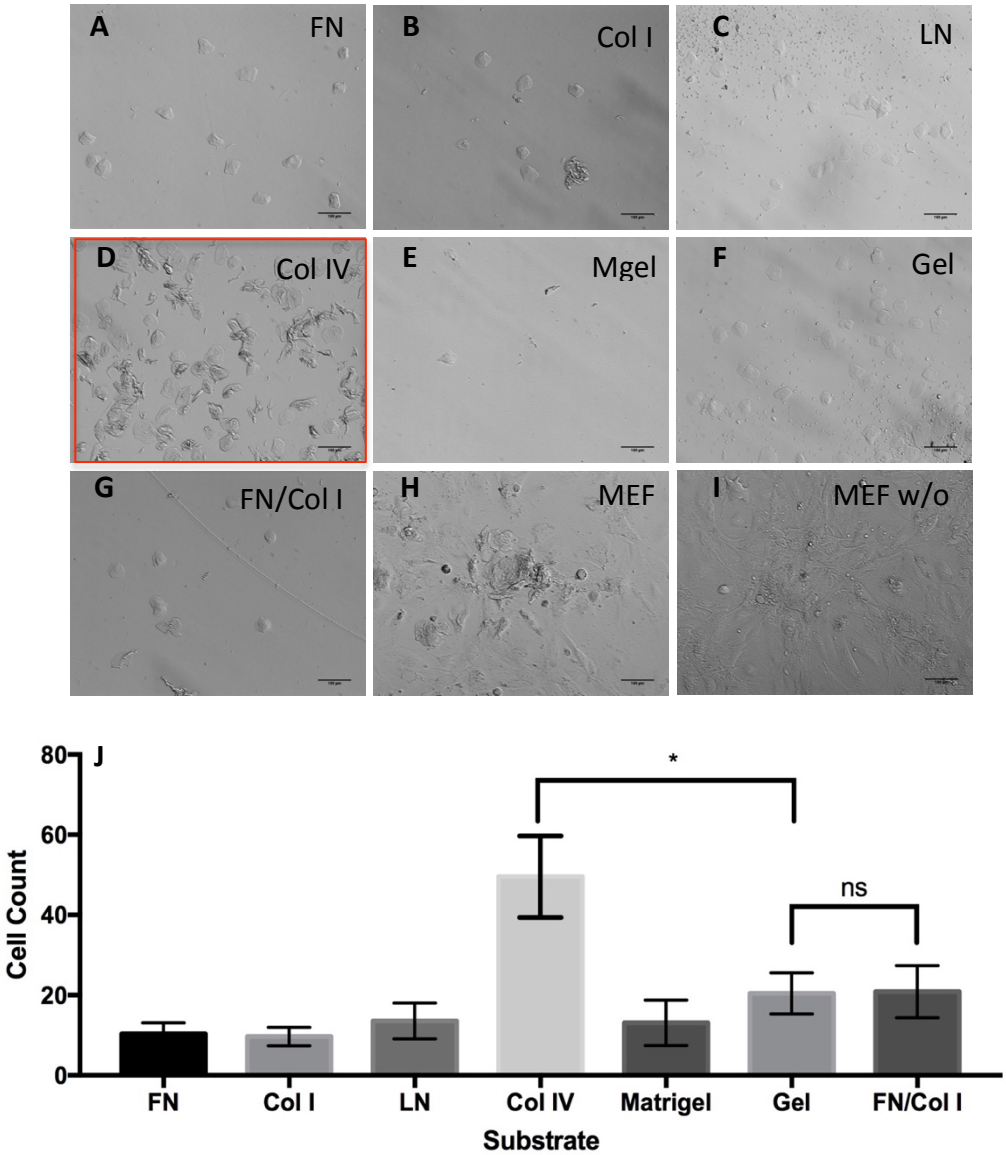

Figure 13: Substrate for buccal cell culture. A-I) Bright-field images of buccal cells at day 5 cultured on various substrates: A) Fibronectin (FN), B) Collagen I (Coll), C) Laminin (LN), D) Collagen IV (Col IV), E) Matrigel (Mgel), F) Gelatin (Gel), G) Fibronectin and Collagen IV combined (FN/Col I), H) Mouse embryonic fibroblast feeder layer (MEF), and I) Mouse embryonic fibroblast feeder layer without any buccal cells on it (MEF w/0). J) Quantification of cell count at day 5 for each substrate used.

When using Gelatin as a substrate, EOM attached right after seeding onto feeder layer at day 0 and survived until day 7, then they all died. However, when seeding on an inactivated MEF layer, there were attached cells until day 12. After day 12, MEF layer started peeling off and cells detach from plate and float. Oral mucosa epithelial cells seeded on the Collagen IV substrate show the most proliferation and were viable for more

than sixty days in culture. On average, there are significantly more cells attached and viable when seeded on Collagen IV than any of the other substrates that we investigated.

2.3.3 Reprogrammed Oral Mucosa Epithelial Cells Have Stem Cell Morphology and Show Pluripotency with Alkaline Phosphate Live Staining.

Commercially available induced pluripotent stem line [iPS DF-19-7T cells (wiCell)] were first characterized to use as a bench mark and establish desired morphology and staining protocol. The iPS cells maintain colony shape and stain for pluripotent markers oct ¾ and SSEA 4 [Figure 14].

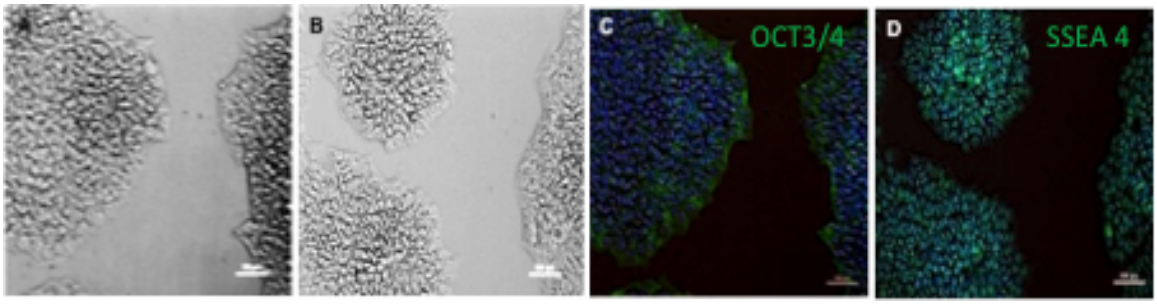

Figure 14: Characterization of iPS cells. A-B) iPS DF-19-7T cells (WiCell) maintain colony shape, and stain positive for the pluripotent markers C) Oct ¾ (green) and D) SSEA4 (green). Counterstained with DAPI nuclear stain (blue). Scale bar = 100µm.

After establishing oral mucosa epithelial cell culture, CytoTune-iPS reprogramming system that uses replication incompetent sendai virus (SeV) to safely deliver and express the yamanaka genetic factors required for reprogramming somatic cells back into a pluripotent stem cell was introduced. Cultured oral mucosa epithelia cells were reprogrammed with manufacturer recommended MOI of each vector. Vector was removed from culture exactly after 24 hours of transfection. As expected, significant amount of cell death was observed at the end of day one (data not shown). To use as a control, the same reprogramming technique to introduce yamanaka genetic factors was utilized to reprogram Normal Human Lung Fibroblasts (NHLF) isolated from adult lung tissues. Figure 15 shows that reprogrammed NHLF (NHLF-iPS cells) maintain colony shape. We examined expression of pluripotency markers in NHLF-iPSC lines using immunostaining. Consistent with their hESC-like morphology, we detected expressions of oct 3/4 and SSEA-4 (Figure 15 C & D), which confirms that reprogramming process resulted in fully reprogrammed cells.

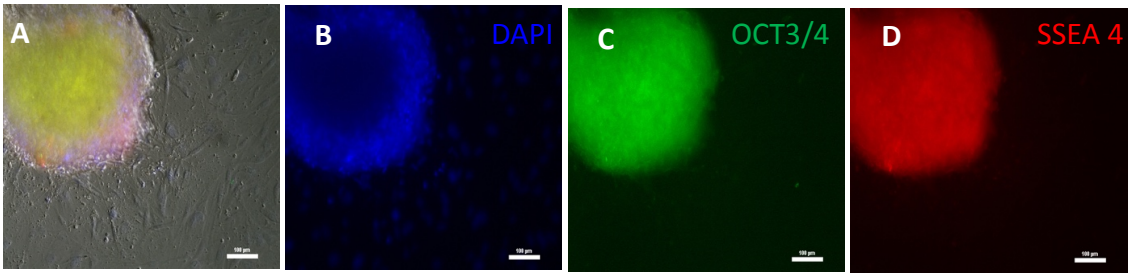

Figure 15: Characterization of iPS cells. NHLF iPS cells maintain colony shape, and stain positive for the pluripotent markers A) DAPI (blue) B) SSEA4 (red) C) Oct ¾ (green). D) Merge scale bar = 100µm.

For the reprogrammed oral mucosa epithelial cells, IPSC colonies were typically formed between days 11 and 18 as shown under phase contrast microcopy [Figure 16 B & F]. Colonies exhibit the characteristic flat shape and distinct crisp borders seen in pluripotent cells. Control plates that have not been transfected do not have such colonies, as seen in figure 16 A & D at days 15 and 18 respectively. Top row, [Figure 16 A – C] high seeding density for feeder layer is utilized and lower density for figure 16 D-F. Variance between cell lines is noticed, as some colonies will not only start at earlier days but they also tend to grow faster and start differentiating and/or disintegrating. MEF layer in some instances started peeling off, lifting the formed colonies (data not shown).

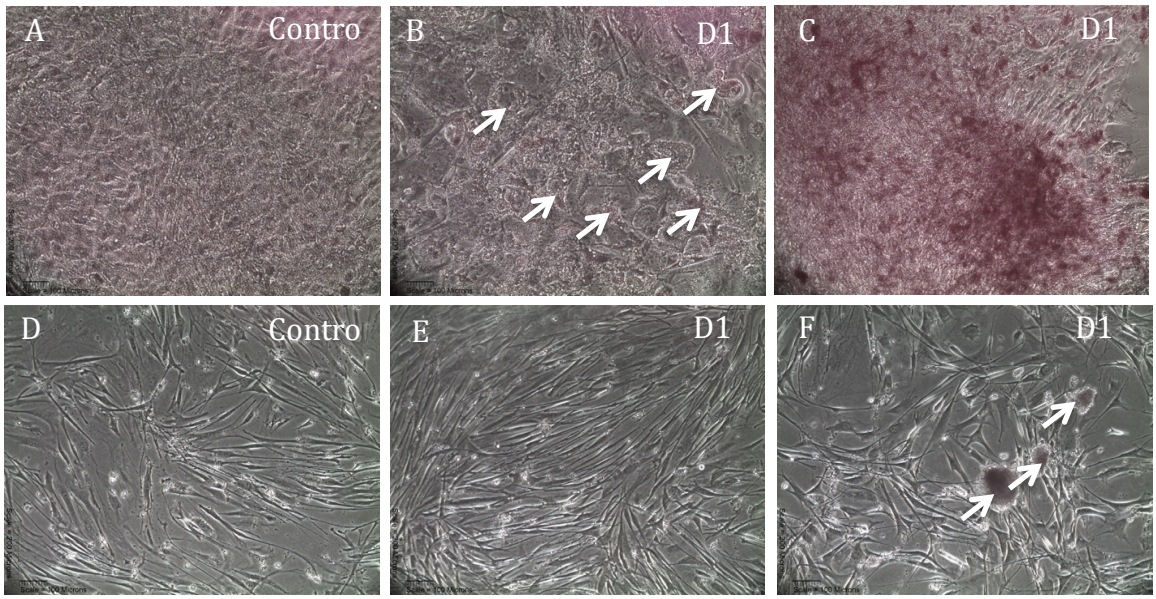

Figure 16: Reprogrammed buccal cells on inactivated MEF feeder layer. A&D) Non transfected buccal cells on MEF B&E) Transfected buccal cells on MEF D11 (colonies) and D12 (no colonies) respectively C&F) Transfected buccal cells on MEF Day 15 overgrew plate and D18 (F) Colonies started emerging. White arrows show emergence of stem cell like colonies).

Stem cell like colonies were identified and stained with alkaline phosphatase transient live staining that differentially stains pluripotent stem cells (PSCs). IPSC colonies stained positive for alkaline phosphatase [Figure 17B].

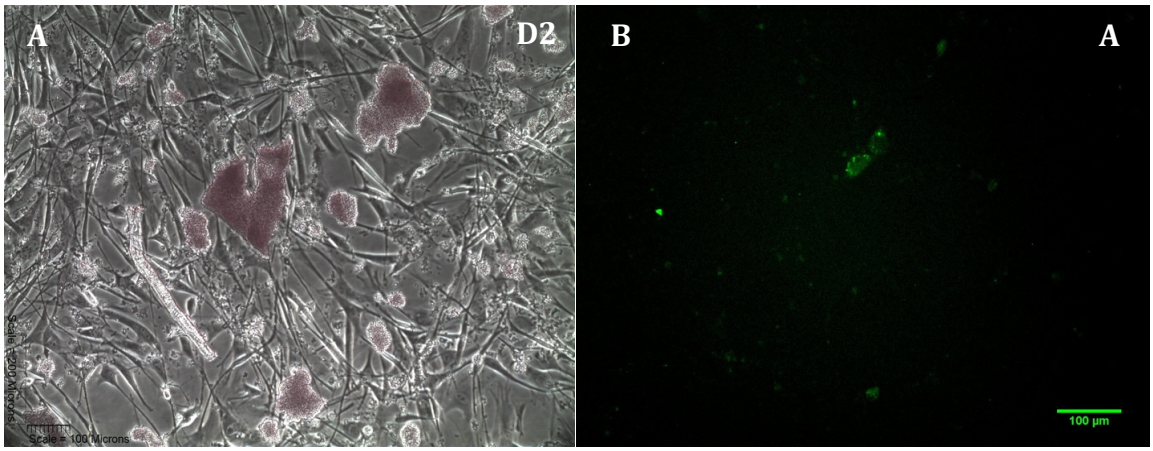

Figure 17: Reprogrammed & stained buccal cells on iMEF feeder layer. A) Transfected buccal cells on MEF with emerging stem cell like colonies at D21. B) Alkaline phosphatase live staining of the stem cell like colonies.

Colonies were then picked and transferred to a new plate to expand. All transferred colonies lifted up and did not survive the transfer. By Day 21 post-transduction, cell colonies on inactivated MEF culture dishes have become large and compact, covering some of the surface area of the culture dish. However, only some of these colonies consist of iPSCs, which exhibit a hESC like morphology characterized by flat cobblestone-like appearance. Alkaline phosphatase live staining was performed to identify pluripotent colonies and recognize undifferentiated hiPS cells [Figure 17].

2.4 Discussions and Conclusions

Epithelial cells from oral mucosa have great potential in serving as a tool for cellular and molecular research. They are usually collected by painful invasive biopsy extraction methods and isolated for culture. However, buccal swabs, pain free non-invasive cell extraction method can potentially yield viable cells for various studies [106]. Traditionally, buccal swabs are utilized to gather one-time molecular or DNA samples from cells for diverse analysis ranging from disease diagnostics to forensic identifications and discarded after use [107]. Here we presented, for the first time, a protocol for culturing oral mucosa epithelial cells after a non-invasive and pain free method of collection, cultured without a feeder layer. This protocol can be utilized as a useful tool for suitable patient specific disease therapy and other new applications.

Unlike skin epithelial cells, even the superficial layer of oral mucosal epithelial cells are viable making them attractive source of starting cell material for reprogramming [108]. Furthermore, oral mucosa epithelial cells are superior candidates for such a study because they are less exposed to mutation agents [99, 109]. Obtaining starting cell material for reprogramming via this non-invasive scraping method avoids discomfort and pain associated with tissue biopsy and venipuncture; thus, is suitable for children and elderly.

To explore whether we are able to generate hiPSCs from non-invasively obtained oral mucosal cells, we collected cheek cell swab samples from different individuals and immediately washed them in PBS supplemented with AAS. We optimized our collection method and were able to consistently gather over 50% live cells that were used in cellular reprogramming. Interestingly, we found that cheek swab cells could be cultured and expanded in check cell medium on Collagen IV substrate to yield enough viable dividing cells for reprogramming. Cells in culture after 2 days were largely CK 13^+, CK 10^+, and transmembrane protein (TfR & ITGB 1) positive epithelial cells. We also confirmed absence of stem cells in the obtained cells in culture before reprogramming. Using non-integrating CytoTune-iPS reprograming system that uses replication incompetent sendai virus, we observed the appearance of hESC like colonies approximately three weeks after transduction (Figure 16 B&F). Reprogramming cheek cells obtained by simple swab method will open a new door for patient specific therapy.

Chapter 3. Stretching Device for Heart Tissue Model Preservation

3.1 Introduction

Mechanical stimulation plays a critical role in cellular structure and function in many organ systems [110]. A wide range of cells in our body are subjected to varying mechanical stimuli such as shear stress, interstitial flow, substrate strain, compression, confinement, etc. Biological responses to these stimuli include: changes in cell differentiation, cell migration, gene expression, and protein secretion [111]. These biological responses not only depend on the nature, duration, and extent of the stimuli, but also the intrinsic cellular mechanical properties of cells themselves and the cells' microenvironment. Thus, mechanical stretching has been utilized to enhance the organization, functionality, and strength of many engineered tissues. Mechanoresponses will then in turn initiate a feedback loop that will alter the longer-term intrinsic mechanical behavior, Figure 18 [112].

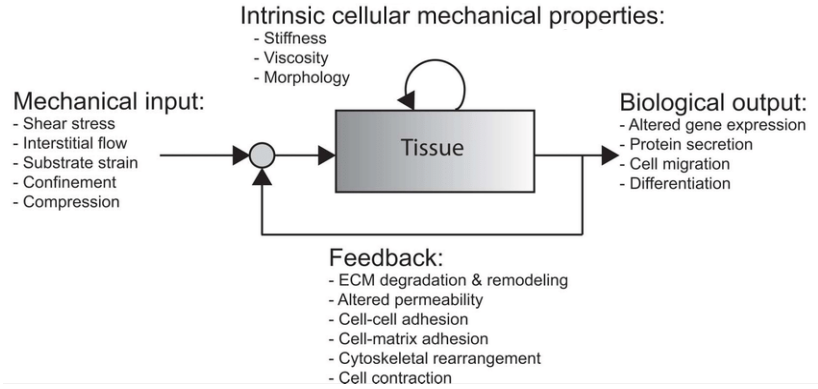

Figure 18: Cellular Mechanotransduction: Cells display biological responses to mechanical cues such as sheer stress, interstitial flow, substrate strain, or compression. The biological outputs (altered gene expressions, protein secretion, cell migration and/or differentiation) from cells and tissues will eventually alter the intrinsic cellular mechanical properties all intertwined in a feedback loop [112].

Every cardiac cycle, i.e. the period of time between onset of atrial systole and ventricular diastole, the heart experiences various mechanical forces [113]. In the heart, cardiac output, i.e. stroke volume, imparts a stretch on cardiac cells during cardiac return, corresponding with the end-diastolic volume (EDV) or preload. Preload denotes length of the sarcomeres in cardiac muscle prior to systole; physiological increase in EDV will increase this preload on the heart, leading to an increase in the amount of blood ejected from the ventricle according to the Frank-Starling mechanism of the heart, Figure 19 [114].

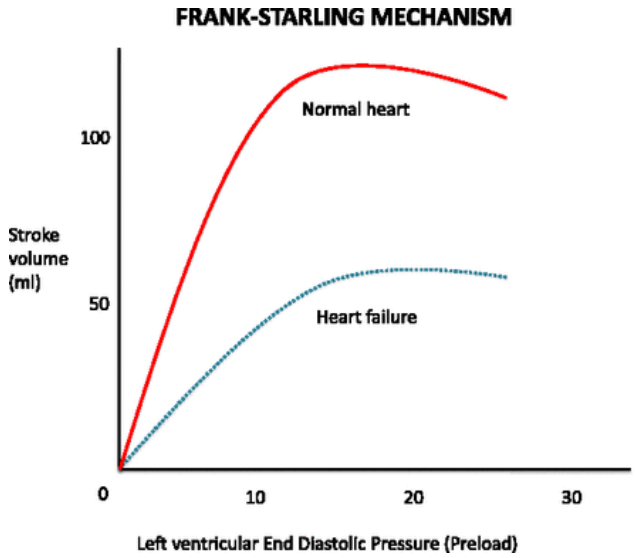

Figure 19: Frank-Starling curve relating the left ventricular end diastolic pressure (EDV) to the stroke volume (SV): Red curve for normal heart and blue curve of a failing heart. The curve shifts downward and to the right as contractility is decreased [115].

Under normal physiological conditions, the heart completes a cardiac cycle approximately every second, contracting against a mechanical load during each heartbeat [116]. The heart performs optimally within a defined range of hemodynamic load and fails if chronically unloaded. Clearly, the heart is a very dynamic organ and cardiac cells sense and respond to their mechanical environment. However, many standard *ex vivo* cardiac tissue platforms do not take mechanical cues into consideration [117-120]. Although organotypic slice preparations have been established for organs such as the brain and liver, [121-123], vital cardiac tissue slice preparation has received less attention. After exploring the use of isolated single cells and whole heart perfused preparations, the use of organotypic slices of the heart has been gaining popularity, especially as sectioning technologies to obtain live cardiac tissue slices have improved. These *ex vivo* tissue slices are currently the most promising candidates for conducting *ex vivo* cardiac research since they maintain native multi-cellularity, present moderate complexity, and retain complex extracellular architecture and well preserved cell-to-cell electrical, mechanical & metabolic connections [124]. In most cardiac slice preparations, slices are subjected to static conditions that will lead to rapid degradation of tissue integrity [117, 125-128]. Here, we report development of a tissue-stretching device to support cardiac tissue slice preparations in order to preserve the structure and function of myocardium long term, and serve as a platform for cardiovascular research, including pharmacological testing and the development of innovative therapeutic strategies.

The specific design goals were to develop and test a uniaxial multi-well cardiac tissue stretcher system capable of delivering cyclic stretch to cardiac tissue slices in a controlled environment. Here, we present the details of the device design.

3.1.1 Advantages and Limitation of Current Tissue/Cell Stretchers

While various cardiac cell/tissue-stretching devices have been designed (reviewed here [129]) [130], to our knowledge, devices that can accommodate 500-micron thin cardiac slice preparations and provide a cyclic stretches to mimic physiological environment for long term preservation have not been popular and only very recently received appropriate attention. Stretching has been shown to impart a unique response compared with other mechanical stimulation modalities. Tissue stretchers attempt to mimic the physiological stress the heart undergoes with every heartbeat. At the cellular level, mechanical stretch has been shown to have influence over cell differentiation [131], proliferation [132], maturation[133], and morphology[134]. Mechanotransduction, a multistep process converting mechanical stimulus into intracellular biochemical activity, arises due to external forces and forces generated inside the cell cytoskeleton. However, the specific cellular response to external stretch depends on the stretch direction, rate, % strain, as well as, properties of extracellular matrix, and presence of other factors in the local environment. Stretching devices have yielded data from strain magnitude (2.5 – 25%) and frequency (0.05 – 2.75 Hz)[135] with 10% and 1 Hz being the accepted physiological values for magnitude and frequency respectively [136, 137]. Over a dozen cell/tissue mechanical stimulating systems have been designed and are available commercially or used in laboratories for *in vitro* studies[138]. The advantages of commercially available stretching device systems such as Flexcell, ElectroForce, and Strex are that they provide relatively well-characterized strain profiles compared to custom lab specific stretching devices.

Advantages and limitations of various systems from earlier days have been described [138]. Most mechanical stretching devices are fitted to support and stretch a membrane that is seeded with cardiac cells, 3D constructs or tissues [139]. The membrane used introduces unwanted elastic recovery of membrane, hinders uniform nutrient diffusion, and constricts these devices. There are very few systems developed to directly attach cardiac tissue slices to the stretching device. Wang et al. developed a device with a single chamber and manual micromanipulator to deliver uniaxial stretch to cardiac slices [140]. Though they were able to perform electrophysiology studies on the effects of mechanical stretch, their device is low throughput (1 chamber) and delivers static uniaxial stretch via manually controlled mechanism. More recently Perbellini et al. utilized a 3D printed A shape primitive device to deliver a static stretch to study the effect of mechanical stretch on cardiac fibroblast [141]. This year, two groups (in Germany and UK) have reported devices that combine mechanical stretch with electrical stimulation to mimic *in vivo* heart environment. Watson et al. developed a sophisticated device for electrical stimulation and continuous media superfusion [142]. They reported a preload equivalent to sarcomere length 2.2μm is optimal for maintenance of slice structure by manually testing static stretches of various magnitudes. The other is a multi-well chamber like our device but has electrical stimulation and sophisticated mechanical collection system in addition to mechanical stimulation. Fixed end of slice was to a spring wire to generate systolic left ventricle wall tension and the moving end was manually operated to a specific preload magnitude [143]. Though these devices are designed for multi

stimulation modalities (electrical, mechanical, and biochemical), to date only our device applies automatic cyclic uniaxial stretches to supported myocardial slices. It must be noted here that it is not difficult to add electrical stimulation to our device and allow for biochemical investigations. We also must note that other systems can easily be accompanied with automatic cyclic stresses delivery mechanism like ours. In any case, these kinds of systems are the future of cardiac research as they present the best imitation of the *in vivo* environment. Types of strain fields induced can be used to categorize devices that are currently being utilized. Devices that exert uniaxial strain are desired because it is simple, produces uniform strain, and consistent stain fields over high strains. However, they are low throughput (one direction at a time), and generate anisotropic strain fields. On the other hand, biaxial strain devices are more desirable for their high throughput. They can also produce uniform anisotropic/isotropic strain fields [144].

For this work, I was interested in developing a system that provides physiologically relevant mechanical stimulation that closely mimics the *in vivo* mechanical conditions to a tissue slice preparation of the left ventricle. Before developing the current DTSD4s, several generations of the same concept has been scrapped because of various shortcomings [Figure 20]. First generation stretcher system (DTSD1) was designed to support a circular left ventricular preparation and provide mechanical stimulation at multiple contact points around the circumference.

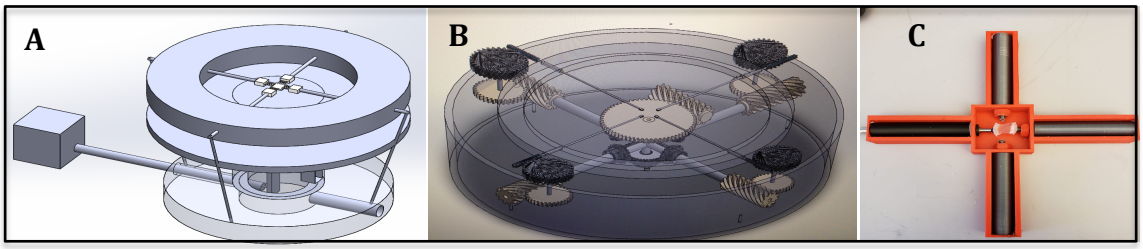

Figure 20: Prior generation devices. A) First generation (DTSD1) motor driven rotational motion to linear motion converting system was too high for data collection. B) Second generation (DTSD2) gear system was prone to getting stuck frequently. C) 3rd generation (DTSD3) was low throughput and can only support one slice at a time.

The final height of 10cm of the device did not allow for data collection, as it was not short enough to fit under a light microscope. Other challenges include difficulties in preparing circular tissue preparations and stretching along fiber direction. I was able to address these issues in subsequent generations of the device by adopting square shape for the tissue preparations and reducing device height.

3.1.2 DTSD 4.0s Design Specifications

The overall design specifications are summarized in Table 3. We aimed to build a uniaxial stretching device to deliver cyclic mechanical stimuli simultaneously to up to five 500-micron thin cardiac tissue slice samples. Device dimensions should be compact enough to be placed inside a laboratory incubator and allow access to samples during

observation and data collection under a light microscope. The device should allow removable parts for easy cleaning. The actuator should deliver precise and accurate mechanical stimulations with a user-friendly interface to control amplitude and frequency of the cyclic stretches.

Table 3: Design specification, constraints that guided the design and considerations taken for the DTSD 4s

	Considerations	Requirements	Constraints
1	Functionality	Support and Provide Cyclic Uniaxial tension to 500μm thin myocardium	Clamping mechanism
2	Usability	Compact to fit in incubator, safety cabinet, and suitable for data collection	Microscope working distance
3	Sterilization	Posses sterile culture chamber, easy to clean and fit in sterile safety Cabinet	Material and machining availability
4	Performance Quality	Provide precise displacement to several samples at a time	Clamping mechanism
5	User interface	Automated Stimulation	Hardware compatibility
6	Manufacturing	Durable, easily modified, in house production	Availability and size of 3D printers
7	Aesthetics	Looks well made	Functionality, corrosion
8	Cost	Affordable for custom laboratory usage	Budget < $3000

3.2 Materials and Methods

3.2.1 Tissue Stretching Device

A Dynamic Tissue Stimulating Device (DTSD-4.0s) has been designed to:

- Provide uniform uniaxial stretch
- 5-15% adjustable elongation
- 0.5-2 Hz adjustable stretch frequency
- Support ~ 500μm thick cardiac tissue preparations
- Keep tissues submerged in media
- Fit under an inverted microscope for imaging
- Possess chamber opening that allows for easy access to observe and manipulate samples
- Compact enough to place inside a cell incubator (37°C, 100% humidity)

It is intended to exert dynamic uniaxial stretching, but can be easily modified to deploy static uniaxial stimulations. DTSD 4s consists of five chambers, each of which can accommodate a sample. Five samples can be stretched simultaneously providing identical stretch to each sample, or several samples can be held at a static strain and serve as controls. Cardiac tissue samples are secured in wells supported by 70μm cell culture inserts. Mechanical stimulation is controlled by a linear actuator, which is powered and

controlled by a high-resolution stepper motor controller. Linear actuator is controlled by motion control software to deliver step and direction pulses through a controller. User-friendly interface is available on the software to control amplitude and frequency of cyclic stretches.

3.2.2 Design and Fabrication

Compact casing for commercially available small M228 linear actuator, chamber casing, and insert holder bars [Figure 21 A-C] are designed using a computer-aided design (CAD) software system available over the Internet via software as a service (SAAS) mode (http://www.onshape.com/). Onshape combines traditional modeling tools and design data management in a secure cloud workspace that can be accessed from any device, circumventing requirement for downloading specific software. Users are able to utilize the system via available web browser while eliminating worries of losing data/design.

CAD designs are saved as .STL file and converted to G-code, Numerical Control (NC) positional programming language suitable to 3D print the objects to precise dimensions. DTSD 4.0s, which measures 240mm x 190mm x 28mm (l x w x h), is designed to fit under inverted microscope for data collection. LASER cutting technology is utilized to accurately cut poly (methyl methacrylate) (PMMA), a transparent shatter-resistant thermoplastic, to utilize as a bottom cover of the device. It is attached to device body with stainless steel screws [Figure 21 E]. Plexiglas bottom is critical for biological imaging using inverted microscope and in some cases removable to permit data collection from individual 35 mm dishes used as culture surface. Carefully selected stainless steel screws diminish effects of corrosion and enhance DTSD 4s aesthetically.

A commercially available M228 10s high-resolution linear actuator with C-663.12 stepper motor was used to deliver precise and accurate mechanical stimulations to tissue samples. Linear actuator is controlled by motion control software PIMikromove to deliver step and direction pulses via user-friendly interface to control amplitude and frequency of cyclic stretches. High microstep resolution C-663.12 Mercury step stepper Motor Controller, 1 axis that has a minimum step size of 1μm is utilized.

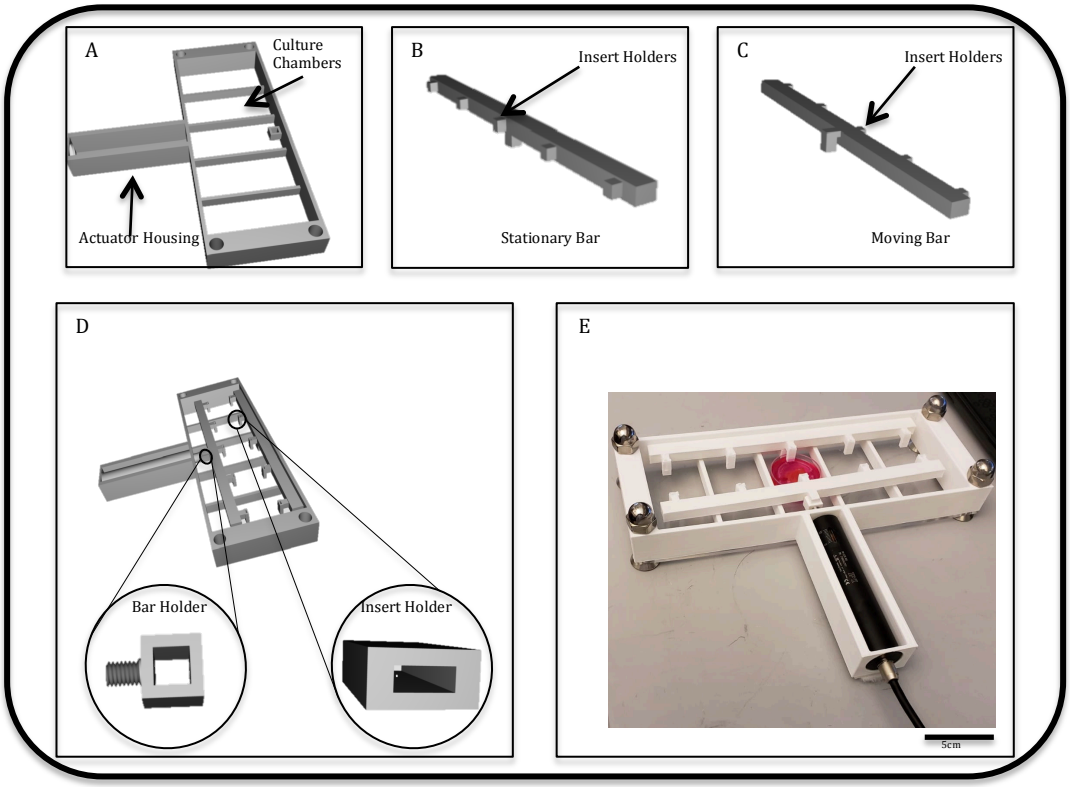

Figure 21: DTSD 4s design and fabrication: A - D) STL files of the various CAD designed parts. E) 3D printed parts put together with a single well and actuator situated in case.

At moving end of linear actuator, a standard M4 thread is exploited to fasten moving bar that holds strainers supporting tissue slice preparation. A small connector is carefully designed with a screw thread to precisely fit M4 opening of linear actuator at one end and provide a hole at the other end to hold moving bar [Figure 21 D]. Both device bars (moving & stationary) are tailored to allow attachment to actuator and chamber wall respectively with other end fitted with 5 holding holes each to secure Nylon cell strainers in each chamber (a zoomed image of one such hole is shown in Figure 21 D). Moving bar moves cardiac tissue slice preparations by specified distances while samples are fixed at the other end with stationary bar to provide uniaxial stretch.

Unlike most devices [145-148], DTSD4s is a multi-well stretcher system allowing multiple (up to 5) samples to be supported and stimulated synchronously and provide a rapid testing to answer questions related to mechanical stimulation. Each of the five chambers has a clear opening that measures at least 4 cm x 4 cm to easily allow 35mm cell culture dishes and provide sterile culture surface for slice preparations. Culture dishes measure 34.8 mm x 10.8 mm (d x h), and can hold up to 3mL of media depending on size of sample. Tissues are supported in suspension in 35mm cell culture dishes to allow superfusion on both top and bottom of the tissue. Culture conditions that allow superfusion on both sides will extend the tissue thickness limitation by two fold from 250µm to 500µm (250 microns on each side).

3.2.3 Slice Preparation

After a careful excision of both atriums and right ventricle using surgical scissors, several cubic chunks slightly larger than 15mm x 15mm x thickness of wall (Length x Width, thickness) of left ventricle wall were meticulously carved out with sterile sharp razor in biosafety cabinet and placed in cardioplegic solution. Tissue blocks are then selected and further interrogated for quality before being trimmed to desired block size. Finally, 500µm-thick heart slices were prepared with Leica VT1000 S Fully Automated Vibrating Blade Microtome. Tissue slices were cut tangential to epicardium, in well-aligned fiber direction. Electromechanical uncoupler 2,3-Butanedione monoxime (BDM) was utilized with tissue blocks to avoid damage during slicing.

3.2.4 Tissue Loading and Device Characterization

To load cardiac slices, high-speed rotary tool, a Dremel was utilized to cut 70µm Nylon mesh sterile cell strainers (Fisher scientific Cat No. 22363548) in half [Figure 22 D&E]. . After cutting, cell strainers were placed in sterile 6 well plates for proper sterilization and placed in UVO cleaner for final safe surface cleaning. Each half was then glued to an end of a section of prepared tissue. Tissue stretching was imaged and length of tissue measured at a start of a cycle (shortest) and halfway through the cycle (longest) on Image J and/or manually using a digital Caliper [Figure 22 C & F respectively].

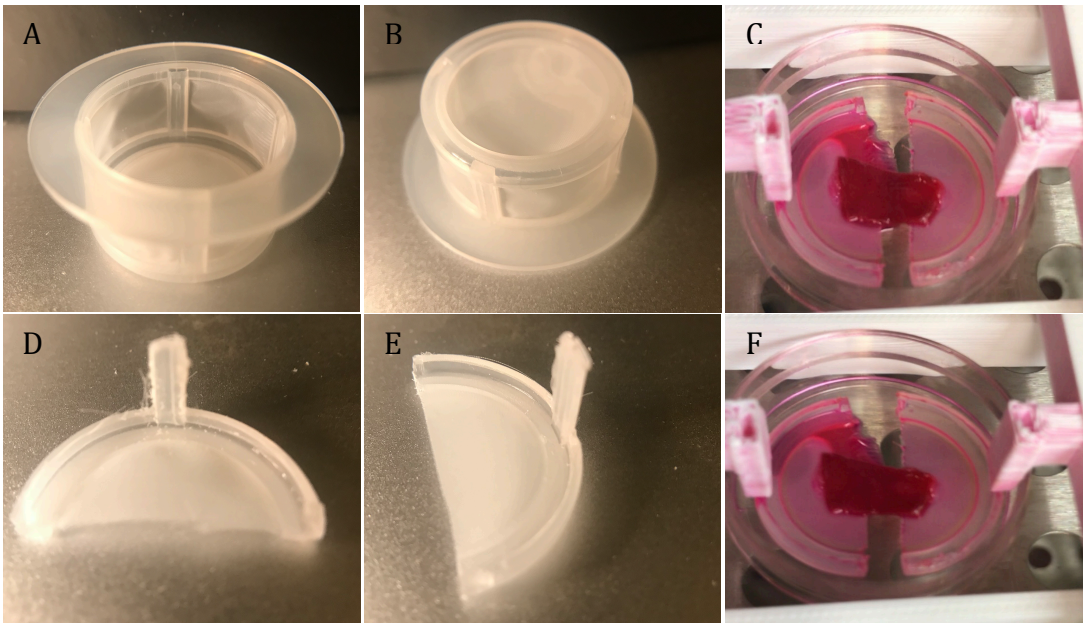

Figure 22: Tissue loading and displacement measurement: A &B) Top and bottom view of sterile cell strainer before cutting. C&F) Tissue slices loaded on device at the end of diastole and at the end of systole respectively. D&E) sterile cell strainers cut in half and ready to be cleaned.

For all five chambers, relationship between input displacement and output stretch distances was determined. Tissue dimension along axis of stretch (along fiber orientation) was measured before 1 Hz stretch and after stretch. The difference (elongation) was also compared for various % strain. Measurements were taken at different time points during stretch. Solidworks, a CAD program, is utilized to simulate and estimate displacement distribution.

3.2.5 Device General Setup

M228 10s stage (linear actuator), C-663.12 step stepper motor controller, PIMikromove motion control software, and connecting wires are purchased as a package (Physik Instrumente, PI). Motor control signals of controller are on the "DC Motor only" Sub-D 15-pin Motor/stage connection (I/O) where cable from M228 stage is connected via an adaptor (C-815.38). Pin includes output, motor control lines and input signals. Mini-B type USB Command routing connects Mercury controller to host PC to interact with motion control software. 15-30 VDC Barrel connector Supplies power to the controller [Figure 23].

Displacement of tissue sample is controlled by a positioner, linear actuator M228 10s stage (Physik Instrumente, PI) powered and controlled by a high microstep resolution stepper motor controller C-663.12 Mercury Step Stepper Motor Controller, 1 Axis that has a minimum step size of 1μm.

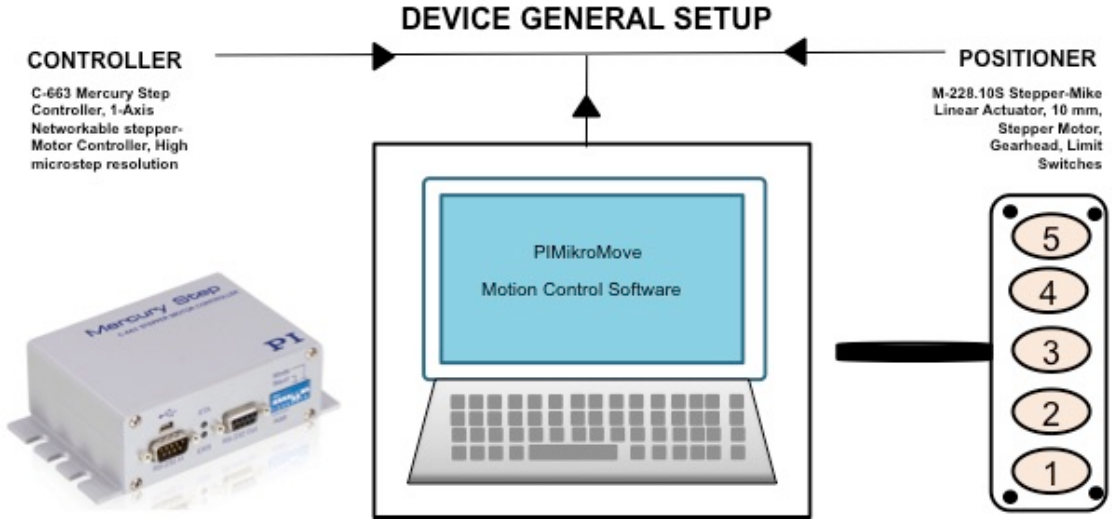

Figure 23: General Device setup: DTSD4s is depicted on the right with the five chambers labeled 1 through 5 (positioner). It is connected to the controller via Sub-D 15-pin Motor/stage connection I/O. In turn, controller is connected to computer running PIMikromove motion control software where motion commands are entered.

Range of actuator is 10mm, which is the maximum stretch that can be applied to any sample. Command to linear actuator is controlled by PIMikromove software to deliver step and direction pulses to the actuator through the C-663 controller. User-friendly interface is available on the software to control amplitude and frequency of the cyclic stretches.

3.2.6 Statistical Analysis

All experiments were performed at least 3 times and analyzed by GraphPad Software Prism.

3.3 Results and Discussions

3.3.1 Device Calibration

The relationship between input and output stretch distances for cyclic stimulation performed at 1 Hz on all culture chambers (five) is shown in Figure 24 below. Only physiologically relevant stretch distances between 0.5mm to 2mm representing 5% to 20% elongation respectively are considered here. The linear fit has a slope of 0.784, 0.773, 0.943, 962, & 0.775 and R^2 of 0.988, 0.952, 0,999, 0.982, & 0.930 respectively for chambers one through five (as indicated in Figure 23) exhibiting that the output distance was consistent and linearly correlated to input distance over entire range of actuator movement. For chamber 5 the relationship is a little distorted especially at the 1.5mm input stretch distance where output was only a little over 1mm. For chamber 3, middle chamber directly in the line of motion of the linear actuator, output value accurately captures the input entered via the computer. Though more runs are required, preliminary runs indicate that output distance may be linearly related to input values for other frequencies [besides 1 Hz; tested frequencies (0.5 & 1.5 Hz, $n < 3$)] in all the five chambers.

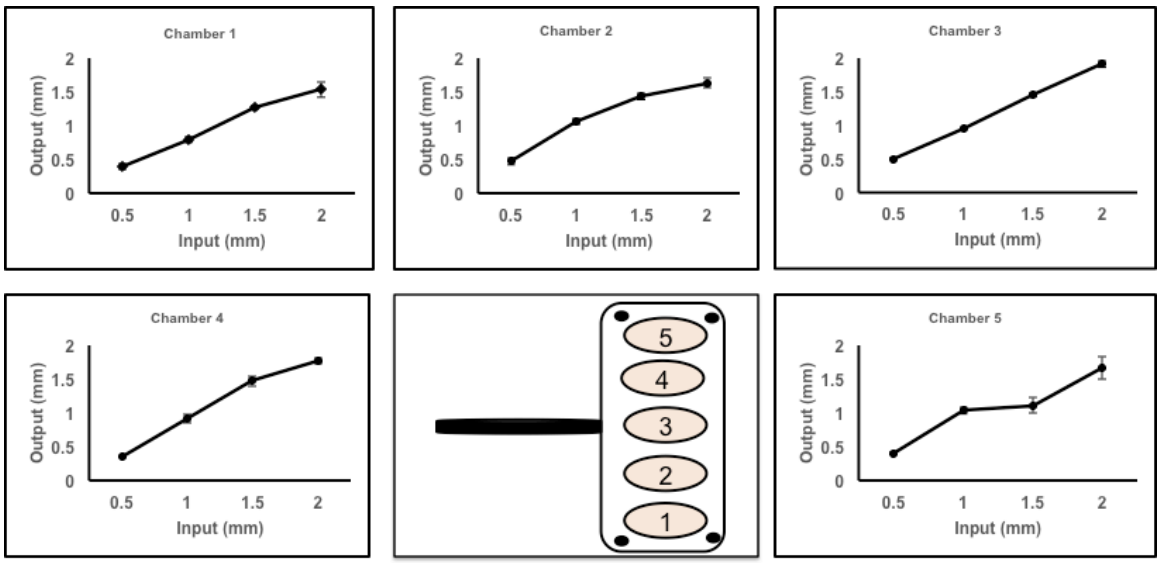

Figure 24: Relationship between Input and Output distances for all five chambers. The linear fit has the following slope and R^2 Value for all chambers; Chamber 1 [m = 0.784, R^2 = 98.8%], Chamber 2 [m = 0.773, R^2 = 95.2%], Chamber 3 [m = 0.943, R^2 = 99.9%], Chamber 4 [m = 962, R^2 = 98.2%], Chamber 5 [m = 0.775, R^2 = 93%]. Middle image in the bottom row represents the order of chambers.

The motion of the actuator was reproducible over several hours of the experiment, as some measurements were taken hours after commencement of continuous cyclic stimulation. Even after 10 days of stimulation, the input and output stretch distance relationship for some samples did not show significant change. We recommend DTSD4s be calibrated before use with a well characterized and well understood soft material.

3.3.2 Device Strain Profile

Next we set out to evaluate displacement and strain profile of cardiac tissue slices supported by our device during applied uniaxial stress. Several videos were recorded (https://drive.google.com/drive/folders/0Bz4Etlpp0yyAS2EwYWhEZkI3eWc?usp=sharing) under an inverted microscope to characterize the strain field using Particle Image Velocimetry-Data Image Correlation (PIV-DIC) analysis. This type of analysis relies on tracing contrast from frame to frame which was lacking from our captures. Perhaps, in the future, it is feasible to utilize some sort of contrast-enhancement techniques to aid analysis [149]. Possibly, we would be able to seed micro-particles on the surface of tissue sample preparations to create a traceable contrast. Poor focusing of samples as they move in the Z direction with every cycle further exacerbates the above-mentioned challenge. Therefore, other ways of determining or estimating strain and displacement profile was explored. We utilized Solidworks static simulation, a structural analysis tool that uses Finite Element Analysis (FEA) to predict a material's mechanical behavior by virtually testing CAD models. One-way uniaxial stretch to material dimensions 10mm x 10mm x .5mm (l x w x h) under linear elastic conditions to produce up to 20% elongation was performed to obtain strain and displacement results [Figure 25].

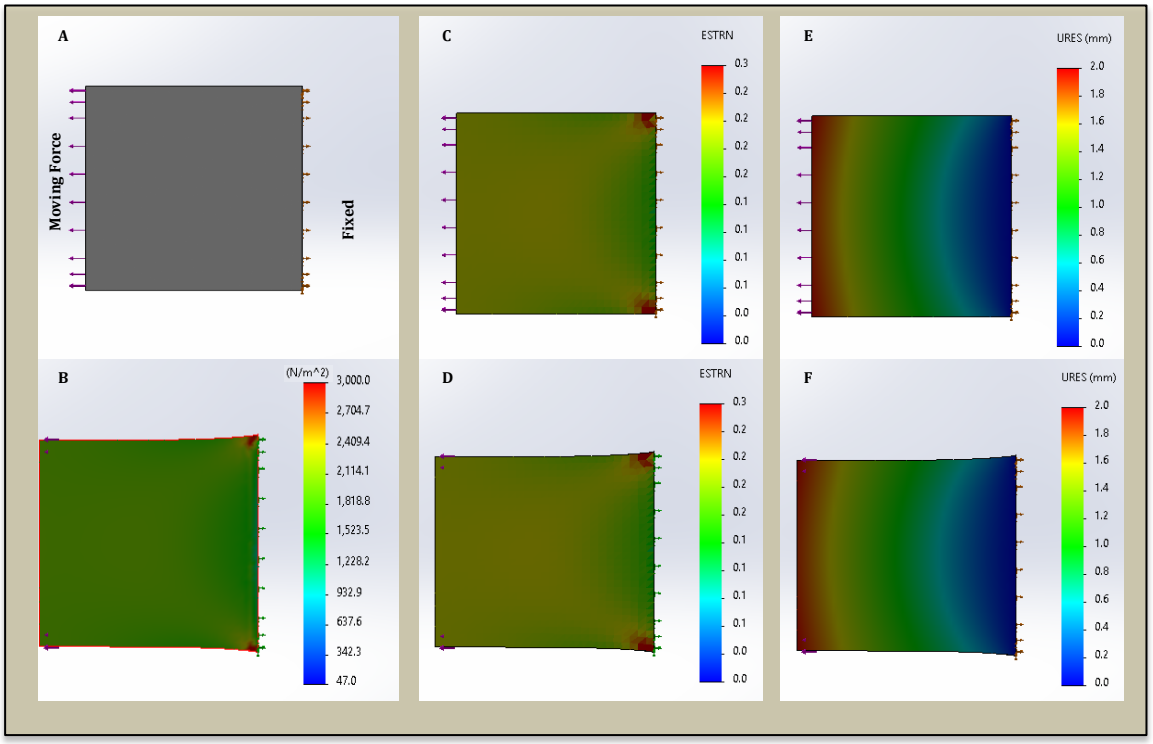

Figure 25: Device characterization: Simulation of force applied on a 3D model of tissue slice preparations (data shown in 2D). A) Material with forces applied (undeformed); right face was fixed and a force of 0.01N is applied on left face (purple arrows). B) Stress profile with mostly uniform distribution of ~2000N/m^2 over material body. C&D) strain (ESTRN) profile of material with uniform [.2] distribution in the middle of sample (yellow space) E&F) Resultant displacement (URES) distribution with varying values with higher displacement where force is applied

Several critical assumptions were made to arrive at the above simulation results. One of the difficulties encountered setting up simulation for the model cardiac slice is the fact that the myocardium is a composite structure (further complicated by slice loading method using glue). In this study, we simplified the problem by assuming the simplest law for solid materials, the theory of linear elasticity, which presents a linear relationship between applied stress and resulting strain. We believed the assumption is fair predicator of response of materials undergoing small deformations. In addition, with applied cyclic load, internal myocardial fibers align in the direction of loading and prompt Pseudoelastic state where the tissue structure no longer changes with cyclic loading. Attempt was made to carefully select all other parameters required to determine the properties of preparations. Young's modulus (E) was set at 10kPa [150] [Figure 26] and because of myocardium's incompressibility, it was simulated with a Poisson's ratio (v) value of 0.499.

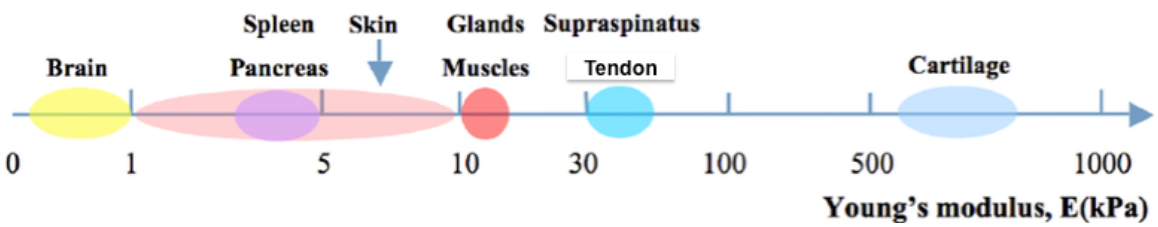

Figure 26: Young's Modulus (E) of biological tissues and Organs. Muscles such as the heart have E value approximately 10kPa [150].

Since DTSD4s is designed to deliver a uniaxial tension in x-direction at one end of tissue sample (along fiber direction) while the other end is stationary, right face of CAD model was fixed and a force of 0.01N force applied on the left face. Stress require was calculated to determine input force needed to cause a 20% elongation (physiological value) via Hooke's law (eq. 3.1) for elastic material

$$\textbf{Stress } (\sigma) = E^{*}\varepsilon \qquad 3.1$$

where E is Young's modulus (10kPa), ε is strain (.2). Force is then calculated using equation 3.2

$$F = \textbf{Stress } (\sigma)\ ^{*}A \qquad 3.2$$

where F is the applied force and A is cross section area of tissue (thickness x Length of tissue). Strain (ESTRN) profile under specified conditioned yielded a uniform distribution of approximately 20% value in "area of interest", middle of tissue sample preparation. ESTRN (ε) displays change in length per unit length. If Δ represents local change in length and L_0 represent initial local length, then the ESTRN is given by equation 3.3.

$$\textbf{ESTRN} = \Delta/L_0 \qquad 3.3$$

Resultant displacement (URES) distribution shows displacement of 0mm at fixed side and progressively increases to 2mm at site of tension application. These displacement values are not local displacement values in the x-direction, rather the local resultant displacement values in all directions as shown in equation 3.4

$$\textbf{URES} = \sqrt{[(\Delta x)^2 + (\Delta y)^2 + (\Delta z)^2]} \qquad 3.4$$

where Δx, Δy, and Δz are local displacements in the x, y, and z direction respectively. These simulations render expected uniform strain field in "area of interest", where we foresee characterization and experimental designs will focus. However, much better and accurate determinations of strain field distributions of actual device-supported slices are

not only insightful but also necessary to validate the use of this platform as a model for cardiovascular research.

3.4 Discussion and Conclusions

Currently established in-vitro cell culture systems are relatively less cumbersome, allow carefully controlled experiments, and have been instrumental in revealing many cellular and molecular mechanisms. However, their oversimplified nature only minimally recapitulates the physiological *in vivo* environment and results obtained can often be inaccurate and/or misleading. Under physiological conditions, cardiac cells are coupled to each other electrically, mechanically and metabolically. Therefore, use of a multi-cellular tissue is a more relevant model that will provide a physiological environment similar to that of a whole intact heart. Models that mimic physiological cardiac niche simultaneously rendering the experimentalist a precisely controlled electromechanical environment are almost a requirement. With lack of adequate *in vitro* tissue explants it is difficult to examine potential therapeutic solutions for MI. In that accord, a stable *in vitro* model with intact cardiac multicellularity, architecture, and physiology is necessary to bridge the gap between conventional cell cultures and *in vivo* animal studies.

Organotypic tissue slice cultures have been a widely utilized platform to study organ systems such as liver, brain, and kidney. In recent years, as superior precision slice preparation technologies and techniques are emerging, living cardiac tissue slices have become an increasingly popular platform to study the heart and supplement findings from isolated cell, co cultures, and perfused whole/wedge heart preparations. These slice preparations preserve the native tissue environment with intact cell to cell and cell to matrix electrical and mechanical communications and have been shown to exhibit similar electrophysiology to the intact heart. They have several advantages as they only present moderate complexity and allow the experimentalist reasonable control while possessing all cell types found in the native tissue. Although these living cardiac tissue slice preparations have previously shown robust survivability in culture, significant mechanical and electrophysiological remodeling has been observed in long-term cultures.

In order to enhance cardiac tissue slice viability and expand experiments beyond an acute time tests, we developed a uniaxial stretching device capable of delivering cyclic stretch to *ex vivo* heart slice to enable long-term studies. Our multi-well cardiac tissue stretcher system (DTSD4s) allows for simultaneous multi sample stimulation for rapid experimental testing. Device characterization revealed that the output distance of actuator was consistent and linearly correlated to input distance over entire range of movement. To our knowledge, this is the first device to directly support thin myocardial slices in a chamber and deliver cyclic mechanical stimulation. Furthermore, our tissue-stretching device is designed as a high throughput system that can stimulate up to five samples under nearly identical mechanical conditions and separate culture condition for

possible biochemical test. Our device has several limitations (tissue loading requires using glue, imaging for data collections needs improvement, chambers on the extremities produce slightly inaccurate output, and doesn't allow to gather any stress or stiffness data) and our characterization techniques should include better strain profile depiction. Nonetheless, we have taken a step in the right direction in establishing an *in vitro* model that will allow long-term cardiac slice studies.

Chapter 4. Characterization of Mechanically Stimulated Cardiac Tissue Slices

4.1 Introduction

4.1.1 Cardiovascular Research Platforms

The main manifestation of cardiovascular disease is the Coronary Heart Disease (CHD) [151], which is defined by thrombosis on inner walls of coronary arteries, impeding flow of blood to downstream areas of cardiac muscle walls. These obstructions lead to perfusion imbalance and hinder oxygen and nutrient delivery locally to parts of the heart muscle, leading to myocardial hypoxia and accumulation of waste metabolites [152, 153]. If blockage is severe enough, it can lead to a myocardial infarction (MI). MI, known commonly as a heart attack, starves the heart tissue of oxygen for a period of time, and subsequent damage and remodeling can often lead to progression towards heart failure. Adult heart muscle cells do not contain a significant pool of endogenous stem cells and do not exhibit substantial proliferative capabilities to effectively regenerate after major injury. Regenerative cell therapy has emerged as a novel and promising candidate to potentially provide curative treatments for various debilitating ailments including cardiovascular diseases [154, 155]. Although translating stem cell therapy to a potential restorative treatment for individuals with cardiovascular disease has become a realistic goal, a great deal remains to be explored at the molecular level in understanding various complex mechanisms involved [156]. Consequently, our ability to develop effective therapeutic approaches to restoratively address cardiovascular maladies has been limited. To elucidate our understanding of cardiac regenerative potential, cardiovascular pathology, and potential therapeutic solutions requires model systems that allow for thorough and applicable investigations.

An ideal cardiac research platform should be physiologically representative of the native human cardiac environment, allow for easy manipulation, permit data collection, fairly inexpensive, ethically sound, and render reproducible results. To date, there is no universal model system that meets all of these desired criteria, as one condition is usually opportunity cost of another. For example, single CM analysis allows for comparatively easy manipulation and divulges vital information on cardiac physiology and CM mechanical properties [157], but is a poor representation of cardiac physiological milieu.

In vitro models range from simple 2D culture system to whole heart Langendorff preparations [Figure 27]. These models have been deployed to capture various aspects of cardiac regeneration and pathology.

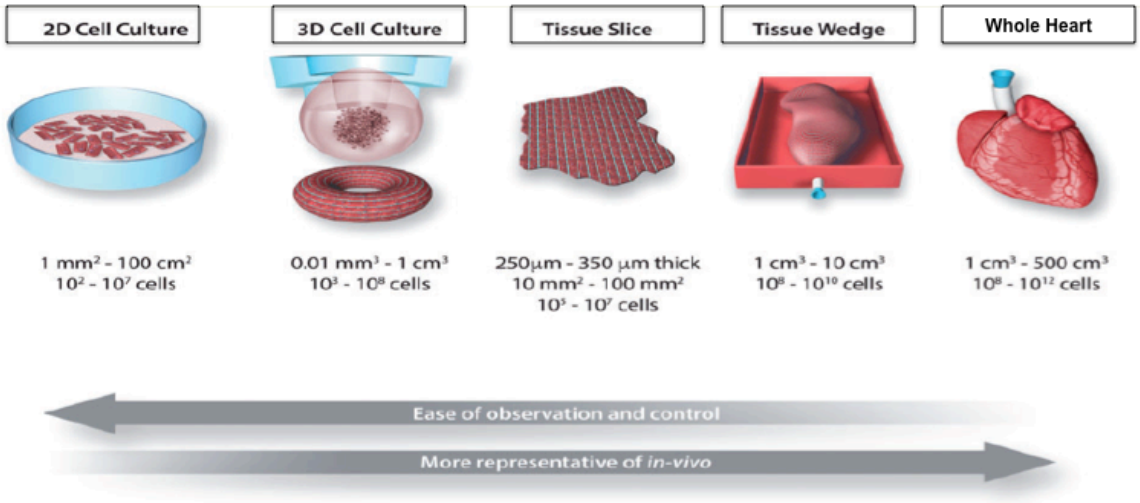

Figure 27: *In vitro* experimental model systems for cardiovascular research: Model systems from left to right are: 2D cell culture, 3D cell culture, tissue slices, coronary perfused tissue wedges, and Langendorff perfused whole heart [158]

As shown in figure 25 above, regenerative research *in vitro* models routinely utilized includes: two-dimensional (2D) cell culture, three-dimensional (3D) cell culture, tissue slice, tissue wedge, and whole heart preparations. CMs grown in 2D culture systems are relatively accessible and have been indispensable in elucidating and validating a wide range of mechanisms such as cardiac regeneration [159], Cardiac physiology [160], signaling pathways [161], and pharmacological investigations [162]. However, their simplified nature only remotely recapitulates *in vivo* physiological environment it attempts to represent. 2D culture systems may contain a single cell type or a co-culture of two or more cell types. Although 2D cultures comprising of a single cell type offer a simplified model for scientific inquiry, they are a poor representation of the complex microenvironment found in multicellular tissues. To assess regenerative medicine potential, relatively physiologically relevant *in vitro* co-culture model systems using human primary cells have been developed to aid in cell-cell and cell-matrix interactions at the cellular and molecular levels (reviewed [163]). For example, arrhythmogenic risk of cardiomyocyte progenitor cells (CMPCs), viable candidates for regenerative cell therapy, were evaluated by co-culturing them with neonatal cardiomyocytes [164]. However useful in elucidating fundamental mechanisms and relatively easy to maintain in culture, expanding cell lines, and investigate them under defined and controlled conditions, results from 2D culture should be considered with skepticism as they are imperfect and can be misleading [112, 165].

Current 3D cultures methods aim to better meet the motivation for developing accurate predictive models to properly inform pre-clinical and clinical studies. Engineered heart tissues (EHT), a scaffold matrix with cells and spheroids, smaller self-assembling cellular aggregates have been the forefronts of 3D culture system addressing physiological and pharmacological inquiries [166-169]. Although these 3D engineering approaches closely mimic intact myocardium and open gates to new opportunities for cellular therapy, they are more expensive, time-consuming, harder to control, do not

contain physiological ECM, and challenging to keep in culture than standardized 2D cultures.

Lastly, the Langendorff perfused whole heart and coronary perfused intact cardiac tissue wedge preparations can provide valuable information to study tissue level physiology, but there are considerable impediments hampering the translation of discoveries made in animal models into human. These preparations allow for limited control by investigators and are difficult and/or expensive, requiring large number of animals. Furthermore, wedge preparations do not allow for long-term studies and only serve as acute heart model as they can be maintained in culture for only a few hours.

Before the turn of this century, vital cardiac tissue slice preparations received less attention than isolated single cells, cell cultures, or whole heart perfused preparation in cardiac research. However, in the last decade, use of organotypic slices of the heart have been gaining popularity as sectioning technologies on live cardiac tissue slices have improved. These are the most promising platforms for conducting cardiac research as they maintain native multicellularity, present moderate complexity, retain complex extracellular architecture and well-preserved cell-to-cell electrical, mechanical & metabolic connections. Myocardial slices are viable, ultrathin (< 500-μm) slices of myocardium of the left ventricle with intact native multicellularity, architecture and physiology of the heart. Although cell and tissue therapies have potential to improve heart function after MI, it is expensive and challenging to conduct controlled studies of graft cells or tissue integration in current *in vivo* MI models. It is difficult to identify precise repair mechanism in the absence of *in vitro* models that allow long-term assessment of transplanted cells. Therefore, there is a need for *ex vivo* model that can help assess the survival, differentiation, and integration of the injected donor cells.

4.1.2 Cardiac Organotypic Tissue Slices as a Model

The need to establish an *in vitro* platform with better physiological representation has been explored as early as the beginning of the 1900s when a group employed a method to isolate pieces of embryonic tissues known to give rise to nerve fibers [170]. However, the first published report with the term "organotypic" was in 1954 on differentiation of chick embryo eye [171]. Since then, organotypic tissue slice cultures have been widely utilized as a platform to study diverse physiological mechanisms in various organs such as lungs, intestine, liver, brain, and kidney [121, 172-175]. The preparation of these ultra-thin slices for *ex vivo* studies utilizes a technique that renders reproducible precision-cut sections, a very good alternative to expensive and time consuming *in vivo* work while possessing many of the attributes of the intact organ. In the past decade, living cardiac tissue slices have become increasingly popular as a platform to study the heart and supplement findings from isolated cell, co-cultures, and perfused whole/wedge heart preparations [74, 147, 158, 176, 177]. These slice preparations preserve the native tissue environment with intact cell to cell and cell to matrix electrical and mechanical communications and have been shown [in slices from various animals] to exhibit similar electrophysiology to the intact heart [126, 178]. They have several advantages as they only present moderate complexity and allow the

experimentalist reasonable control while possessing all cell types (and ratio) found in the native tissue.

Extracting ultra-thin slices also makes it possible to generate numerous slices from the same heart, reducing the need for a large number of animals. Their thinness permits the diffusion of oxygen and other necessary small molecules even to cells at the innermost part of the slice, avoiding the need for coronary perfusion, as is the case for other preparations. Although these living cardiac tissue slice preparations have previously shown robust survivability in culture, significant cellular mechanical and electrophysiological dedifferentiation is a problem [118, 146]. Brandenburger et al. observed decline in the action potential (AP) and conduction velocity in cardiac tissue slices cultured in liquid air interface over 28 days. The characteristic phase 2 (plateau phase) of the AP was diminished, conduction velocity dropped dramatically, and action potential duration 20 (APD_{20}) declined to half its value compared to acute slices [Figure 28 A - C]. Similar decline manifested in the mechanical properties with significant loss in contractility just after a day in culture [Figure 28 D – F].

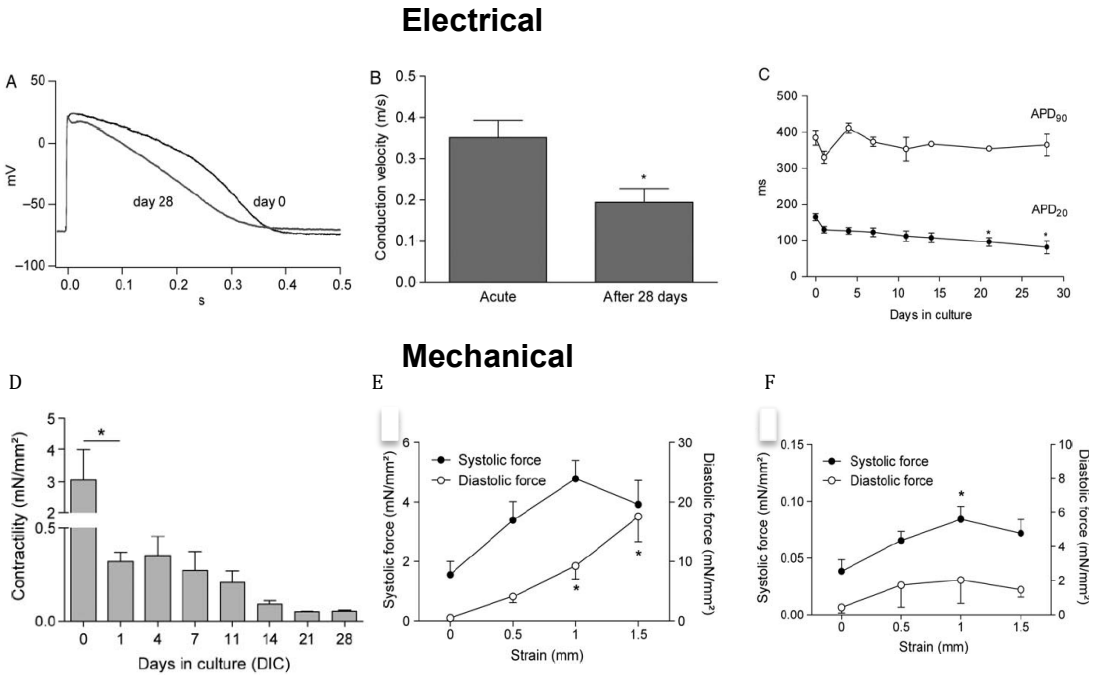

Figure 28: Electrophysiological parameters and mechanical properties of acute vs. cultured slices. A) Representative action potential of acute slices and slices at 28 days in culture, with diminished characteristic phase 2. B) Conduction velocity has dropped < 0.2 m/s in cultured slices. C) APD_{20} declined from 180ms to under 100ms. D) Contractility of slices had significantly declined even after one day in culture. E & F) Kinetics of diastolic force has dramatically altered in cultured slices (F) compared to acute slices (E). (Figure adapted from published work[118])

The exact factors involved in CM dedifferentiation and structural degradation in tissue slice cultures or immature phenotypes observed in standardized cell cultures are not well understood. However, one fact is clear, there are several factors at play

influencing cardiac phenotypes, one of which is presence of all native cell types along with the supporting ECM. Despite the presence of multicellularity with intact cell- cell and cell-matrix interaction in cardiac slice preparations, tissue integrity continues to be compromised over time in culture, limiting their use to acute studies and not allowing critical long-term investigations necessary to delineate mechanism in cardiovascular research. Introducing mechanical stimulation to cardiac tissue slices has been shown to modulate structure and function of CMs and other supporting cells [146, 147, 177]. In 3D engineered human myocardium for example, it was observed that cyclic stress conditioning resulted in significant increase in CM hypertrophy and proliferation [179].

4.1.3 Role of Mechanical Stimulation in Cardiac Remodeling

Under physiological conditions, the myocardium undergoes stress with every heartbeat. When the heart muscle is stretched (increased EDV), its force of contraction increases according to the Frank-Sterling law. Cultured human ESC and iPSC-CM express fetal-like spontaneous contraction, ion channel expression [180], electrical propagation [181], and physical characteristics. In order to further CM maturation, researchers are beginning to engineer stem cell microenvironments that incorporate mechanical signals along with the cell-cell contacts and soluble growth factors that have been previously optimized [182, 183]. Over the past decade, it has become increasingly apparent that mechanical signaling is a critical component of this cardiovascular microenvironment. Mechanical loading has a dramatic effect on the ECM production of CM [184], increases intracellular protein content [185], as well as their cytoskeletal organization, alignment, and proliferation [186]. Therefore, a number of groups have begun using micromanipulation devices for stretching cardiac cells [187]. Specifically, when cyclic strain was applied to stem cell-derived CM, the fetal-like CM exhibited elevated cardiac markers. When implanted into a mouse, the stretched cells also had less scar tissue formation, lower apoptotic activity, higher VEGF expression, and increased angiogenic activity [188].

External load also plays a critical role in determining muscle mass and phenotype in CM. The cells have the ability to sense mechanical stretch and convert it into the intracellular growth signals, which lead to hypertrophy. Mechanical stretch of CM *in vitro* increases the calcium sensitivity of the heart's contractile machinery and causes activation of multiple second messenger systems that are very similar to growth factor-induced cell signaling systems. Another significant component of heart tissue is the micro and nano extracellular architecture. Mature adult CM exhibit an elongated rod-like shape with well-developed contractile apparatus and intercalated discs as electromechanical cell end-to-end couplings. The existence of an organized structure in the cardiac cells can be identified by the striated pattern observed after staining for contractile proteins. Gap junctions, located in intercalated discs at the ends of cardiac cells, are responsible for rapid propagation of electrical signals between the cells. However, in standard tissue culture set-ups, the CM will often undergo dedifferentiation and lose many of these key physiological features, including their elongated shape and defined contractile apparatus. It is thought that the dedifferentiation is due to the lack of appropriate micro-

environmental cues in prolonged cultures. It has been shown that the alignment of cardiac cells, not only helps limit cell dedifferentiation by increasing the continuity of cell-to-cell connections, but also has a profound effect on impulse initiation and propagation velocities [189]. Moreover, cell culture systems that additionally provide signals to induce anatomical anisotropy of cardiac cells lead to larger cellular coupling resistance in the transverse (along short cell axis) compared with the longitudinal (along long cell axis) direction, resulting in a smaller velocity, but larger maximum slope of action potential upstroke [190]. Mimicking the heart's unique topographical signals induces alignment of both CM [190] and endothelial cells (EC) [69], facilitating more uniform electrical propagation and subsequent mechanical contraction of the heart cells [190]. In order to enhance cardiac tissue slice viability and counteract dedifferentiation, we designed and developed a simple user-friendly tissue-stretching device that provides cyclic mechanical stimulation to *ex vivo* heart slices allowing their maintenance and manipulation. Here, we report that cyclic uniaxial physiological relevant load maintains tissue integrity for up to ten days in culture.

The specific goals were to optimize cardiac tissue slice preparation for use as a model system and utilize our multi-well cardiac tissue stretcher developed to deliver uniaxial cyclic stretch to the cardiac tissue slices in a controlled environment. Here, we compared 10-day results from connexin43 & α-actinin expression of tissues supported with our device and those that were chronically unloaded. We also compared alignment data.

4.2 Materials and Methods

4.2.1 Heart Collection

Porcine hearts were obtained from a local slaughterhouse (Clausen Meat Co., 19455 E Clausen Rd, Turlock, CA). They immediately remove the heart after slaughtering and immerse it in a bag with ice while we are in route to collect it. Heart is then transferred to an ice filled chest cooler while in its original bag for transportation, and delivered to laboratory in approximately 40 minutes of travel time (making total time since removal approximately one hour). In the laboratory biological safety cabinet, tissue blocks are carefully and methodically prepared as quickly as possible. On arrival, the heart is taken out of the chest cooler and bag and placed in ice-cold (4°C) cardioplegia solution (Table 4) in biological safety cabinet. As much blood as possible is flushed out of the coronary arteries with the solution by inserting a syringe in aorta and other openings. The heart is then ready to be cut into blocks that will produce the organotypic slices.

Table 4: Preparation of 1 liter of cardioplegia solution.
Add the following to 1 liter of dH_2O

Solid reagents		
	Mass (g)	Final concentration (mM)
Glucose	0.99	5.50
Magnesium sulfate	0.13	0.50
Potassium chloride	1.79	24.00
Sodium bicarbonate	1.68	20.00
Sodium chloride	6.37	109.00
Sodium phosphate monobasic monohydrate	0.12	0.90
Solution		
	Volume (ml)	Final concentration (mM)
1 M Calcium chloride	1.80	1.80

4.2.2 Slice Preparation

After excision of both atriums in dissection container filled with Tyrode's solution with the excitation-contraction uncoupler 2,3 butanedione-monoxime (BDM), the right ventricle was carefully removed by using surgical scissors to cut the heart along the interventricular septum so that the septum remains intact with the left ventricle. The septum is then cut longitudinally from the superior side down to the inferior side (the apex) to open the left ventricle. The trabeculae and papillary muscles revealed were removed from the endocardium, and several cubic chunks slightly larger than 30mm x 30mm x thickness of wall of left ventricle wall were meticulously carved out with sterile sharp razor in biosafety cabinet and placed in a conical tube filled with Tyrode's solution containing BDM. Tissue blocks are then selected and further interrogated for quality before being trimmed to desired block size (20mm x 15mm x 6mm) [Figure 29]. Desired tissue blocks have minimal visible damages, do not possess fatty like areas, do not contain an artery filled with blood clot, and are generally healthy looking. Tissue blocks were glued with the epicardium face down to provide a flat surface. Finally, 500µm-thick heart slices were prepared with Leica VT1000 S Fully Automated Vibrating Blade Vibratome. Tissue slices were cut tangential to epicardium, in well-aligned fiber direction.

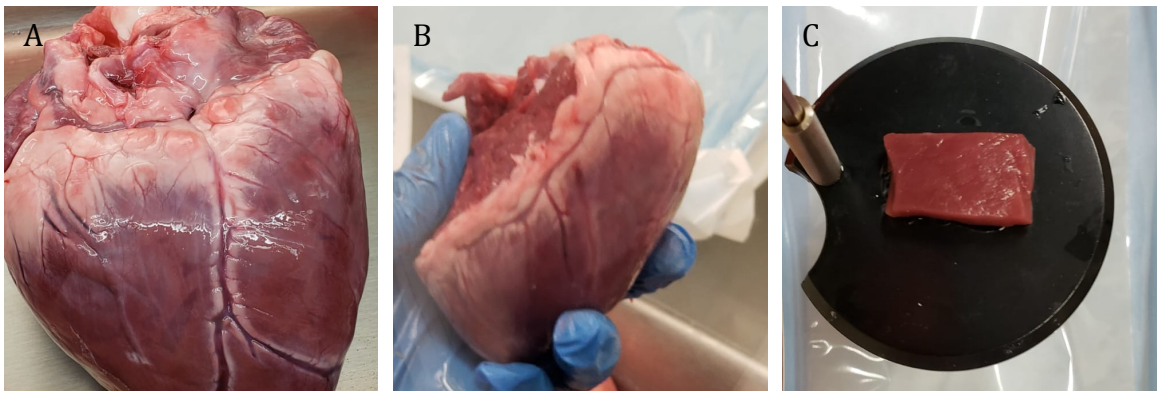

Figure 29: Porcine heart block preparation for slicing: A) Heart with the right ventricle on the right and atriums on the back (some blood can be seen in the coronary arteries). B) Heart after both atriums and right ventricle are removed and intact interventricular septum. C) Final 20mm x 15mm x 6mm tissue block on removable vibratome stage base.

The stage of the vibratome was submerged in tyrode's solution with electromechanical uncoupler 2,3-Butanedione monoxime (BDM) (Slicing solution Table 5) to immobilize tissue blocks and avoid damage during slicing. The bath was bubbled with oxygen via a tube connected to a small external min oxygen cylinder. Each tissue slice produced is transferred to a 60 mm tissue culturing well with medium 199.

Table 5: Preparation of 1 liter of slicing solution (Tyrode's solution + 30 mM BDM).
Add the following to 1 liter of dH_2O

Solid reagents		
	Mass (g)	Final Concentration (mM)
BDM	3.00	30.00
Glucose	1.86	1.00
HEPES	2.38	10.00
Potassium chloride	0.45	6.00
Sodium chloride	8.18	140.00
Solutions		
	Volume (ml)	Final Concentration (mM)
1 M Magnesium chloride	1.00	1.00
1 M Calcium chloride	1.80	1.80

4.2.3 Tissue Culture

Each tissue slice is transferred to a 60 mm tissue culturing well with medium 199 to a biosafety cabinet to prepare for culture. All transfers are done carefully using a Pasteur pipette to avoid dropping and/or sucking tissue and causing damage. Slice was washed with PBS containing 3% penicillin–streptomycin at room temperature. Then we transferred slices onto the surface of cell strainers positioned in a 6 well plate submerged in medium 199 (with 3% penicillin–streptomycin + 0.001% ITS liquid media supplement) or load onto device for mechanical stimulation. In culture dish, slices were rested flat on strainers. Unloaded culture slices in 6 well plate and loaded culture slices

supported by device were transferred to humidified incubator at 37 °C with 5% CO_2. We replaced medium every day, monitoring for any contamination.

4.2.4 Hematoxylin & Eosin (H&E) Staining

To observe cell morphology and viability we stained slices using Haematoxylin and Eosin staining protocols. Tissue was processed and paraffin block embedded for microtomy where they were sliced into thin sections and several slides generated for chronically unloaded slices and slices subjected to cyclic uniaxial stimulations at different days of interest (Day 0, Day 1, Day 3, Day 5, Day 7 and Day 10 - Day 3, 5, and 10 not reported). We then followed standard protocol adopted from Baylor College of medicine. Briefly: Slides containing paraffin sections were placed in a slide holder to deparaffinize and rehydrate sections. After blotting excess water, slices were stained with hematoxalin. Once again, excess water blotted from slide holder before staining with eosin. Finally, cover slip was carefully placed without formation of bubbles.

4.2.5 Fixation and Histological/Immunohistochemical Staining

The explanted heart slice was assessed by standard histology followed by staining for structural and functional proteins at Day 0, Day 1, Day 3, Day 5, Day 7 and Day 10 (only reported Day 0 and Day 10). Specifically, formalin-fixed sections were stained for cardiac structural and electromechanical proteins: alpha-sarcomeric actin and connexin43, respectively. Fixed cardiac slices were permeablized and blocked, incubated in a conjugated primary antibody in PBS at 4 °C overnight, and washed in PBS for three times.

4.2.6 Stimulation Protocol

Cardiac tissue slice preparations were loaded onto all five chambers at the same time and subjected to mechanical stimulation starting on day zero, and stored in the incubator with daily media changes. Samples were attached to the device by gluing them onto a modified (cut in half and trimmed) tissue culture insert and stretching was performed on the five samples simultaneously. Chronically unloaded cardiac tissue preparations were maintained as controls for each of the days of interest (day 0, day 1, day 3, day 5, day 7, and day 10) with daily media change as well. The stimulus delivered was a uniaxial cyclic stretch with fixed strain amplitude and frequency. Strain amplitude of 12 - 20% and frequency of 1 Hz were utilized for the purpose of this study. Stretched samples were removed from each chamber at the different dates of interest and portion of the sample that were glued were discarded and only the portion of the sample that is in the middle was collected for analysis.

4.2.7 Statistical Analysis

Quantified was done using Image J and analyzed by GraphPad Software Prism.

4.3 Results

4.3.1 Cardiac Slice Preparations

Cardiac tissue slices bridge the gap between cell culture and whole heart preparations. In our preparation, we directly glue the epicardium to the vibratome stage and produce 6-7 slices per tissue block [Figure 30].

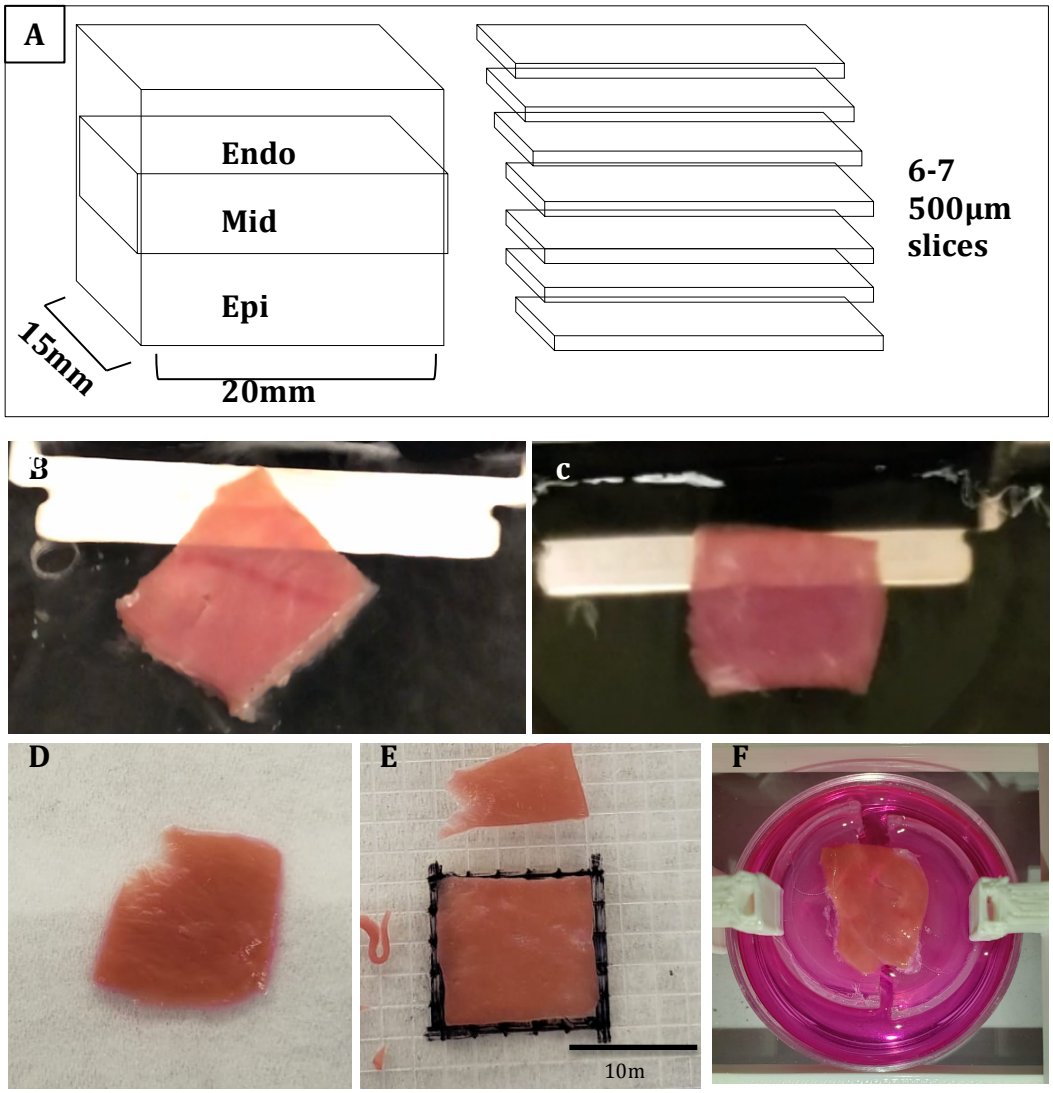

Figure 30: Myocardial tissue slice preparation: A) schematic drawing showing the position and slice direction of ventricular tissue blocks. B &C) Cardiac slices images captured from video while vibratome is running (0.05mm/s) D) Fresh slice, photograph taken right after slicing E) slice trimmed to desired dimensions and uneven edges removed. Aligned area of the slice was confirmed under a microscope before trimming. F) Tissue slices [both loaded and unloaded] were cultured in the same manner glued onto inserts

Schematic is intended to show the orientation of the tissue block during slicing and not the proportion of the various layers. Since the mid myocardium in normal hearts is the

thickest, leading to optimized cardiac output [191], slices produced from our 6mm thick pre-slicing tissue blocks are mostly from this layer alone.

Changing the orientation of tissue blocks on vibratome stage further optimized cutting slices. We reduced the blade-tissue contact from about 10mm line to a point (approximately 1mm) simply by altering orientation of tissue blocks from "side" to "diagonal" [Figure 30 B & C]. The orientation in B presents a small contact area to start slicing and gradually increase then at the other end decrease again to finish slicing at a point allowing better cutting efficiency. Blade speed was increased from 0.03mm/s as reported by others [119, 176] to 0.2 mm/s, significantly decreasing the amount of time from 6 minutes to under 2 minutes to obtain a slice. During cutting with "side" orientation, tissue buckling (folding under blade) makes it impossible to generate a slice at 0.2mm/s speed [Figure 31].

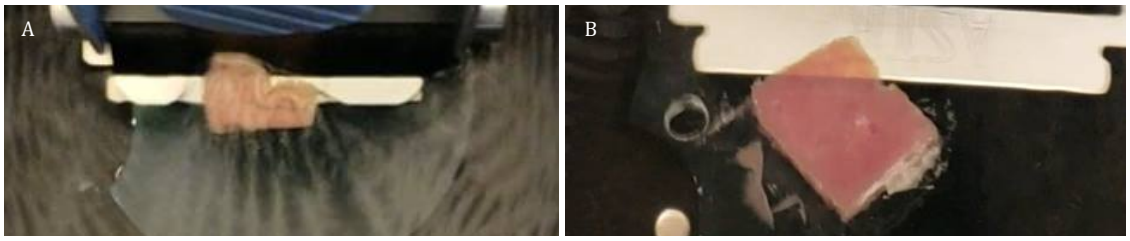

Figure 31: Optimization of tissue slicing speed by altering cutting orientation. A) Slice in "side" orientation at 0.2mm/ s buckles under the blade and B) Slice in "diagonal" orientation at 0.2mm/s does not buckle. .

Our 500µm slice dimension (for better anchorage) is slightly thicker than other groups reported at 300µm - 400µm [73, 142, 143]. Diagonal orientation may not significantly disrupt tissue fiber orientation any more than the side orientation. A slightly higher frequency of almost 100 Hz was used in all slicing.

4.3.2 Static Cultured slices lose their tissue integrity over time

H&E staining confirmed that tissue slices lose structural integrity and display compromised morphology in culture [118] [Figure 32].

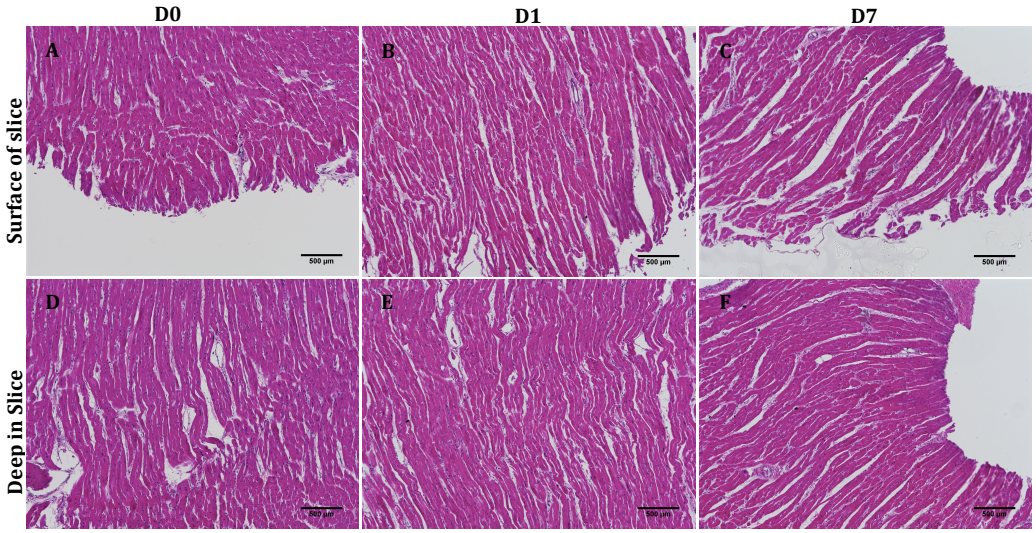

Figure 32: H&E staining reveals chronically unloaded tissue slices lose structural integrity. A) Acute slice (D0) section from the surface of slice. B) Chronically unloaded slice after one day in culture (D1). C) Chronically unloaded slice after seven days in culture (D7). D –F) H&E staining of sections deep within slices at day 0, day 1, and day 7 respectively.

Sections displayed in the top row [Figure 32 A-C] were obtained from the surface of the slice and sections displayed in the bottom row [Figure 32 D-F] were obtained from approximately 100µm – 200µm deep within the tissue slices. Chronically unloaded slices exhibit smaller numbers of cell nuclei, less alignment of fibers, and loss of overall mass indicated by spaces between fibers. The average separation distance (between fibers) increases significantly by two-fold from 30µm at day one to 60µm just after one day in culture. At day seven the average separation surges to 80µm (data not shown).

4.3.3 Mechanical stimulation improves structure and function

In order to enhance cardiac tissue slice structure and function over time, we developed a uniaxial stretching device capable of delivering cyclic stretch to *ex vivo* heart slice and enabling long-term investigations (Chapter 3). Five slices were loaded on our multi-well cardiac tissue stretcher system (DTSD4s) at a time, and subjected to 12% - 20% strain at 1Hz frequency. Figure 33 below shows images from 3 different conditions: Acute slice, slice cultured in a tissue culture (unloaded) for ten days, and slice supported with our device under continuous cyclic stimulation.

Gap junctions, located in intercalated discs at the ends of cardiac cells, are responsible for rapid propagation of electrical signals between cells and play a critical role in the synchronized contraction of the heart [192]. The protein α-actinin is the main component of the Z-disk that bounds each sarcomere and maintains their structure and function [193]. As expected, acute cardiac slices extensively expressed a gap junction protein connexin43 shown in red and display aligned fibers indicated by α-actinin staining in green [Figure 33 A]. Figure 33 B is a representative image of day 10 unloaded

cardiac slice cultures stained for structural protein α-actinin and functional protein connexin43. The aligned and elongated structure seen in acute slices is lost, accompanied by highly diminished cell-cell gap junction.

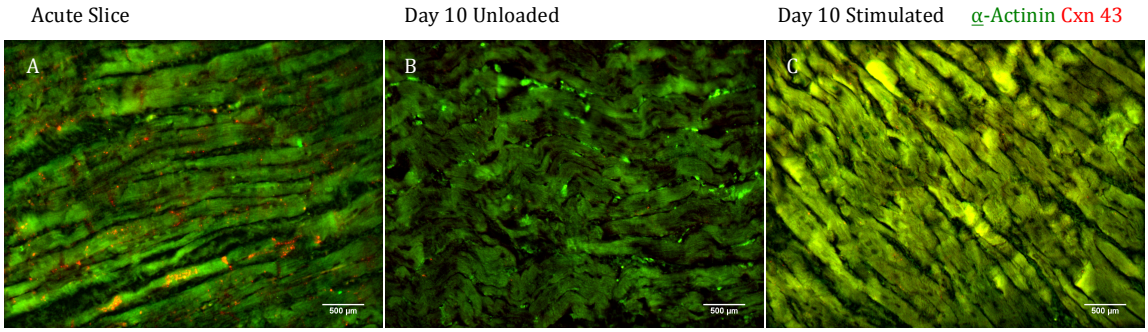

Figure 33: Cardiac tissue slices stained for structural and functional proteins. A) Acute slice with aligned fibers connected to each other with connexin43, gap junction protein. B) Tissue slice in culture without stimulation shows disrupted structural integrity and lack of junction protein connnexin43 after 10 days. C) Tissue slice in culture with stimulation shows mostly intact fiber alignment and ample gap junction protein after 10 days. α-actinin shown in green & Connexin43 (Cxn43) shown in red.

Cardiac slices stimulated with continuous uniaxial cyclic mechanical load for ten days displayed similar structural and functional properties to that of acute slices [Figure 33 C]. A representative image of day 10 cardiac slice supported by our device suggests that uniaxial cyclic stimulations could preserve structural and functional properties of slices to enable long-term maintenance of physiology and validate our platform as a suitable *in vitro* model system.

4.4 Discussions and Conclusions

Changing the orientation of tissue blocks on vibratome stage further optimized cutting slices. By altering tissue orientation on cutting surface we reduced the blade-tissue contact surface area at the beginning and ending of slicing, leading to increased efficiency of cutting. We were able to decrease slicing time by increasing cutting speed from 0.03mm/s to 0.2mm/s. We confirmed that tissue slices lose structural integrity and display distorted morphology when chronically unloaded, by performing H&E staining. Since our slice thinness of 500µm is slightly larger than dimensions reported by other groups (300µm - 400µm), we obtained our H&E samples from deep within our blocks in addition to surface for comparison. Slices both from surface and deep within blocks exhibited similar structural degradation.

We compared three conditions (1) slices at day 0, acute slice, (2) slices at day 10 that were in culture without mechanical stimulation, day 10 unloaded, (3) slices at day 10 that were supported with our device delivering continuous cyclic mechanical stimulation, day 10 stimulated. Slices at day 0 generally expressed the gap junction protein connexin43. This expression has diminished by almost 90% in slice cultures that

were unloaded for 10 days, while slices supported by our device preserved 70% of the expressions. Similarly, cell alignment has been lost with chronically unloaded slices, while alignment seems to be preserved by slices supported by device. These results suggest that continuous uniaxial cyclic mechanical stimulations preserve structural and functional properties of slices to enable long-term preservation of physiology and validate our model system.

Cardiovascular research requires a model system to enhance our basic understanding of cardiac biology, electrophysiology, and pathology, and to serve as a platform for cardiac toxicology, drug discovery and most importantly understand cardiac repair mechanisms. To reveal cardiovascular regenerative potential, we need to identify a suitable *in vitro* model system that will allow us to conduct long-term experimentations in the proliferation, differentiation, maturation, and integration of donor cells to improve cardiac function. Viable organotypic cardiac tissue slices could potentially present such a platform and maybe are the best *in vitro* model system of the future. They are the promising candidates for conducting cardiac research as they maintain native multicellularity (correct cell type ratio), present moderate complexity, retain complex extracellular architecture and well preserved cell-to-cell electrical, mechanical & metabolic connection. In addition, their ultra thin dimension permits diffusion of oxygen and other necessary small molecules even to cells at the inner most part of slice avoiding need for coronary perfusion, as is the case with other preparations.

In 2012, Brandenburger et al. observed decline in the electrical properties of cardiac tissue slices cultured in liquid air interface over 28 days. The characteristic phase 2 (plateau phase) of the AP was diminished, conduction velocity dropped dramatically, and action potential duration 20 (APD_{20}) declined to half its value compared to acute slices. Similar decline manifested in the mechanical properties with significant loss in contractility just after a day in culture [57]. The obvious conclusion from their work is that introducing directional forces can better preserve physiology. In some studies since then, mechanical load did not appear to be sufficient to prolong physiology and indicated preservation for more than 4 days [141, 194]. Very recently, in work parallel to ours, Watson et al. and Fischer et al. have demonstrated that the application of electromechanical stimulation with physiological preload improves preservation of myocardial structure and function [142, 143]. Their setups are more sophisticated than ours in that they combine other stimulations in addition to mechanical; however, our system is unique in allowing continuous cyclic mechanical stimulation to supported tissues. The finding by Watson et al, that the application of a preload equivalent to sarcomere length 2.2μm (exact % elongation) should be implemented in our system in the future to produce best possible results. In any case, the ability to maintain myocardial slices in a fictional state *in vitro* or taking a step towards a stable *in vitro* model of the adult myocardium, provides a suitable and desired platform for cardiovascular research. Though very beneficial, this has not been possible with published techniques until this year. Improved model provides prolonged preservation of cardiac phenotype, intact native multicellularity & architecture, and allows for long-term cardiac repair studies and

data collection In this study, we confirmed that cyclic uniaxial mechanical stimulation preserves cardiomyocyte structure and function.

The major downside in preparing and eventually utilizing quality myocardial slices is the manual nature of tissue block preparation from ventricles. This step requires a lot of practice to collect viable slices and needs to be standardized/automated in the future. In this study, we were able to optimize slicing speed by altering tissue orientation, which we believe should aid in efficiency of experiments. Although living cardiac tissue slice preparations have previously shown robust survivability in culture, with dedifferentiation others and us have noticed significant structural and functional remodeling in long-term cultures. In order to enhance cardiac tissue slice viability and counteract dedifferentiation, we designed and developed a simple user-friendly tissue-stretching device that provides cyclic mechanical stimulation to *ex vivo* heart slices allowing their maintenance and manipulation. Our results here suggest that uniaxial cyclic stimulations could preserve structural and functional properties of slices to enable long-term maintenance of physiology and validate our platform as a suitable *in vitro* model system.

Chapter 5. Derivation of Cardiomyocyte from Pluripotent Stem Cells: Optimizing Culture Substrate

5.1 Introduction

5.1.1 Cardiac Cell Therapy

The heart is traditionally considered a terminally differentiated organ as it is unable to effectively regenerate after notable injury, since it does not contain a significant pool of endogenous stem cells [6, 7] The limited intrinsic regenerative capacity in adult heart is not adequate to compensate for considerable loss of cardiomyocytes during a significant injury such as a MI [195]. Treatments of heart attack over the last century have been palliative, focused on managing, reducing, or preventing further damages to the heart and fail to address the underlying problem: loss of functional cardiomyocytes. Even though improved clinical outcomes for patients with heart failure have been realized with pharmacological treatments such as β-blockers and angiotensin converting enzyme (ACE) inhibitors, they are not able to address the fundamental problem and diminish the size of scar tissue on the heart[196]. The current gold standard therapy, and usually the last option, is a heart transplant. However, heart transplants are significantly limited by donor supply, organ mismatch, and need for immunosuppression. At any given time, there are ten times more patients who would benefit from cardiac transplantation than available donor hearts. In addition, the long-term prognosis of heart transplants remains disappointing with only marginal improvement in quality of life. Given these facts, regenerative medicine using cell and tissue transplantation approaches have garnered much attention as they could restore cardiac functions in failing hearts.
However, their application in regenerative medicine is hampered by several limitations. These include identification or generation of a mature cell source, best methods for cell or tissue delivery, as well as cell survival (retention), engraftment, and integration within the ischemic environment. Furthermore, there are issues with an appropriate model system, long-term product storage, and risks associated with immunogenicity and potential tumorigenicity from the graft implant. Here, we focus on preparation and characterization of the cell source.

5.1.2 Cell Sources

In stem cell transplantation, stem cells can be introduced into damaged areas of a tissue to initiate myocardial repair and potentially improve cardiac function after MI via several direct and indirect mechanisms [197] [Figure 34]. However, there remains the question of cell source maturation, and/or purification methodologies [198]. Numerous types of stem/progenitor-like cells have been described to contribute to cardiac repair in CHD. Pluripotent stem cells (PSCs), including multipotent adult stem cells, embryonic stem cells (ESCs) and induced-pluripotent stem (iPS) cells have emerged as promising

therapeutic options for repairing cardiac damage. Various methods for generating CMs from PSCs have been reported (reviewed in [15]), but these methods still produce heterogeneous mixtures of CMs and non-CMs cells.

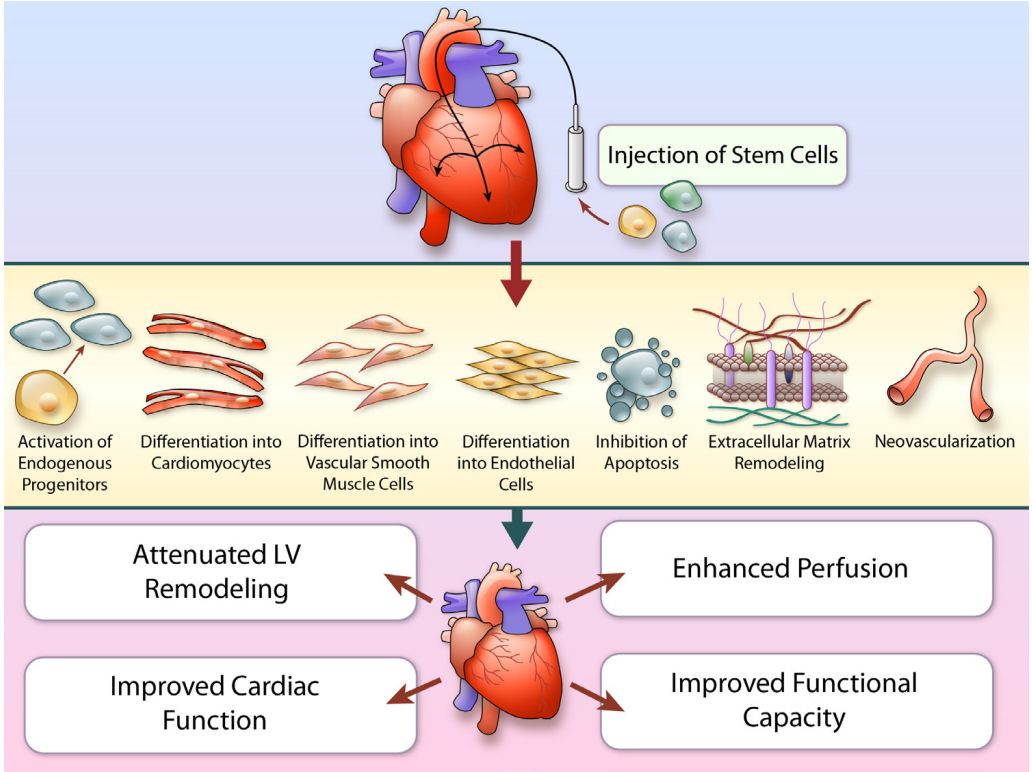

Figure 34: Injected cells can potentially improve cardiac function. Cardiac repair can potentially be the result of one or more of the following: Differentiation into cardiac/vascular cells, activation of neovascularization, modulation of ECM, inhibition of apoptosis/hypertrophy, activation of endogenous precursors [199]

Methodologies that require genetic modifications are accompanied by several risk factors and complications that include, but are not limited to, incompatibility with clinical use, potentially silenced extrinsic genes, need for species specific constructs, possibility of tumor formation & genetic instability, and cumbersome integration process. It is extremely clear and important that non-genetic methods for purification are necessary for clinical applications of PSC derived CMs to repair MI. Moreover, non-genetic methods of purification have been shown to yield higher percentages of CM using CM-specific molecular beacons (MBs) [16], CM-specific surface markers such as VCAM-1 [17], and other metabolic/ morphology differences between CM and non-CM [18-21]. Even before the stages of derivation and injection for integration, we are faced with a challenge of choosing suitable and non-controversial cell sources for regeneration therapy.

5.1.3 Cardiac Differentiation

The McCloskey laboratory has over ten years of expertise in the cell line-specific and stage specific optimization of critical activin A/BMP4 signals for induction of H7, H9, and HES2 human ESC [200-202]. This work led to protocols that reproducibly generate cultures containing between 50-60% cardiomyocytes (CM) and has been published as a research paper in the *Journal of Stem Cells and Regenerative Medicine* [53] and a step-by-step protocol paper in *Stem Cell Reviews and Reports* [200]. Moreover, the McCloskey lab further examined the role of matrix signaling in the CM differentiation, and found that a 70:30 blend of fibronectin (FN) and laminin (LN) directed significantly more cells towards the CM fate (60-70%) [202]. Based on our own experience and cited reports [203], these protocols will need to be optimized for each new iPS cell line. The general protocol is outlined as follows [Figure 35].

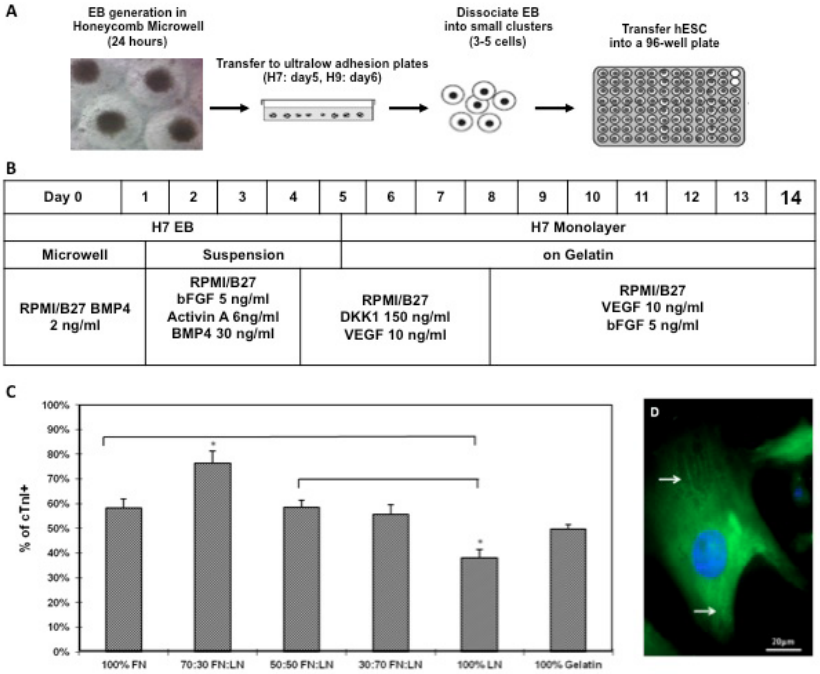

Figure 35: CM induction from human ESC (hESC). (A) Scheme for hESC cell culture manipulation. Embryoid bodies (EB) were generated from small clumps (3-5 cells) in honeycomb microwells and then transferred to suspension culture. At the indicated time points (day 5 for H7 and HES2, day 6 for H9), EB were dissociated into small clumps (3-5 cells) and plated down as monolayer on gelatin in 96-well flat bottom plate. (B) Table of the overall optimized stage-specific differentiation schemes for the first 14 days of cardiac induction for H7. (C) Percentage of cTnI+ cardiac cells from H7 hESC expressing cardiac markers at day 14. (D) Immunostaining for cTnI at day 14. The H7 were imaged after immunofluorescent staining with cardiac troponin I (green) and DAPI (blue). The arrow indicates the presences of sacromeric structures. Scale = 10µm. (Image adapted from published works [204-206]).

In order to verify the role of integrin β (ITGB)4 [receptor for LN] and ITGB5 [receptor for FN] signaling in CM differentiation, we blocked both receptors at the same time showing that the expression of CM specific markers (cTnI and Nkx2.5) was attenuated [206]. In addition, the work revealed some interesting dynamics between the two receptors. Co-staining shows cells are not double positive for both integrins, and only expressing either ITBG4 or ITGB5 with the latter being expressed more. Their expression pattern showed ITGB 5 expressing cells localized next to ITGB 4 expressing cells.

Since the specific components of the mechanism and how the two signals are distinct is not well understood, we decided to investigate further in hopes of revealing mechanisms and its active components. First, we explored combining a less expensive method to direct high numbers of CM from hPSC by modulating Wnt/ β-Catenin signaling using a high cell seeding density [77] with our own data on using FN/LN matrix. In this work, we created an improved derivation method for directing CM populations from stem cells.

5.2 Materials and Methods

5.2.1 Stem Cell Culture

A Matrigel-coated six-well plate was set at room temperature for 15 minutes. A frozen vial of cells were removed from liquid Nitrogen and immersed in 37°C aluminum bead bath/water bath to thaw. The vials were swirled gently until the contents were completely thawed. In a tissue culture hood, the cells were gently transferred into a sterile 15-ml conical tube containing 5 ml of room temperature mTeSR1 medium. The conical tubes were then centrifuged at 200g for 5 minutes. The supernatant was aspirated with sterile Pasteur pipette and discarded to resuspend the cell pellet in 6 ml of mTeSR1 medium + 5 mM Y27632. Excess Matrigel was aspirated from prepared Matrigel-coated 6 well plate and 2 ml of the cell suspension were added into three wells. The plate was then placed inside a 37°C, 5% CO_2 incubator and carefully moved in three short back and forth and side-to-side motions to disperse the cells across the surface of the wells. On the next day, the medium in each well were aspirated and replaced with 2 ml of fresh room temperature mTeSR1 medium. Medium was replaced daily until cells were ready for passage or induction. Cells were cultured in 6well, 60mm, 100mm plates on MEF feeder layer in hESC media (HES2) and Matrigel in mTeSR1 (H7, H9, and iPSC).

5.2.2 Differentiation

EB method: Briefly, cells were detached using Accutase, and dissociated into small 3-5 cell clumps. The cells were then spun down and re-suspended in 2ml Roswell

Park Memorial Institute (RPMI) medium supplemented with 2% B27. To generate embryoid bodies (EB), a 400-µm Honeycomb Microwell microchip was placed into each well of a standard 24-well plate and 6 x 10^5 cells were added to each Microwell chip. 10µM of ROCK inhibitor (Y-27632; EMD) was added during EB formation to enhance cell survival. After 24 hours, uniform EB were formed in Microwell and then transferred to ultra-low attachment plates in RPMI/B27 media with bFGF, BMP4, and Activin A until Day 4. On day 5, media was changed to RPMI/B27 with DKK1 and VEGF. EBs were then dissociated into small clusters (3-5 cells) by gentle pipetting on day 6 and plated on 60 mm tissue culture treated plate coated with FN: LN (70:30) as a monolayer. Once again media change to RPMI/B27 with VEGF and bFGF was administered on day 9 (fresh media added every other day). This temporally controlled addition of various growth factors mimics cardiogenesis during development and was optimized for H7, H9 and HES2. However, this has to be optimized for our generated iPSC to yield comparable CMs expressing cardiac specific markers (cTnT, cTnI, Nkx2.5).

Monolayer method [Figure 36]: Briefly, cells were detached using accutase and 0.5mL of mTeSR1 was added into each well to collect cells in 15mL conical tube. The cells were then counted and spun down and resuspended in mTeSR1 + 5 µM Y27632 at a cell density of 2 million cells/mL. We cultured 0.5–1.5 million cells per well in each well of a 12-well plate and added media for a total volume of 2mL in each well.

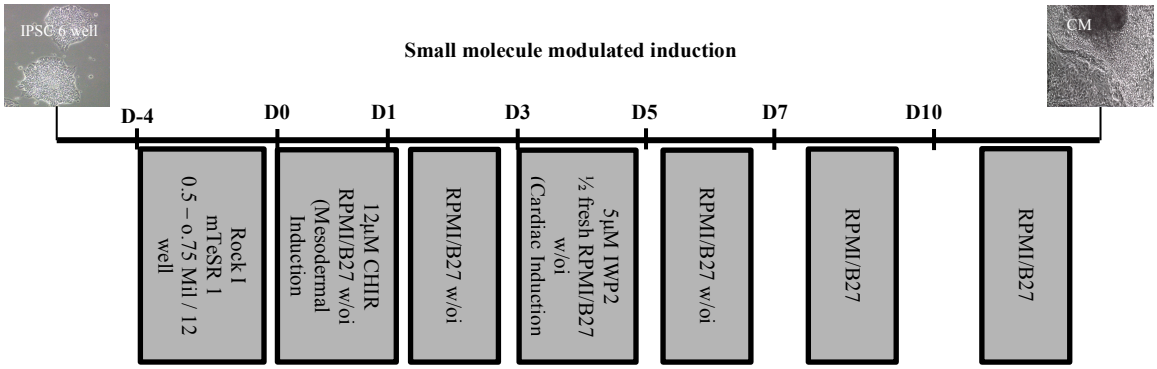

Figure 36: Time line and description of small molecule modulated induction. CM differentiation from hPSC by modulating Wnt/ β-Catenin signaling using small molecules.

This time point corresponds to day −4. Media was replaced daily for the next three days. At day 0, old media was aspirated and 2mL RPMI/B27-insulin with CHIR99021 was added to each well. 24 hours later, media was aspirated from each well and replaced with 2mL RPMI/B27. Day one, medium was aspirated from each well and replaced with 2mL RPMI/B27 –insulin. On day 3, combined medium of 1ml old media, 1mL of fresh RPMI/B27 –insulin media, and IWP2 was prepared and added to each well. On day 5, the medium from each well was aspirated and 2mL RPMI/B27 –insulin was added. Day 7 and every three days following, old medium was replaced with fresh 2mL/well RMPI/B27 media [77].

5.2.3 Fixing and Staining

Our lab uses antibody-staining protocols to stain cell surface or intracellular markers to confirm identity and/or characterize cells/tissues. After staining, qualitative and quantitative analysis is performed via immunohistochemistry and flow cytometry, respectively.

Media was aspirated from culture dish containing cells/tissue and washed with PBS. For flow, 5ml Accutase added (amount added varies with cell type) and incubated at room temperature for 5 minutes. Cells were observed under microscope to check for commencement of detachment (i.e. if cells were balling up). Cells were then transferred to a 15mL conical tube and centrifuged at 1200 RPM for 5 minutes. We added 300 – 500 µL of 4% Formaldehyde (PFA) to tissue/cell (if attached) in a dish or re-suspend cells in 300 – 500 µL of 4% PFA. Blocking solution (1mg/mL Bovine Serum Albumin (BSA) + 5% Donkey Serum) and Block & Perm solution (Blocking solution + 0.7% TritonX-100) were prepared. PFA was removed from fixed cells/tissue and washed with PBS to add/re-suspend cells in Block & Perm solution (for intracellular staining). After 1 hour, appropriate marker specific primary antibodies were added. Cells were then incubated overnight at 4 degrees and rinsed with PBS the next day to add secondary antibody. One hour after adding secondary, plates were rinsed again and samples were ready for flow cytometer or fluorescent microscope (add DAPI for nuclei staining).

5.3 Results and Discussions

5.3.1 Cardiac Induction: EB method

We commenced our investigation with two objectives in mind. Even though our lab has established a protocol that reproducibly generates cultures containing 50-60% CMs, it has to be optimized from each new cell line. Therefore, our first objective was to further optimize the protocol for directing CMs from stem cells. Our second objective was to verify the integrin receptor localization findings in this new cell line before we commence further investigation into understanding the dynamic mechanism involved. Three human ESC (HES2, H7, and H9) and one iPSC were utilized to generate CM via EB method using microchips. We first noticed morphological differences between the cell lines during the induction process. Figure 37 shows representative images of the process at different time points in the induction. Stem cells with characteristic round colonies with distinct margins for all cell lines is shown at the top row. Second, third, and fourth row show EB in suspension at day 4, monolayer on 70:30 FN/LN substrate at day 7, and monolayer on 70:30 FN/LN substrate at day 12 respectively for the four cell lines tested.

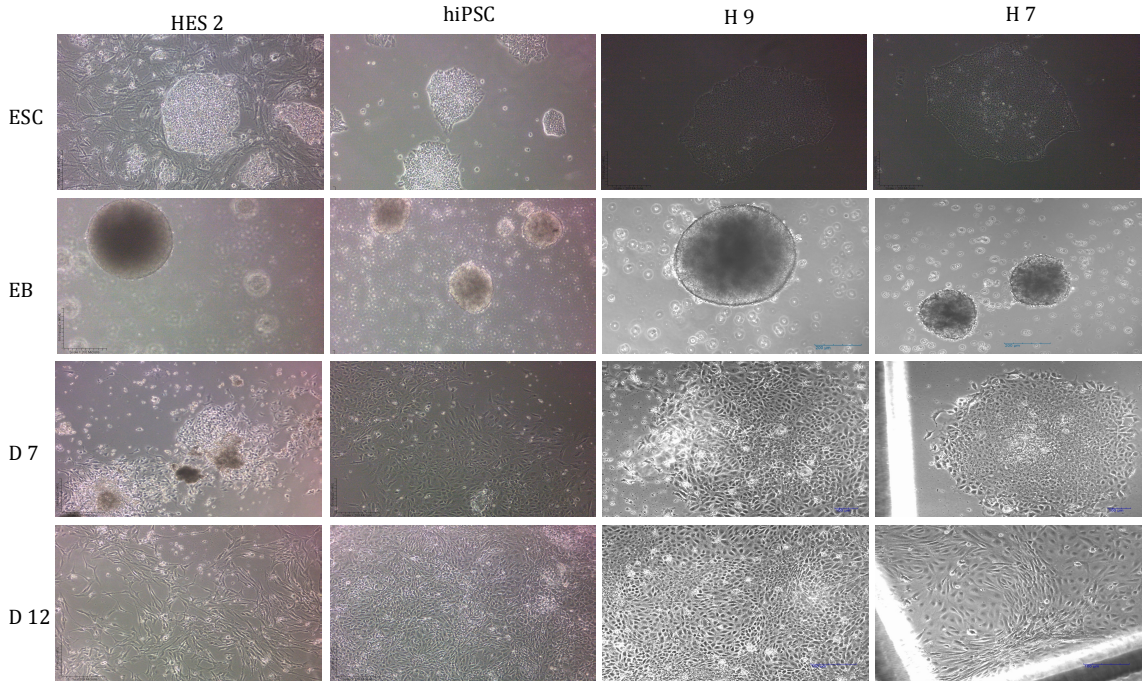

Figure 37: Induction of CM from hESC-HES2, iPSC, H9, and H7 via EB method. Top row are the stem cell colonies of the different cell lines. Second row EB were generated and cultured in suspension plate for 5 days (image at day 4) before transferring partially dissociated cells onto adhesive plates. The adhesive cells imaged at day 7 the third row and day 12 the last row. Scale =200µm for all [except the last two in the bottom row 100µm]

It must be noted that the microwell chip utilized is 400µm (each microwell size) for HES2 and H9 and 300µm for iPSC and H7 cell lines. These can be seen from the sizes of EBs in suspension at day four (second row above). The difference in EB size may contribute to the morphological difference seen in the derived CM in culture, but it is not the only factor since the morphology across the board is unique. Initial results were promising in all cell lines, generating over 50% $cTnI^{+}$ as reported [Figure 38]. However, our mold for generating the microwell chips was deteriorating, and failing to consistently produce EBs. Simultaneously our lab was adopting a popular monolayer induction method with higher CM yields at lower costs.

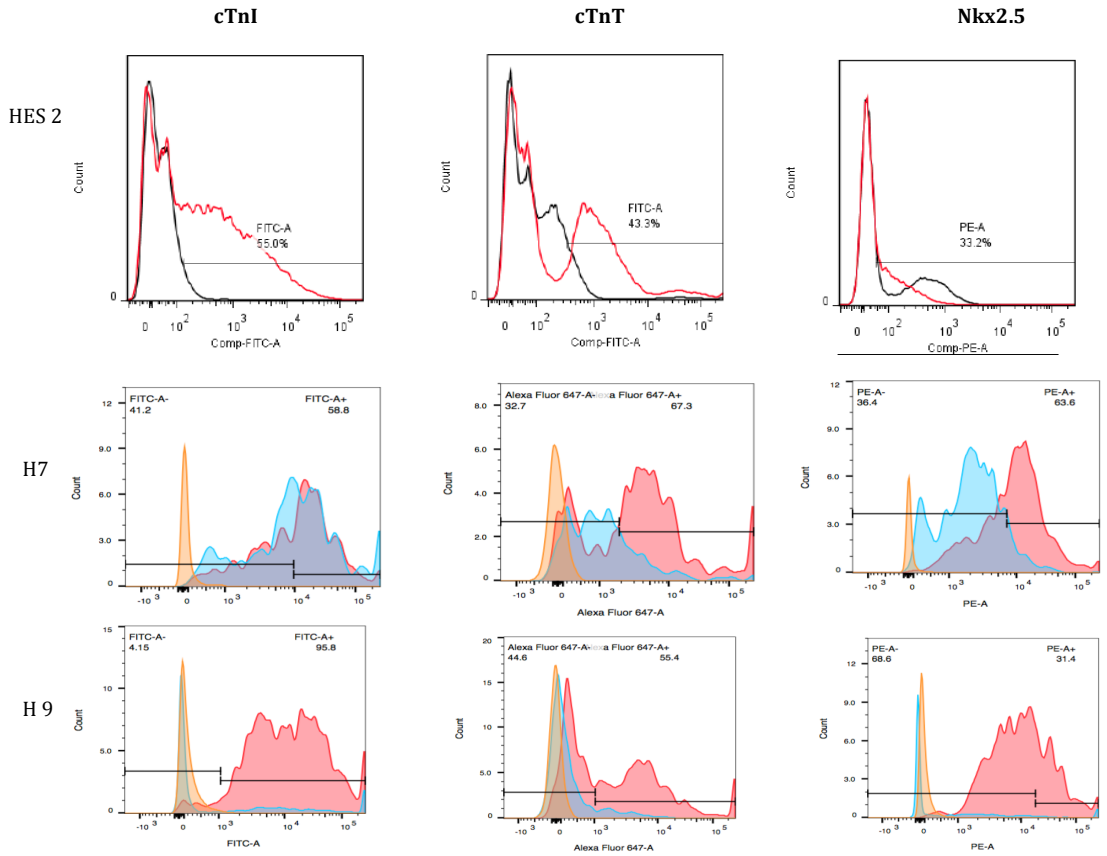

Figure 38: After 21 days of induction, CM were stained for cardiac specific markers. Cardiac troponin I (cTnI) cTnT, and Nkx2.5 by flow cytometry for cell lines HES2 top, H7 middle, and H9 last rows. Note that although isotype controls were not included in this analysis, data indicates cultures contain over 50% CM. This is comparable induction efficiency to the best-reported values via this method.

5.3.2 Cardiac Induction: Monolayer Method

The induction of CMs using the high cell density induction on Matrigel did not generate CMs with ITGB5 and only poor expression of ITGB4. We suspected that the type of substrate used in the protocol, Matrigel, a mixture of ECM materials extracted from Engelbreth-Holm, Swarm (EHS) mouse sarcoma that contains mostly laminin and collagen IV (60:30 ratio), was the reason for the lack of ITGB5 expression in our CMs. Moreover CM generated on Matrigel may not be safe for clinical setting.

To address these concerns and to optimize the protocol for our purpose (integrin receptors study), we focused our efforts on utilizing the optimized substrate (70:30 FN:LN) [206] from the EB method established in our lab for defined xeno-free substrate that was shown to support robust CM derivation. Others have reported that the usage of a combination of collagen IV, laminin, fibronectin, and victonectin can replace Matrigel to expand hPSCs [207]. Initially, cells were not adhering properly on FN:LN (70:30)

substrate and we spent some time exploring the use of Matrigel layered with FN:LN on top before seeding cells.

Figure 39: Induction of CM from ESC H9 via small molecule monolayer method. A) Induction on Matrigel, B) Induction on Matrigel and FN/LN at 70:30 ratio, and C) Induction on FN/LN 70:30 ratio.

Representative Day 12 CMs under three conditions (Matrigel, Matrigel + FN:LN, and FN:LN) are shown in figure 39. We were able to consistently generate robustly beating CM at day 6 of induction (half the time previously reported). We have not explored this finding any further. In this work we were able to generate xeno-free CMs by optimizing an existing protocol with substrate findings in our lab. After much practice, we were able to drive robust CMs using monolayer method on FN:LN substrate [Figure 39], as planned.

5.3.3 ITGB 4 and ITGB 5 localization

Before deep interrogation of hESC-CM to understand specific mechanisms involved in the distinct expression of the two receptors, we first wanted to confirm if the same phenomenon holds true for our newly optimized CM derivation. Results in Figure 40, confirms that ITBB 4 and ITGB5 are not expressed on the same cells, but expressed on distinct cells.

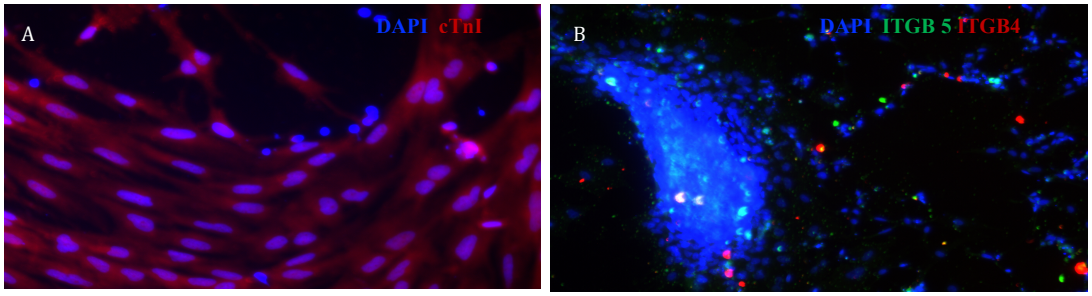

Figure 40: Human ESC-CMs (H9) stained from Cardiac Troponin I (A) & ITGB4, and ITGB5 (B). The two receptors are not co-expressed but they seem to be expressed next to each other.

ITGB5 (green) and ITGB4 (red) are distinctly expressed as expected, however, we still have to dig deeper in our future works to understand mechanisms involved.

5.4 Conclusions

In this work we optimized an already robust CM derivation method [77] with an optimized substrate combination established in our lab [206] to realize xeno-free production of CMs. We also verified the distinct expression of ITGB4 and ITGB5 observed in our lab on cells derived via EB method. There still remains further characterization and confirmation of our results. We also believe robust beating of cells at day 6 introduces a story to be explored in the future.

Chapter 6. Conclusions

Various cell sources have been explored as cell therapy products to replace lost cardiac muscle and/or improve cardiac performance [208-214]. Stem cell therapy can improve heart function after MI; however, cell injection alone does not provide sufficient environmental support for the injected cells to survive. Moreover, it is difficult to conduct controlled studies of graft cell or tissue integration in current *in vivo* MI models. Therefore, the work in this thesis aimed to establish primary cheek swab oral epithelia cell culture and use them for reprograming of noninvasively obtained starting material (Chapter 2), and develops a tissue stretching device for cardiac slices (Chapter 3&4) as an *ex vivo* platform for examining cell therapy engraftment on/in a slice of dynamically strained heart tissue. Additionally, studies were conducted on improving current CM derivation protocols. The overall aims of the work are illustrated in the diagram below [Figure 41].

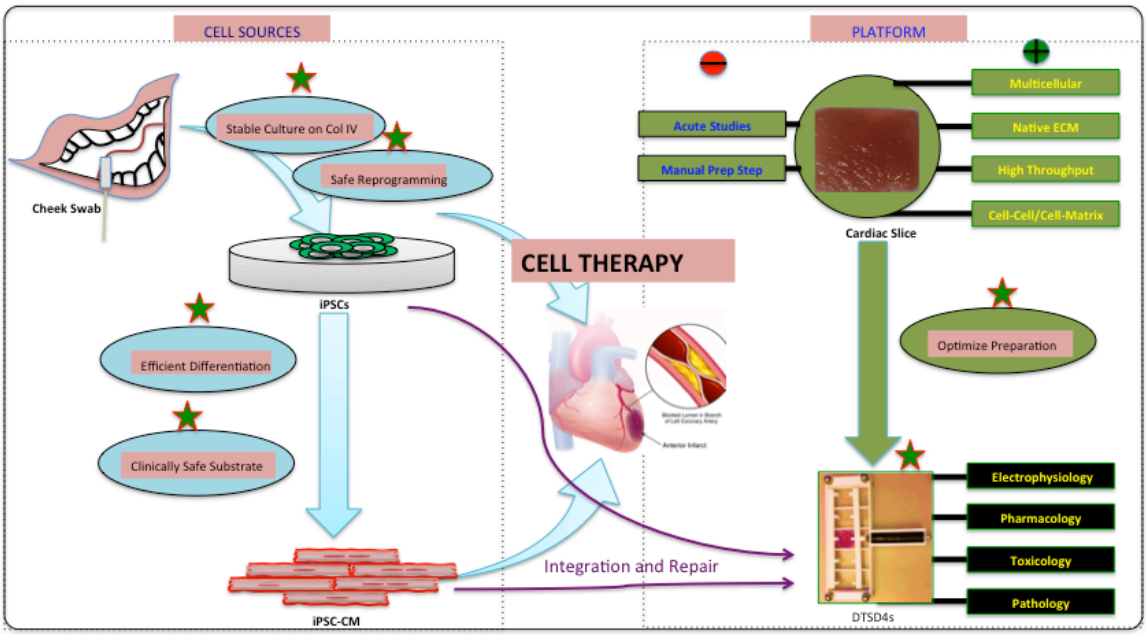

Figure 41: Summary of our work towards realizing cardiac cell therapy focused on tackling challenges in two areas of cardiac cell therapy; finding suitable and convenient cell sources and innovating a model system that allows for long term studies. Combined, they will potentially enable investigation of integration and repair mechanisms. Green stars denote our unique contributions within the context of the larger picture. First we established a stable culture of non-invasively obtained cells (cheek swab cells) and reprogramming them to iPSC. Second, we developed a device to support and provide mechanical signal to a cardiac slice to enable long-term preservation of cardiac structure and function. Finally, we improved on current CM derivation methods to include clinically relevant culture substrate.

Although a few minimally invasive starting cell sources have been explored [42], to date, there has not been any published work describing the generation of iPSCs from a simple cheek swab. We were interested in exploring the possibility of using buccal

swabs, because it is a simple method of obtaining primary cells that requires no special skills and it is non-invasive and pain free. Furthermore, the process to obtain cells takes minimum time, effort, and finding donors to conduct the study extremely easy. Buccal swabs are routinely collected for extraction of DNA for one-time cellular or molecular studies or forensic identifications, and discarded after use [107]. However, there is only one published study describing their use in a stable culture [106], which required using a supportive cell feeder layer. The cell cultures studies described in chapter 2 found that oral mucosa epithelial cells can be expanding as proliferating cells on collagen-type IV substrate without the need of a supportive cell feeder layer. Although several substrates (fibronectin, collagen I, laminin, matrigel, gelatin, and combination of fibronectin and collagen I) were examined as a possible substrate, buccal cells seeded on all these substrates showed significant loss of cell on day 1 in culture and supported 20k – 50k adherent cells after 5 days. After one week in culture, all cells were either dead or floating in culture medium. In contrast, cells cultured on Collagen-type IV showed superior survivability in culture for several days. On day 5, 130k (up to 6 fold more) cells were viable and adhering to substrate. We then explored the reprogramming potential of our cultured cheek cells (CK 13^+, CK 10^+, TfR^+ & $ITGB1^+$) using non-integrating reprogramming method. We observed the appearance of hESC like colonies approximately three weeks after transduction. Our reprogramming efficiency (number of colonies per input cell) of approximately 0.01% is comparable to reported efficiencies [215]. However, it has proved to be challenging to expand the colonies in culture to establish a stem cell line.

Next, we considered the development of an *ex vivo* heart model for studies examining cell delivery and integration. Living organotypic tissue slice cultures are emerging as a popular platform to study the heart. Although living cardiac tissue slice preparations have previously shown robust survivability in culture, significant mechanical and electrophysiological degeneration has been observed in cultures even after a few days [57]. In order to enhance cardiac tissue slice viability up to two months, we developed a uniaxial stretching device capable of delivering cyclic stretch (~15% elongation and 1 Hz frequency) to *ex vivo* heart slice. We set out to develop a system that provides a physiologically relevant mechanical stimulation to circular tissue slice sample. First generation stretcher system (DTSD1) was designed to provide several support points around the circumference of the samples and provide mechanical stretch in several directions. The final height of 10cm of the device introduced challenges in allowing device under a microscope for data collection. The circular sample shape proved to be extremely challenging to attain. Furthermore, the multipoint stretching didn't allow for differential stretch along fiber direction. Subsequent device design and development addressed these issues of stretch direction and data collection. Rectangular/square sample shape was preferred to allow biaxial stretching and device height was reduced by 50% on the next design to eventually by 80% on our final device to about 20mm allowing for data collection. Even though a differential biaxial stretch could better mimic the *in vivo* mechanical stretch, we settled for a uniaxial mode to easily accommodate for a multi-well system. Our initial goal for anchorage was to develop a clamp system but that was demonstrated to be difficult for such ultra thin samples and we adopted the usage of glue

as all other groups extensively use it. Although the glue is biodegradable and compatible to use with tissue cultures, future efforts in developing a system that avoids the usage of glue for anchorage could potentially be beneficial.

Our multi-well cardiac tissue stretcher system (DTSD4s) allows for simultaneous multi sample stimulation for rapid experimental testing. Device characterization revealed that the output distance of actuator was consistent and linearly correlated to input distance over entire range of movement. To our knowledge, this is the first device to directly support thin myocardial slices in a chamber and deliver cyclic mechanical stimulation. Furthermore, our tissue-stretching device is designed as a high throughput system that can stimulate up to five samples under nearly identical mechanical conditions and separate culture condition for possible biochemical test. We have taken a step in the right direction in establishing an *in vitro* model that allows long-term (up to 3 months) cardiac slice studies. By altering tissue orientation to diagonal during slicing, we were able to increase slicing speed from 0.03 mm/second to 0.2 mm/second decreasing slice time from 6 minutes to about 2 minutes per slice. Full characterization of obtained slices is required for conclusive claim. Tissue preparations supported with our device under continuous uniaxial cyclic mechanical stimulation for 10 days, showed 40% connexin43 expression that is comparable to the 55% expression by slices at day 0 and significantly better than the less than 10% expression seen in samples that received no mechanical stimulation. Samples that received mechanical stimulation also show better alignment of fibers as seen from alpha actinin stain than chronically unloaded slices. These results suggest that uniaxial cyclic stimulations may preserve structural and functional properties of slices for up to 10 days or more to enable long-term maintenance of physiology and validate our platform as a suitable *in vitro* model system.

Finally, we explored a suitable CM derivation method to use as a source for cell transplantation to potentially restore cardiac function for failing hearts. Cell transplantation has several limitations including risks associated with tumorigenicity from pluripotent (iPS or ES) cell implant. Therefore, it maybe a requirement to transplant suitable differentiated mature CM to circumvent this important risk. With that accord, we were able to optimize a robust CM derivation method that constantly yields over 90% CM with a xeno-free defined substrate condition by switching from undefined Matrigel substrate to a 70:30 ratio of FN and LN optimized in our lab. We also observed distinct expression of ITGB 4 and ITGB5 in the culture we established.

Cardiac cellular therapy is far from use in patients, and a lot of work needs to be done to understand the various mechanisms involved. Superior cell source exploration and establishing a suitable platform are a worthwhile effort to make an impact on the field and eventually make a difference in the lives of many who are waiting for such a groundbreaking intervention. My work on developing an *ex vivo* heart tissue stretching device enables further studies exploring delivery and long-term integration of cardiovascular cell products for patient use, and development of devices/bioreactors able to combine mechanical, electrical, and biochemical cues to provide the most physiologically relevant model system possible.

References

1. Mozaffarian, D., et al., *Heart Disease and Stroke Statistics-2015 Update A Report From the American Heart Association.* Circulation, 2015. p. e310 - e313.
2. Mensah, G., et al., *Decline in Cardiovascular Mortality: Possible Causes and Implications.* Circ Res, 2017. **120**(2): p. 366-380.
3. Benjamin, E., et al., *Heart Disease and Stroke Statistics-2018 Update: A Report From the American Heart Association.* Circulation, 2018. **137**(12): p. e67-e492.
4. Thygesen, *Third universal definition of myocardial infarction American college of Cardiology* Circulation 2012(126): p. 2020-2035.
5. Thygesen, *Universal definition of myocardial infarction.* European Heart Journal 2007. **28**(20): p. 2525-2538.
6. Carvalho, A. and A. Carvalho, *Heart regeneration: Past, present and future.* World J Cardiol, 2010 **2**: p. 107-111.
7. Mallory, G. and P. White, *The speed of healing of myocardial infarction: a Study of the pathologic anatomy in seventy-two cases* The American Heart Journal. 1939(18): p. 647- 671.
8. Weisfeldt, M. and S. Zieman, *Advances in the prevention and treatment of cardiovascular disease.* Health Aff (Millwood), 2007. **26**(1): p. 25-37.
9. Sandison, A., *Degenerative vascular disease in the Egyptian Mummy.* Med Hist, 1962. **6**(1): p. 77-81.
10. Go, A., et al., *Heart Disease and stroke statistics - 2013 update: a report from the American Heart Association.* Circulation 2013. **127**(1): p. e6-e245.
11. Murry, C., *Haematopoietic stem cells do not transdifferentiate into cardiac myocytes in myocardial infarcts.* Nature, 2004. **428**(6983): p. 660-664.
12. Editor, *Global burnden of disease: Cause of death.* W.H. Organization, 2004: p. 2-26.
13. Braunwald, E., *The rise of cardiovascular medicine.* European Heart journal, 2012. **33**(838-846).
14. Passier, R., et al., *Stem-Cell-based therapy and lessons from the heart.* Nature 2008. **453**(7193): p. 322-329.
15. Mummery, C., et al., *Differentiation of Human Embryonic Stem Cells and Induced Pluripotent Stem Cells to Cardiomyocyts: A methods overview* Circ Res, 2012: p. 344-358.
16. Ban, K., et al., *Purification of cardiomyocytes from differentiating pluripotent stem cells using molecular beacons that target cardiomyocyte-specific mRNA.* Circulation 2013. **128**: p. 1897-1909.
17. Uosaki, H., et al., *Efficient and scalable pruification of cardiomyocytes from human embryonic and induced pluripotent stem cells by VCAM1 surface expression.* PLoS One 2011. **6**(8): p. e23657.
18. Lian, X., et al., *Robust cardiomyocyte differentiation from human pluripotent stem cells via temporal modulation of canonical Wnt signaling* PNAS, 2012. **109**(27): p. E1848-1857.
19. Hattori, F., et al., *Nongenetic method for purifying stem cell-derived cardiomyocytes.* Nature Methods 2010. **7**(1): p. 61-66.

20. Nomura, F., et al., *Label-free shape-based selection of cardiomyocytes with on-chip imaging cell sorting system.* Journal of Bioprocessing and Biotechniques, 2011: p. 1-6.
21. Tohyama, S., et al., *Distinct Metabolic flow enables large-scale purification of mouse and human pluripotent stem cell-derived cardiomyocytes.* Cell Stem Cell, 2013. **12**(1): p. 127-137.
22. Laflamme, M., et al., *Formation of human myocardium in the rat heart from human embryonic stem cells.* Am J Pathol, 2005. **167**(3): p. 663-671.
23. Kehat, I., et al., *Electromechanical integration of cardiomyocytes derived from human embryonic stem cells.* Nat Biotechnol, 2004. **22**(10): p. 1282-1289.
24. Laflamme, M., et al., *Cardiomyocytes derived from human embryonic stem cells in pro-survival factors enhance function of infarcted rat hearts.* Nat Biotechnol, 2007. **25**(9): p. 1015-1024.
25. Caspi, O., et al., *Transplantation of human embryonic stem cell---derived cardiomyocytes improves myocardial performance in infarcted rat hearts.* J Am Coll Cardiol, 2007. **50**(19): p. 1884-1893.
26. Leor, J., et al., *Human embryonic stem cell transplantation to repair the infarcted myocardium.* Heart, 2007. **93**(10): p. 1278-1284.
27. Laake, L., et al., *Improvement of mouse cardiac function by hESC-derived cardiomyocytes correlates with vascularity but not graft size.* Stem Cell Res, 2009. **3**(2-3): p. 106-112.
28. Steele, A. and P. Steele, *Stem cells for repair of the heart.* Curr Opin Pediatr, 2006. **18**(5): p. 518-523.
29. Smits, A., et al., *Human cardiomyocyte progenitor cell transplantation preserves long-term function of the infarcted mouse myocardium.* Cardiovasc Res, 2009. **83**(3): p. 527-535.
30. Segers, V. and R. Lee, *Stem-cell therapy for cardiac disease.* Nature 2008. **451**(7181): p. 937-942.
31. Noort, W., et al., *Stem cells from in or outside of the heart: isolation, characterization, and potential for myocardial tissue regeneration.* Pediatr Cardiol, 2009. **30**(5): p. 699-709.
32. Gonzales, C. and T. Pedrazzini, *Progenitor cell therapy for heart disease.* Experimental Cell Research, 2009. **315**(18): p. 3077-3085.
33. Laflamme, M. and C. Murry, *Regenerating the heart.* Nat Biotechnol, 2005. **23**(7): p. 845-856.
34. Menasché, P., et al., *The Myoblast Autologous Grafting in Ischemic Cardiomyopathy (MAGIC) trial: first randomized placebo-controlled study of myoblast transplantation.* Circulation, 2008. **117**(9): p. 1189-1200.
35. Novotny, N., et al., *Stem cell therapy in myocardial repair and remodeling.* J Am Coll Surg, 2008. **207**(3): p. 423-434.
36. Doetschman, T., et al., *The in vitro development of blastocyst-derived embryonic stem cell lines: formation of viscral yolk sac, blood islands and myocardium.* Journal of Embryology and Experimental Morphology, 1985. **87**: p. 27-45.

37. Kattman, S., et al., *Stage-specific optimization of activin/nodal and BMP signaling promotes cardiac differentiation of mouse and human Pluripotent stem cell lines.* Cell Stem Cell, 2011. **8**: p. 228-240.
38. Nussbaum, J., et al., *Transplantation of undifferentiated murine embryonic stem cells in the heart: teratoma formation and immune response.* FASEB J, 2007. **21**: p. 1345-1357.
39. Takahashi, K. and S. Yamanaka, *Induction of pluripotent stem cells from mouse embryonic and adult fibroblast cultures by defined factors.* Cell, 2006. **126**: p. 663-676.
40. Mauritz, C., et al., *Generation of functional murine cardiac myocytes from induced pluripotent stem cells.* Circulation, 2008. **118**: p. 507-517.
41. Beltrami, A., et al., *Adult cardiac stem cells are multipotent and support myocardial regeneration.* Cell, 2003. **114**(6): p. 763-775.
42. Raab, S., et al., *A comparative view on human somatic cell sources for iPSC generation.* Stem Cells International, 2014: p. 1-12.
43. Takahashi, K., et al., *Induction of Pluripotent stem cells from adult human fibroblasts by defined factors.* Cell, 2007. **131**: p. 861-872.
44. Yu, J., et al., *Human induced pluripotent stem cells free of vector and transgene sequences.* Science 2009. **324**: p. 797-801.
45. Okita, K., et al., *Generation of mouse induced pluripotent stem cells without viral vectors* Science 2008. **322**: p. 949-953.
46. Ban, H., et al., *Efficient generation of transgene-free human induced pluripotent stem cells (iPSCs) by temperature-sensitive Sendai virus vectors.* PNAS 2011. **108**(34): p. 14234-14239.
47. Shi, Y., et al., *Induction of pluripotent stem cells from mouse embryonic fibroblasts by Oct4 and Klf4 with small-molecule compounds.* Cell Stem Cell, 2008. **3**: p. 568-574.
48. Huangfu, D., et al., *Induction of pluripotent stem cells by defined factors is greatly improved by small-molecule compounds.* Nat Biotechnol, 2008. **26**(7): p. 795-797.
49. Warren, L., et al., *Highly efficient reprogramming to pluripotency and directed differentiation of human cells with synthetic modified mRNA.* Cell Stem Cell 2010. **7**(5): p. 618-630.
50. Zhang, J., et al., *Functional cardiomyocytes derived from human induced pluripotent stem cells.* Circ Res, 2009. **104**(4): p. e30-41.
51. Sanganalmath, S. and R. Bolli, *Cell therapy for heart failure: a comprehensive overview of experimental and clinical studies, current challenges, and future directions.* Circ Res, 2013. **113**(6): p. 810-834.
52. Vunjak-Novakovic, G., et al., *Challenges in Cardiac Tissue Engineering* Tissue Engineering 2010. **16**(2): p. 169-187.
53. Sa, S. and K. McCloskey, *Activin A and BMP4 Signaling for Efficient Cardiac Differentiation of H7 and H9 Human Embryonic Stem Cells.* J stem Cells Regen Med, 2012. **8**(3): p. 198-202.
54. Croft, C., et al., *Preparation of organotypic brain slice cultures for the study of Alzheimer's disease.* F1000Res, 2018. **7**.

55. Arakawa, I., et al., *Usefulness of kidney slices for functional analysis of apical reabsorptive transporters.* Scientific Reports 2017. **7**.
56. Verrill, C., et al., *Organotypic liver culture in a fluid-air interface using slices of neonatal rat and adult human tissue--a model of fibrosis in vitro.* J Pharmacol Toxicol Methods 2002. **48**(2): p. 103-10.
57. Brandenburger, M., et al., *Organotypic slice culture from human adult ventricular myocardium.* Cardiovasc Res 2012. **93**(1): p. 50-59.
58. Beqqali, A., et al., *Genome-wide transcriptional profiling of human embryonic stem cells differentiating to cardiomyocytes* Stem Cells 2006. **24**(8): p. 1956-1967.
59. David, R., et al., *Induction of MesP1 by Brachyury(T) generates the common multipotent cardiovascular stem cell.* Cardiovasc Res, 2011. **92**(1): p. 115-122.
60. Ghafar-Zadeh, E., et al., *Engineered approaches to the stem cell microenvironment for cardiac tissue regeneration* Lab Chip 2011. **11**(18): p. 3031-3048.
61. Parker, K. and D. Ingber, *Extracellular matrix, mechanotransduction and structural hierarchies in heart tissue engineering* Philos Trans R Soc Lond B Biol Science, 2007. **362**(1484): p. 1267-1279.
62. Gupta, V. and K. Grande-Allen, *Effects of static and cyclic loading in regulating extracellular matrix synthesis by cardiovascular cells* Cardiovasc Res, 2006. **72**(3): p. 375-383.
63. Kira, Y., et al., *Effect of long-term cyclic mechanical load on protein synthesis and morphological changes in myocardial cells from neonatal rat.* Cardiovasc Drugs Ther, 1994. **8**(2): p. 251-262.
64. Tulloch, N., et al., *Growth of engineered human myocardium with mechanical loading and vascular coculture.* Circ Res, 2011. **109**(1): p. 47-59.
65. Simmons, C., et al., *Microsystems for biomimetic stimulation of cardiac cells.* Lab Chip, 2012. **12**(18): p. 3235-3248.
66. Gwak, S., et al., *The effect of cyclic strain on embryonic stem cell-derived cardiomyocytes.* Biomaterials 2008. **29**(7): p. 844-856.
67. Bursac, N., et al., *Cardiomyocyte cultures with controlled macroscopic anisotropy: a model for functional electrophysiological studies of cardiac muscle.* Circ Res, 2002. **91**(12): p. e45-54.
68. Luna, J., et al., *Multiscale biomimetic topography for the alignment of neonatal and embryonic stem cell- derived heart cells.* Tissue Engineering Part C Methods, 2011. **17**(5): p. 579-588.
69. Hatano, R., et al., *Endothelial cells derived from embryonic stem cells respond to cues from topographical surface patterns.* J Biol Eng, 2013. **7**: p. 18.
70. Verrill, C., et al., *Organotypic liver culture in a fluid-air interface using slices of neonatal rat and adult human tissue-a model of fibrosis in vitro.* Pharmacological and Toxicological Methods 2002. **48**(2): p. 103-110.
71. Humpel, C., *Organotypic brain slice cultures: a review.* Neuroscince 2015. **305**: p. 86-98.
72. Stribos, E., et al., *Precision-cut human kidney slices as a model to elucidate the process of renal fibrosis.* Translational Reserach 2016. **170**: p. 8-16.

73. Wang, K., et al., *Cardiac tissue slices: preparation, handling, and successful optical mapping.* American Journal of Physiology 2015.
74. Watson, S., et al., *Preparation of viable adult ventricular myocardial slices from large and small mammals.* Nature Protocols, 2017. **12**: p. 2623-2639.
75. Kang, C., et al., *Human Organotypic Cultured Cardiac Slices: New Platform For High Throughput Preclinical Human Trials.* Scientific Reports 2016.
76. Schneider-Warme, F., et al., *Organotypic myocardial slices as model system to study heterocellular interactions.* Cardiovasc Res, 2017. **114**(1): p. 3-6.
77. Xiaojun, L., et al., *Directed cardiomyocyte differentiation from human pluripotent stem cells by modulating Wnt/β catenin signaling under fully defined conditions.* Nat Protoc. , 2013. **8**(1): p. 162-175.
78. Thomson, J., et al., *Embryonic Stem Cell Lines Derived from Human Blastocysts.* Science 1998. **282**(5391): p. 1145-1147.
79. Waite, L. and G. Nindl, *Human embryonic stem cell research: an ethical controversy in the US & Germany.* Biomed Sci Instrum 2003. **39**: p. 567-572.
80. Bernard, L. and L. Parham, *Ethical Issues in Stem Cell Research.* Endocr Rev, 2009. **30**(3): p. 204-213.
81. Doss, M. and A. Sachinidis, *Current Challenges of iPSC-Based Disease Modeling and Therapeutic Implications.* Cells 2019. **8**(403): p. 1-16.
82. Invitrogen, *CytoTune-iPS 2.0 Sendai Reprogramming Kit*, in *USER GUIDE*. 2016.
83. Loh, Y., et al., *Generation of induced pluripotent stem cells from human blood.* Blood, 2009. **113**(22): p. 5476-5479.
84. Aasen, T., et al., *Efficient and rapid generation of induced pluripotent stem cells from human keratinocytes.* Nat Biotechnol, 2008. **26**(11): p. 1276-1284.
85. Zhou, T., et al., *Generation of induced pluripotent stem cells from urine.* J Am Soc Nephrol 2011. **22**(7): p. 1221-1228.
86. Harty, L., et al., *Self-Collection of Oral Epithelial Cell DNA under Instruction from Epidemiologic Interviewers.* Am J of Epidemilogoy **151**(2): p. 199-205.
87. Borthakur, G., et al., *Exfoliated Buccal Mucosa Cells as a Source of DNA to Study Oxidative Stress.* Cancer Epidemiol Biomarkers Prev, 2008. **17**(1): p. 212-219.
88. Sun, D., et al., *Buccal Mucosa as an Alternative Source of DNA for Molecular Tests.* Am J of Clinical Pathology 2015. **144**(2): p. 235.
89. Heath, E., et al., *Use of buccal cells collected in mouthwash as a source of DNA for clinical testing.* Arch Pathol Lab Med, 2001. **125**(1): p. 127-133.
90. Trevisan, M., et al., *Generation of a transgene-free induced pluripotent stem cells line(UNIPDi002-A) from oral mucosa epithelial stem cells carrying theR304Q mutation in TP63 gene.* Stem Cell Res, 2018. **28**: p. 149-152.
91. Kashiwagi, T., et al., *Accelerated generation of human induced pluripotent stem cells from human oral mucosa using episomal plasmid vectors and maternal transcription factor Glis1.* J Oral Science Rehabilitation, 2016. **2**(2): p. 26-35.
92. Miyoshi, K., et al., *Generation of human induced pluripotent stem cells from oral mucosa.* J of Bioscience and Bioengineering 2010. **110**(3): p. 345-350.

93. Groeger, S. and J. Meyle, *Oral Mucosal Epithelial Cells.* Frontiers in Immunology 2019. **10**.
94. Squier, C. and M. Kremer, *Biology of oral mucosa and esophagus.* J Natl Cancer Inst Monogr, 2001. **29**: p. 7-15.
95. Kullaa, A., et al., *Microstructure of oral epithelial cells as an underlying basis for salivary mucosal pellicle.* Ultrastruct Pathol. , 2014. **38**(6): p. 382-386.
96. Amemiya, T., et al., *Autologous transplantation of oral mucosal epithelial cell sheets cultured on an amniotic membrane substrate for intraoral mucosal defects.* PLoS One, 2015. **10**(4): p. e0125391.
97. Sheth, R., et al., *Culture and Characterization of Oral Mucosal Epithelial Cells on a Fibrin Gel for Ocular Surface Reconstruction.* Curr Eye Res, 2015. **40**(11): p. 1077-1087.
98. Walker, D., *Oral mucosal immunology: an overview.* Ann Acad Med Singapore, 2004. **33**(4): p. 27-30.
99. Marchetto, M., et al., *Gene transduction in skin cells: preventing cancer in xeroderma pigmentosum mice.* Proc Natl Acad Sci, 2004. **101**(51): p. 17759-17764.
100. Sen, S., et al., *Molecular characterization of explant cultured human oral mucosal epithelial cells.* Invest Ophthalmol Vis Sci, 2011. **52**(13): p. 9548-9554.
101. Ang, L., et al., *Autologous serum-derived cultivated oral epithelial transplants for severe ocular surface disease.* Arch Ophthalmol, 2006. **124**(11): p. 1543-1551.
102. Moharamzadeh, K., *Oral mucosa tissue engineering*, in *Biomaterials for Oral and Dental Tissue Engineering*, L.T.a.K. Moharamzadeh, Editor. 2018, Woodhead Publishing p. 223-244.
103. Khoshnoodi, J., et al., *Mammalian collagen IV.* Microscopy Research and Technique, 2008. **71**(5): p. 357–370.
104. Yurchenco, P. and J. Orear, *Basal lamina assembly.* Current Opinion in Cell Biology, 1994. **6**(5): p. 674-681.
105. Timpl, R., *Macromolecular organization of basement membranes.* Current Opinion in Cell Biology, 1996. **8**(5): p. 618-624.
106. Russo, F., et al., *Epithelial cells from oral mucosa: How to cultivate them?* Cytotechnology 2016. **68**(5): p. 2105-2114.
107. Isaiah, I. and M. Joseph, *Comparative Dynamics of DNA Isolated from Buccal Swab for Forensic Investigation "Pro and Post Brushing from Some Adult Males in Benin Metropolis, Nigeria".* Journal of Forensic Science & Criminology 2016. **4**(5): p. 1-6.
108. Deborah, V., et al., *Organization, barrier function and antimicrobial lipids of the oral mucosa.* Int J Cosmet Sci, 2013. **35**(3): p. 220-223.
109. Souto, L., et al., *Model for human skin reconstructed in vitro composed of associated dermis and epidermis.* Sao Paulo Med J, 2006. **124**(2): p. 71-76.
110. Martino, F., et al., *Cellular Mechanotransduction: From Tension to Function.* Frontiers in Physiology 2018. **9**.
111. Janmey, P. and R. Miller, *Mechanisms of mechanical signaling in development and disease.* J Cell Sci, 2011. **124**(1): p. 9-18.

112. Polachecka, W., et al., *Microfluidic platforms for mechanobiology.* Lab Chip 2013. **13**(12): p. 2252-2267.
113. Secomb, T., *Hemodynamics.* Compr Physiol, 2017. **6**(2): p. 975-1003.
114. Solaro, R.J., *Regulation of Cardiac Contractility*. 2011: Morgan & Claypool Life Sciences
115. Sahni, M., et al., *Role of the Renin-Angiotensin-Aldosterone System in the Management of Neonatal Heart Failure.* NeoReviews 2015. **16**(10).
116. Makaryus, J., *Physiology, Cardiac Cycle*. 2019: StatPearls Publishing
117. Kang, C., et al., *Human Organotypic Cultured Cardiac Slices: New Platform For High Throughput Preclinical Human Trials.* Scientific Reports 2016. **6**.
118. Brandenburger, M., et al., *Organotypic slice culture from human adult ventricular myocardium.* Cardiovasc Res, 2012. **93**(1): p. 50-9.
119. Wang, K., et al., *Cardiac tissue slices: preparation, handling, and successful optical mapping.* AM J Physiol Heart Circ Physiol. , 2015. **308**(9): p. H1112-H1125.
120. Wang, K., et al., *Living cardiac tissue slices: an organotypic pseudo two-dimensional model for cardiac biophysics research.* Prog Biophys Mol Biol, 2014. **115**(2-3): p. 314-27.
121. Humpel, C., *Organotypic brain slice cultures: A review.* Neuroscience 2015. **305**: p. 86-98.
122. LeCluyse, E., et al., *Organotypic liver culture models: Meeting current challenges in toxicity testing.* Critical Reviews in Toxicology 2011. **42**(6): p. 501-548.
123. Stribos, E., et al., *Murine Precision-Cut Kidney Slices as an ex vivo Model to Evaluate the Role of Transforming Growth Factor-β1 Signaling in the Onset of Renal Fibrosis.* Front. Physiol., (2017). **8**.
124. De Boer, T., et al., *Myocardial tissue slices: organotypic pseudo-2D models for cardiac research & development.* Future Cardiol. , 2009. **5**(5): p. 425-430.
125. Watson, S., et al., *Myocardial Slices: an Intermediate Complexity Platform for Translational Cardiovascular Research.* Cardiovasc Drugs Ther. , 2019. **33**(2): p. 239-244.
126. Camelliti, P., et al., *Adult human heart slices are a multicellular system suitable for electrophysiological and pharmacological studies.* J Mol Cell Cardiol, 2011. **51**(3): p. 390-8.
127. Wang, K., et al., *Cardiac tissue slices: preparation, handling, and successful optical mapping.* AM J Physiol Heart Circ Physiol., 2015. **308**: p. H1112-H1125.
128. Bussek, A., et al., *Cardiac tissue slices with prolonged survival for in vitro drug safety screening.* J Pharmacol Toxicol Methods, 2012. **66**(2): p. 145-51.
129. Riehl, B., et al., *Mechanical Stretching for Tissue Engineering: Two-Dimensional and Three-Dimensional Constructs.* Tissue Eng Part B Rev. , 2012. **18**(4): p. 288-300.
130. Perbellini, F., et al., *Investigation of cardiac fibroblasts using myocardial slices.* Cardiovasc Res. , 2017. **114**: p. 77–89.

131. Geuss, L. and L. Suggs, *Making Cardiomyocytes: How Mechanical Stimulation Can Influence Differentiation of Pluripotent Stem Cells.* Biotechnol. Prog 2013 **29**(5): p. 1089-1096.
132. Mai-Dung, N, et al., *Effects of Physiologic Mechanical Stimulation on Embryonic Chick Cardiomyocytes Using a Microfluidic Cardiac Cell Culture Model.* Anal Chem, 2014. **87**(4): p. 2107-2113.
133. Jia-Ling, R., et al., *Mechanical Stress Conditioning and Electrical Stimulation Promote Contractility and Force Maturation of Induced Pluripotent Stem Cell-Derived Human Cardiac Tissue.* Circulation, 2016. **134**(20): p. 1557-1567.
134. Vandenburgh, H., et al., *Mechanical stimulation of organogenic cardiomyocyte growth in vitro.* Am J Physiol 1996. **270**(5 Pt 1): p. 1284-92.
135. Gupta, V. and Grande-Allen, K., *Effects of static and cyclic loading in regularting extracellular matrix synthesis by cardiovascular cells* Cardiovasc Res, 2006: p. 375-83.
136. Ono, S., et al., *Effect of coronary artery reperfusion on transmural myocardial remodeling in dogs* Circulation, 1995. **91**: p. 1143 - 53.
137. Lee, A. and McCullockh, A., *Multiaxial myocardial mechanics and extracellular matrix remodeling: mechanochemical regulation of cardiac fibroblast function* Adv Exp Med Biol 1997. **430**: p. 227 - 40.
138. Riehl, B., et al., *Mechanical Stretching for Tissue Engineering: Two-Dimensional and Three-Dimensional Constructs.* Tissue Engineering Part B Rev. , 2012. **18**(4): p. 288-300.
139. Brown, T., *Techniques for mechanical stimulation of cells in vitro: a review.* Journal of Biomechanics 2000. **33**(1): p. 3-14.
140. Wang, K., et al., *Living cardiac tissue slices: An organotypic pseudo two-dimensional model for cardiac biophysics research.* Progress in Biopysics and Molecular Biology 2014. **115**(2-3): p. 314-327.
141. Perbellini, F., et al., *Investigation of cardiac fibroblasts using myocardial slices.* Cardiovasc Res 2018. **114**(1): p. 77-89.
142. Watson, S., et al., *Biomimetic electromechanical stimulation to maintain adult myocardial slices in vitro.* Nat Commun, 2019. **10**.
143. Fischer, C., et al., *Long-term functional and structural preservation of precision-cut human myocardium under continuous electromechanical stimulation in vitro.* Nat Commun, 2019. **10**.
144. Simmons, C., et al., *Microsystems for biomimetic stimulation of cardiac cells* Lab Chip 2012. **12**: p. 3235 - 48.
145. Wang, K., et al., *Living cardiac tissue slices: An organotypic pseudo two-dimensional model for cardiac biophysics research.* Progress in Biophysics and Molecular Biology 2014. **115**(2-3): p. 314-327.
146. Perbellini, F., et al., *Investigation of cardiac fibroblasts using myocardial slices.* Cardiovasc Res, 2018. **114**(1): p. 77-89.
147. Watson, S., et al., *Biomimetic electromechanical stimulation to maintain adult myocardial slices in vitro.* Nature communications 2019. **10**.

148. Friedrich, O., et al., *Stretch in Focus: 2D Inplane Cell Stretch Systems for Studies of Cardiac Mechano-Signaling.* Front. in Bioengineering and biotechnology 2019. **7**.
149. Dellenback, P., et al., *Contrast-enhancement techniques for particle-image velocimetry.* Appl Opt. , 2000. **39**(32): p. 78-90.
150. Liu, J., et al., *Hydrogels for Engineering of Perfusable Vascular Networks.* Int J Mol Sci. , 2015. **16**(7): p. 15997-16016.
151. Mozaffarian, D., et al., *Heart Disease and Stroke Statistics—2015 Update. A Report From the American Heart Association.* Circulation, 2015: p. e310 - e313.
152. Thygesen, *Third universal definition of myocarial infarction* American college of Cadiology 2012. **60**: p. 1 - 18.
153. Thygesen, K., et al., *Universal definition of myocardial infarction.* European Heart Journal, 2007. **28**: p. 2525–2538.
154. Choi, E., *Adult Stem Cell Therapy for Autoimmune Disease.* Int J Stem Cells, 2009. **2**(2): p. 122-128.
155. Sun, R., et al., *Advances in stem cell therapy for cardiovascular disease (Review).* Int J Mol Med, 2016. **38**(1): p. 23-29.
156. Kumar, J., et al., *Comparative Aspects of Animal Regeneration.* Annu. Rev. Cell Dev. Biol. , 2008. **24**: p. 525-549.
157. Russell, M., et al., *Micromechanical Regulation in Cardiac Myocytes and Fibroblasts: Implications for Tissue Remodeling.* Pflugers Arch. , 2011. **462**(1): p. 105-117.
158. Schneider-Warme, F., et al., *Organotypic myocardial slices as model system to study heterocellular interactions.* Cardiovasc Res, 2018. **114**(1): p. 3-6.
159. Lee, S., et al. , *Identification of cell-specific soluble mediators and cellular targets during cell therapy for the treatment of heart failure.* Regen Med 2008. **3**(6): p. 953-62.
160. White, S., et al., *Cardiac physiology at the cellular level: use of cultured HL-1 cardiomyocytes for studies of cardiac muscle cell structure and function.* AM J Physiol Heart Circ Physiol., 2004. **286**(3): p. H823-9.
161. Yong, F., et al., *Wnt/β-catenin-mediated signaling re-activates proliferation of matured cardiomyocytes.* Stem Cell Research & Therapy 2018. **9**.
162. Donck, L., et al., *Isolated rat cardiac myocytes as an experimental model to study calcium overload: the effect of calcium-entry blockers.* Life Sci, 1986. **38**(9): p. 765-72.
163. Kirkpatrick, C., et al., *Co-culture systems for vascularization--learning from nature.* Adv Drug Deliv Rev. , 2011. **63**(4-5): p. 291-9.
164. Smit, N., et al., *Human Cardiomyocyte Progenitor Cells in Co-culture with Rat Cardiomyocytes Form a Pro-arrhythmic Substrate: Evidence for Two Different Arrhythmogenic Mechanisms.* Front. Physiol., 2017. **8**.
165. Savoji, H., et al., *Cardiovascular disease models: A game changing paradigm in drug discovery and screening.* Biomaterials 2019. **198**: p. 3-26.
166. Mannhardt, I., et al., *Human Engineered Heart Tissue: Analysis of Contractile Force.* Stem cell Reoprts, 2016. **7**(1): p. 29-42.

167. Polonchuk, L., et al., *Cardiac spheroids as promising in vitro models to study the human heart microenvironment.* Sci Rep. , 2017. **7**.
168. Campbell, M., et al., *Stem Cell-Derived Cardiac Spheroids as 3D In Vitro Models of the Human Heart Microenvironment.* Methods Mol Biol., 2019. **2002**: p. 51-59.
169. Lemoine, M., et al., *Human Induced Pluripotent Stem Cell–Derived Engineered Heart Tissue as a Sensitive Test System for QT Prolongation and Arrhythmic Triggers.* Circulation: Arrhythmia and Electrophysiology 2018. **11**(7).
170. Harrison, R., et al., *Observations of the living developing nerve fiber.* The Anatomical Record 1907. **1**(5): p. 116-128.
171. Reinbold, R., *Organotypic differentiation of the eye of the chick embryo in vitro.* C R Seances Soc Biol Fil 1954. **148**: p. 1493-1495.
172. Rosales Gerpe, M., et al., *Use of Precision-Cut Lung Slices as an Ex Vivo Tool for Evaluating Viruses and Viral Vectors for Gene and Oncolytic Therapy.* Molecular Therapy Methods &Clinical Development 2018. **10**: p. 245-256.
173. Chokshi, E., et al., *Precision-cut liver slices: a versatile tool to advance liver research.* Hepatology International 2019. **13**(1): p. 51-57.
174. Poosti, F., et al., *Precision-cut kidney slices (PCKS) to study development of renal fibrosis and efficacy of drug targeting ex vivo.* Disease Models & Mechanisms 2015. **8**: p. 1227-1236.
175. Gähwiler, B., et al., *Organotypic slice cultures: a technique has come of age.* Trends Neurosci 1997. **20**: p. 471-477.
176. Watson, S., et al., *Preparation of viable adult ventricular myocardial slices from large and small mammals.* Nature Protocols 2017. **12**: p. 2623-2639.
177. Fischer, C., et al., *Long-term functional and structural preservation of precision-cut human myocardium under continuous electromechanical stimulation in vitro.* Nature communications, 2019. **10**.
178. Bussek, A., et al., *Tissue slices from adult mammalian hearts as a model for pharmacological drug testing.* Cell Physiol Biochem 2009. **24**(5-6): p. 527-36.
179. Tulloch, N., et al., *Growth of engineered human myocardium with mechanical loading and vascular coculture.* Circulation Research, 2011. **109**(1): p. 47-59.
180. Beqqali, A., et al., *Genome-wide transcriptional profiling of human embryonic stem cells differentiating to cardiomyocytes.* Stem Cells, 2006. **24**(8): p. 1956-67.
181. David, R., et al., *Induction of MesP1 by Brachyury(T) generates the common multipotent cardiovascular stem cell.* Cardiovasc Res, 2011. **92**(1): p. 115-22.
182. Ghafar-Zadeh, E., et al., *Engineered approaches to the stem cell microenvironment for cardiac tissue regeneration.* Lab Chip, 2011. **11**(18): p. 3031-48.
183. Parker, K. and D. Ingber, *Extracellular matrix, mechanotransduction and structural hierarchies in heart tissue engineering.* Philos Trans R Soc Lond B Biol Sci, 2007. **362**(1484): p. 1267-79.
184. Gupta, V. and K. Grande-Allen, *Effects of static and cyclic loading in regulating extracellular matrix synthesis by cardiovascular cells.* Cardiovasc Res, 2006. **72**(3): p. 375-83.

185. Kira, Y., et al., *Effect of long-term cyclic mechanical load on protein synthesis and morphological changes in cultured myocardial cells from neonatal rat.* Cardiovasc Drugs Ther, 1994. **8**(2): p. 251-62.
186. Tulloch, N., et al., *Growth of engineered human myocardium with mechanical loading and vascular coculture.* Circ Res, 2011. **109**(1): p. 47-59.
187. Simmons, C., et al., *Microsystems for biomimetic stimulation of cardiac cells.* Lab Chip, 2012. **12**(18): p. 3235-48.
188. Gwak, S., et al., *The effect of cyclic strain on embryonic stem cell-derived cardiomyocytes.* Biomaterials, 2008. **29**(7): p. 844-56.
189. Bursac, N., et al., *Cardiomyocyte cultures with controlled macroscopic anisotropy: a model for functional electrophysiological studies of cardiac muscle.* Circ Res, 2002. **91**(12): p. e45-54.
190. Luna, J., et al., *Multiscale biomimetic topography for the alignment of neonatal and embryonic stem cell-derived heart cells.* Tissue Eng Part C Methods, 2011. **17**(5): p. 579-88.
191. Dusturia, N., et al., *Effect of myocardial heterogeneity on ventricular electro-mechanical responses: a computational study.* Biomed Eng Online 2019. **18**.
192. Del Rya, S., et al., *Altered expression of connexin 43 and related molecular partners in a pig model of left ventricular dysfunction with and without dipyrydamole therapy.* Pharmacol. Res., 2015: p. 28-31.
193. Frank, D., et al., *The sarcomeric Z-disc: a nodal point in signalling and disease.* Journal of molecular medicine, 2006. **84**: p. 446-468.
194. Qiao, Y., et al., *Multiparametric slice culture platform for the investigation of human cardiac tissue physiology.* Prog Biophys Mol Biol 2019. **144**: p. 139-150.
195. Madonna, R., et al., *Recent developments in cardiovascular stem cells.* Circulation Research, 2014. **115**(12): p. e71-8.
196. Berliner, D., *Current Drug Therapy in Chronic Heart Failure: the New Guidelines of the European Society of Cardiology (ESC).* Korean Circ J, 2017. **47**(5): p. 543-554.
197. Sun, R., et al., *Advances in stem cell therapy for cardiovascular disease (Review).* Int J Mol Med, 2016. **38**(1): p. 23-29.
198. Passier, R., et al., *Stem-Cell-based therapy and lessons from the heart.* Nature, 2008. **453**: p. 322-329.
199. Bolli, S., et al., *Cell Therapy for Heart Failure: A Comprehensive Overview of Experimental and Clinical Studies, Current Challenges, and Future Directions.* Circulation Research. **113**(6): p. 810-834.
200. Sa, S. and K. McClsokey, *Stage-specific cardiomyocyte differentiation method for H7 and H9 human embryonic stem cells.* Stem Cell Rev 2012. **8**(4): p. 1120-1128.
201. Sa, S. and K. McCloskey, *Activin A and BMP4 Signaling for Efficient Cardiac Differentiation of H7 and H9 Human Embryonic Stem Cells.* J Stem Cells Regen Med, 2012. **8**(3): p. 198---202.
202. Sa, S., et al., *Combinatorial Fibronectin and Laminin Signaling Promote Highly Efficient Cardiac Differentiation of Human Embryonic Stem Cells.* Biores Open Access, 2014. **3**(4): p. 150-161.

203. Kattman, S., et al., *Stage-specific optimization of activin/nodal and BMP signaling promotes cardiac differentiation of mouse and human pluripotent stem cell lines.* Cell Stem Cell, 2011. **8**(2): p. 228-40.
204. Sa, S. and K. McCloskey, *Stage-specific cardiomyocyte differentiation method for H7 and H9 human embryonic stem cells.* Stem Cell Rev, 2012. **8**(4): p. 1120-8.
205. Sa, S. and K. McCloskey, *Activin A and BMP4 Signaling for Efficient Cardiac Differentiation of H7 and H9 Human Embryonic Stem Cells* J Stem Cells Regen Med., 2012. **8**(3): p. 198---202.
206. Sa, S., et al., *Combinatorial Fibronectin and Laminin Signaling Promote Highly Efficient Cardiac Differentiation of Human Embryonic Stem Cells.* Biores Open Access, 2014. **3**(4): p. 150-161.
207. Ludwig, T., et al., *Derivation of human embryonic stem cells in defined conditions.* Nat Biotechnol. , 2006. **24**(2): p. 185-7.
208. Rao, M., *iPSC-based cell therapy: an important step forward.* Stem cell Reports 2013. **1**: p. 281 - 282.
209. Orlic, D., et al., *Transplanted adult bone marrow cells repair myocardial infracts in mice* Ann N Y Acad Sci. , 2001: p. 221 - 30
210. Jackson, K., et al., *Regeneration of ischemic cardiac muscle and vascular endothelium by adult stem cells.* J clinical investigation, 2001. **107**: p. 1395 - 402.
211. Murry, C., et al., *Skeletal myoblast transplantation for repair of myocardial nacrosis* The Journal of Clinical investigation, 1996. **98**(11): p. 2512-2523.
212. Tongers, J., D. Losordo, and L. U, *Stem and progenitor cell-based therapy in ischaemic heart disease: promise, uncertainties, and challenges.* Eur Heart J 2011. **32**(10): p. 1197-1206.
213. Menasché, P., et al., *Autologous skeletal myoblast transplantation for severe postinfarction left ventricular dysfunction.* J Am Coll Cardiol, 2003. **41**(7): p. 1078-1083.
214. Beltrami, A., et al., *Evidence that human cardiac myocytes divide after myocardial infarction.* N Engl J Med 2001. **344**(23): p. 1750-1757.
215. Schlaeger, T., et al., *A comparison of non-integrating reprogramming methods.* Nat Biotechnol, 2015. **33**(1): p. 58-63.